สำนักหอสมุดกลาง พระจอมเกล้าลาดกระบัง

EFFECT OF BIODIESEL ON METAL PARTS IN AUTOMOTIVE FUEL SYSTEM

E077727

KHEMMACHAT RUNGSAWAT

เลขหมู่.....
เลขทะเบียน 077727
วัน,เดือน,ปี - 3 มิ.ย. 2559
.b.....
.i.....

A THESIS SUBMITTED IN PARTIAL FULFILLMENT

OF THE REQUIREMENT FOR THE DEGREE OF

MASTER OF ENGINEERING IN AUTOMOTIVE ENGINEERING

(INTERNATIONAL PROGRAM)

INTERNATIONAL COLLEGE

KING MONGKUT'S INSTITUTE OF TECHNOLOGY LADKRABANG

2011

KMITL-2011-IC-M-004-011

This material is reserved for educational use only, not allowed for commercial use.
Forbidden to modify the content, and cite the document when use.

COPYRIGHT 2011

INTERNATIONAL COLLEGE

KING MONGKUT'S INSTITUTE OF TECHNOLOGY LADKRABANG

NATIONAL SCIENCE AND TECHNOLOGY DEVELOPMENT AGENCY

This material is reserved for educational use only, not allowed for commercial use.

Forbidden to modify the content, and cite the document when use.

Thesis Title	Effects of biodiesel on metal parts in automotive fuel system
Student	Mr.Khemmachat Rungsawat
Student ID.	50061919
Degree	Master of Engineering
Program	Automotive Engineering (International Program)
Year	2011
Thesis Advisor	Asst. Prof. Dr. Chinda Charoenphonphanic
	Dr. Subongkoj Topaiboul
	Assoc. Prof. Dr. Kunio Takahashi

ABSTRACT

The use of biodiesel is rapidly expanding around the world due to oil crisis and global warming concerns. Despite the fact that biodiesel is a renewable and environmentally friendly fuel, which provides cleaner combustion and hence less emissions, there are some arguments regarding to the compatibility of the fuel and diesel engine, making it worthwhile to fully understand the impacts of biodiesel on engine parts. The objective of this study is to investigate the effect of 100% biodiesel (B100) on fuel system, focusing on metal parts. Under fuel system durability for period of 500 hours test on 4-cylinder, a mechanical pump system, diesel engine will be performed with full analysis of the effects on the fuel system. Furthermore, some components such as fuel injection pumps, fuel lines and fuel nozzles (injector) were tested by mechanical simulation test and fuel tanks will be sampled and tested in the laboratory by mean of static immersion test method in order to study the corrosion characteristics of those components.

This material is reserved for educational use only, not allowed for commercial use.
Forbidden to modify the content, and cite the document when use.

ACKNOWLEDGEMENT

This thesis could not be completed without the assistance of many persons to whom I would like to express my sincere appreciation.

First, I would like to sincerely thank my advisor, Dr. Subongkoj Topaiboul, Dr. Nuwong Chollacoop, Bioenergy Laboratory at MTEC, who has given me many helpful suggestions, useful advice and fruitful discussions during the undertaken research.

I would also like to sincerely thank Asst. Prof. Dr. Chinda Charoenphonphanic, Dr.Preechar Karin, KMITL, for kind advise and help, and Assoc. Prof. Dr. Kunio Takahashi for the suggestion regarding test conditions.

Moreover, I would like to show gratitude to the National Metal and Materials Technology Center (MTEC), especially the Bioenergy Laboratory for providing the laboratory equipments and instruments as well as financial support.

I am grateful to the National Science and Technology Development Agency (NSTDA), which provided the full scholarship for studying this master program.

Special thanks go to MTEC Bioenergy Laboratory's members and other MTEC staffs for helping me during the experiment.

Finally, I am very grateful to my family for all love, caring, understanding and motivation throughout my life.

Khemmachat Rungsawat

This material is reserved for educational use only, not allowed for commercial use.

Forbidden to modify the content, and cite the document when use.

CONTENTS

Page

ABSTRACT I

ACKNOWLEDGEMENT II

CONTENTS III

LIST OF TABLES VIII

LIST OF FIGURES IX

NOMENCLATURE XIII

CHAPTER 1 INTRODUCTION

1.1 Significance and Background 1

1.2 Objectives 1

1.3 Scopes 2

1.4 Expected Benefits 2

CHAPTER 2 THEORY AND LITERATURE REVIEW

2.1 Transesterification of Vegetable Oils 3

2.1.1 Acid-Catalyzed Processes 4

2.2 Biodiesel 5

2.2.1 Biodiesel's Attributes 5

2.2.2 Biodegradability 5

2.2.3 Flash Point 6

2.2.4 Toxicity 6

2.2.5 Emission Reductions 7

2.2.6 Health Effects 7

2.2.7 Lubricity 8

2.2.8 Stability 8

2.2.9 Infrastructure 9

2.3 Properties of Diesel Fuels 9

2.3.1 Cetane number (CN) 10

This material is reserved for educational use only, not allowed for commercial use.
Forbidden to modify the content, and cite the document when use.

CONTENTS (CONT.)

Page

2.3.2 Cetane Index (CI) 10

2.3.3 Heating value 11

2.3.4 Density 11

2.3.5 Viscosity 12

2.3.6 Boiling Range 13

2.3.7 Distillation Curve 13

2.3.8 Volatility 13

2.3.9 Flash point 13

2.3.10 Pour point 14

2.3.11 Cloud point 14

2.3.12 Low – Temperature Filterability 14

2.3.13 Stability 15

2.3.14 Color 15

2.3.15 Diesel Index 15

2.4 Diesel engine 15

2.5 The Diesel Combustion Process 17

2.6 Combustion of Diesel Fuel Oils 18

2.7 Combustion Type of Diesel Engines 18

2.7.1 Direct injection (DI) systems 18

2.7.2 Indirect-Injection System 19

2.8 Thermal Efficiency of Diesel Engine 20

2.9 Fuel system of diesel engine 20

2.9.1 Injection pump 21

2.9.2 In-line fuel-injection pump 22

2.10 Electrochemical mechanisms 24

2.10.1 The dry-cell analogy and Faraday's law 24

2.10.2 Definition of anode and cathode 26

2.10.3 Types of cells 28

This material is reserved for educational use only, not allowed for commercial use.

Forbidden to modify the content, and cite the document when use.

CONTENTS (CONT.)

Page

2.10.4 Types of corrosion damage 30

2.10.5 Iron and steel 33

2.10.6 Aqueous environments 35

2.10.6.1 Effect of Dissolved Oxygen 35

2.10.6.2 Higher Partial Pressures of Oxygen 35

2.10.6.3 Action of Anaerobic Bacteria 37

2.10.6.4 Effect of Temperature 38

2.10.6.5 Effect of pH 39

2.10.6.6 Corrosion of Iron in Acids 42

2.11 Literature review 44

CHAPTER 3 EXPERIMENTAL PROCEDURES

3.1 Methodology diagram 48

3.2 Tested Fuels 48

3.3 Model of diesel engine 49

3.4 Apparatus 51

3.4.1 Measuring Instruments for Physical and Chemical Property Tests 51

3.4.2 Equipment for analyzed component parts of fuel system 51

3.5 Experiments 53

3.5.1 Simulation test apparatus and methodology 53

3.5.2 Immersion test of fuel tank and methodology 55

CHAPTER 4 EFFECT OF B100 ON SIMULATION OF FUEL SUPPLY LINE

4.1 Results of inline-pump 57

4.1.1 Weight of inline pump parts 58

4.1.2 Delivery valve and holder investigation 59

4.1.3 Pump plunger surface investigation 60

4.2 Injector investigation 63

This material is reserved for educational use only, not allowed for commercial use.
Forbidden to modify the content, and cite the document when use.

CONTENTS (CONT.)

Page

4.2.1 Weight of injector parts 65

4.2.2 Injector housing investigation 66

4.2.3 Needle investigation 67

4.2.4 Spring investigation 68

4.3 Properties of B100 during 510 hour test 69

CHAPTER 5 EFFECT OF B100 ON FUEL TANK

5.1 Testing Environment 72

5.2 Biodiesel properties evaluation 73

5.3 Fuel tank corrosion 74

5.3.1 Area of corrosion 74

5.3.2 Fuel tank observation by Scanning Electron Microscope (SEM) 76

5.3.3 Analysis of chemical components by EDS technique 76

5.3.4 Corrosion of fuel tanks by using Reflected Light Microscope 78

CHAPTER 6 CONCLUSIONS AND SUGGESTIONS

6.1 Conclusions 79

6.1.1 The effect of B100 on fuel supply line 79

6.1.2 The effect of B100 on fuel tank 79

6.2 Suggestions 80

6.2.1 Biodiesel (B100) 80

6.2.2 Quality Specifications 81

6.2.3 B100 Material Compatibility 82

REFERENCES 84

APPENDIX

A: Conference Proceeding 86

A-1: The 2nd Thammasat University International Conference on 86

This material is reserved for educational use only, not allowed for commercial use.

Forbidden to modify the content, and cite the document when use.

CONTENTS (CONT.)

Page

B: ASTM Standard 87

B-1: Flash Point (ASTM D93) 87

B-2: Copper Strip Corrosion (ASTM D130) 88

B-3: Carbon Residue (ASTM D524) 89

B-4: Kinematic Viscosity (ASTM D445) 89

B-5: Ash Content (ASTM D482) 91

B-6: Density (ASTM D4052) 91

B-7: Water Content (ASTM D6304) 92

C: Diesel Standard of Department of Energy Business 94

BIOGRAPHY 95

This material is reserved for educational use only, not allowed for commercial use.
Forbidden to modify the content, and cite the document when use.

LIST OF TABLES

Table	Page
2.1 Corrosion Rates of Various Steels When Oxygen Diffusion is controlling	41
2.2 Effect of Dissolved Oxygen on Corrosion of Mild Steel in Acids	43
3.1 Properties of PSME	49
3.2 Engine specification	50
3.3 Injection pump specification	50
4.1 Weight of metal parts for inline pump (B100 and diesel)	58
4.2 Diameter of delivery-valve holder	59
4.3 Surface Roughness, Ra (μm) of pump plunger skirt surface after diesel and biodiesel fuel usage	62
4.4 Weigh of metal parts for injector (B100 and diesel)	65
4.5 Injector orifice after diesel and biodiesel fuel usage	67
4.6 Diameter of needle tip and diameter of needle after diesel and biodiesel fuel usage	68

This material is reserved for educational use only, not allowed for commercial use.
Forbidden to modify the content, and cite the document when use.

LIST OF FIGURES

Figure Page

2.1 Transesterifications of vegetable oils 3

2.2 Operating cycle of a four-stroke diesel engine 16

2.3 Direct injection engine (DI) systems 19

2.4 Indirect injection engine (IDI) systems 20

2.5 Fuel system of diesel engine 21

2.6 In-line fuel-injection pumps 23

2.7 In-line fuel-injection pumps on 6-cylinder diesel engine 23

2.8 In-line fuel-injection pump (sectional view) 24

2.9 Dry cell 25

2.10 Metal surface enlarged, showing schematic arrangement of local-action cells 26

2.11 Salt concentration cell 28

2.12 Differential aeration 28

2.13 Differential aeration cell formed by rust on iron 29

2.14 Differential aeration cell illustrated by water-line corrosion 29

2.15 Sketch of deepest pit with relation to average metal penetration and the pitting factor 31

2.16 Effect of oxygen concentration on corrosion of mild steel in slowly moving water containing 165 ppm $CaCl_2$, 48-h test, 25°C 35

2.17 Effect of oxygen concentration on corrosion of mild steel in slowly moving distilled water. 48-h test, 25°C 36

2.18 Effect of temperature on corrosion of iron in water containing dissolved oxygen 38

2.19 Effect of pH on corrosion of iron in aerated soft water, room temperature 39

3.1 Methodology diagram 48

3.2 Model of diesel engine 49

3.3 Instruments for physical and chemical property tests 51

(a) Automatic Titrator, (b) Oxidation stability measurement,

(c) Karl Fisher coulometer, (d) Viscosity measurement

3.4 Equipment for analyzed component parts of fuel system 52

(a) Surface Roughness Tester, (b) Injection Tester,

This material is reserved for educational use only, not allowed for commercial use.
Forbidden to modify the content, and cite the document when use.

LIST OF FIGURES (CONT.)

Figure Page

(c) Mechanical pump Tester, (d) Scanning Electron Microscope (SEM),

(e) Optical Microscopy (OM), (f) Temperature and humidity sensor

3.5 Schematic drawing of fuel supply system simulation test apparatus 53

3.6 Controller 54

3.7 The pump rig test 54

3.8 Test procedure for study the effect of biodiesel on fuel tank 56

(a) fuel tanks at the indoor area, (b) fuel tanks at the outdoor area,

(c) sampling biodiesel from the fuel tank every week, (d) observation of fuel tank corrosion

4.1 Dismantled Inline Pump 57

4.2 parts of inline pump (a) holder, (b) delivery valve, (c) pump plunger 58

4.3 Weigh of metal parts for inline pump which is analyzed by using statistics 58

(a) weight of holder and error bar with stdev,

(b) weight of delivery valve and error bar with stdev,

(c) weight of pump plunger and error bar with stdev

4.4 Delivery- valve holder 59

4.5 Diameter of delivery-valve holder which is measured by using microscope 60

(a) Inside diameter of delivery-valve holder and error bar with stdev,

(b) Outside diameter of delivery-valve holder and error bar with stdev

4.6 Pump elements with leakage return channel 60

4.7 Pump plunger design variation (a) helix at bottom, (b) helix at top and bottom, ... 60

(c) helix at bottom and starting groove

4.8 Pump plunger skirt surface 61

4.9 Pump plunger skirt surface after diesel fuel usage 62

4.10 Pump plunger skirt surface after biodiesel usage 62

4.11 Surface Roughness, Ra (μm) by statistics shows average of Ra 62

and error bar with stdev which compare between diesel fuel group and biodiesel group

4.12 Dismantled Injector, the type is DSLA 154 P018, 6 hole 64

4.13 The injection pressure during the diesel fuel and B100 usage on the test rig 64

This material is reserved for educational use only, not allowed for commercial use.
Forbidden to modify the content, and cite the document when use.

LIST OF FIGURES (CONT.)

Figure Page

4.14 Metal parts of injector (a) injector housing, (b) needle, (c) spring 65

4.15 Weigh of metal parts for injector which is analyzed by using statistics 65

(a) weight of injector housing and error bar with stdev,

(b) weight of needle and error bar with stdev,

(c) weight of spring and error bar with stdev.

4.16 Injector orifice investigation 66

4.17 Orifice of injector were analyzed by statistics 67

4.18 Needle investigation focus on diameter of needle tip and diameter of needle 67

after diesel and biodiesel fuel usage

4.19 Needle investigations were analyzed by statistics which shows error bar with stdev 68

4.20 Spring tester 68

4.21 Results of spring 69

4.22 Properties of B100 during 500 hours test 71

(a) viscosity of B100 during 500 hours test, (b) water content of B100 during 500 hours test,

(c) oxidation stability of B100 during 500 hours test, (d) acid value of B100 during 500 hours test.

5.1 History plots of outdoor storage condition for 3 months showing: 73

(a) temperature (degree Celsius); (b) %relative humidity.

5.2 Biodiesel property evaluations: (a) pH value, (b) acid value (mg KOH/g), ... 73

(c) water content (ppm), and (d) conductivity value (μs)

5.3 The corrosion of fuel tank after containing biodiesel for : 75

(a) 1 month at the indoor area, (b) 2 months at the indoor area,

(c) 3 months at the indoor area (d) 1 month at the outdoor area,

(e) 2 months at the outdoor area, and (f) 3 months at the outdoor area

5.4 The corrosion of fuel tanks at indoor area taken by SEM during and after 76

containing biodiesel for 3 months, (a) smooth surface without corrosion,

This material is reserved for educational use only, not allowed for commercial use.

Forbidden to modify the content, and cite the document when use.

LIST OF FIGURES (CONT.)

Figure Page

(b) corrosion surface after 1 month, (c) corrosion surface after 2 months,

(d) corrosion surface after 3 months.

5.5 The corrosion of fuel tanks at the outdoor area taken by SEM during and 76

after containing biodiesel for 3 months, (a) smooth surface without corrosion,

(b) corrosion surface after 1 month, (c) corrosion surface after 2 months,

(d) corrosion surface after 3 months

5.6 The chemical components of fuel tank by EDS technique at outdoor area , ... 77

(a) the elemental compositions of the corrosion product for non-corroded surface,

(b) the elemental compositions of the corrosion product after 1 month,

(c) the elemental compositions of the corrosion product after 2 months,

(d) the elemental compositions of the corrosion product after 3 months

5.7 The chemical components of fuel tank by EDS technique at outdoor area , ... 78

(a) the elemental compositions of the corrosion product for non-corroded surface,

(b) the elemental compositions of the corrosion product after 1 month,

(c) the elemental compositions of the corrosion product after 2 months,

(d) the elemental compositions of the corrosion product after 3 months

5.8 The cross section of fuel tank after containing biodiesel by using 78

Reflected Light Microscope at the indoor area

(a) the cross section of fuel tank for smooth surface,

(b) the cross section of fuel tank after 1 month,

(c) the cross section of fuel tank after 2 months,

(d) the cross section of fuel tank after 3 month.

5.9 The cross section of fuel tank after containing biodiesel by using 78

Reflected Light Microscope at the outdoor area :

(a) the cross section of fuel tank for smooth surface,

(b) the cross section of fuel tank after 1 month,

(c) the cross section of fuel tank after 2 months,

(d) the cross section of fuel tank after 3 months.

This material is reserved for educational use only, not allowed for commercial use.
Forbidden to modify the content, and cite the document when use.

NOMENCLATURE

Acronym

ASTM = American Society for Testing and Materials International

B5 = Biodiesel 5% blending with diesel

B100 = Biodiesel fuel

CN = Cetane number

CI = Cetane Index

CFPP = Cold filter plugging point

DOEB = Department of Energy business standard

DI = Direct injection engines

EN = European Committee for Standardization

IDI = Indirect injection engines

LTFT = Low temperature flow test

OM = Optical Microscopy

PSME = Palm stearin methyl ester

SEM = Scanning Electron Microscope

Symbols

C = Carbon

Fe = Iron

H = Hydrogen

HC = Hydrocarbon

H_2O = Water

N_2 = Nitrogen

CO = Carbon monoxide

CO_2 = Carbon dioxide

NO/NO_X = Nitric Oxide/Oxides of Nitrogen

O_2 = Oxygen

Zn = Zinc

This material is reserved for educational use only, not allowed for commercial use.

Forbidden to modify the content, and cite the document when use.

CHAPTER 1

INTRODUCTION

1.1 Significance and Background

Nowadays, Thailand is facing with fuel crisis as the same as other countries that are dependent on petroleum import. It is caused by continuously increasing petroleum oil's price. At the same time, we are encountering with double increasing of environmental problem caused by non-renewable energy use which also contributes to global warming. One of the solutions is to find an alternative source such as biodiesel. Thai government has issued policy to support and realized about biodiesel fuel. This benefits to energy consumption within the country, balances quantity of agriculture products and lowers environmental problem at the same time. However, the use of biodiesel fuel may have effects on engine parts and performance, especially when using at high concentration. This research offers the study on the effect of 100% biodiesel on fuel system of diesel engine. It focuses on metal parts under sets of experiment and durability test in laboratory to investigate corrosion of various parts.

The Ministry of Energy has issued biodiesel standard in Thailand based on ASTM (American Society of Testing and Materials International) and EN (European Committee for Standardization) which were derived from soybean and rapeseed oil whereas raw material for Thai biodiesel fuel is palm or jatropha oil. In Thailand, the use of biodiesel fuel in agriculture sector has been promoted but there are no automobile manufacturer accept B100 (100%biodiesel). Only B5 (5% biodiesel blended with diesel) can be used to ensure the fuel quality will not much different from diesel fuel. In other words, there are some arguments regarding to the compatibility of biodiesel and diesel engine. It is then worthwhile to fully understand the impacts of biodiesel on engine, focusing on metal parts. Series of experiment will be performed in order to analyze the effects on diesel fuel system and also to determine lifetime of metal parts when using pure biodiesel.

1.2 Objectives

1.2.1 To study the effect of 100% biodiesel on injectors, fuel pumps by designed mechanical simulation of diesel fuel system.

1.2.2 Determine corrosion characteristics and compatibility of biodiesel on fuel tank.

This material is reserved for educational use only, not allowed for commercial use.
Forbidden to modify the content, and cite the document when use.

1.3 Scopes

This research offers the study on the effect of 100% biodiesel on fuel system of diesel engine. It focuses on metal parts under experiments and mechanical simulation test for determining the parts, durability and corrosion behavior of various parts. It is intended to analyze the problems occurring during the experiment and suggest accurate approaches in practical.

To look at material and biodiesel compatibility, the metal parts from fuel system components of a farm truck 4100QB-2 Diesel Engine, including fuel tank, fuel pump, fuel line and fuel injection, which parts are affected directly on 100% biodiesel use, are investigated by the followings

1.3.1 500-hour screening test on 4-cylinder, mechanical pump system, diesel engine will be performed with full analysis of the effects on the fuel system.

1.3.2 Static immersion test method by filling fuel tank with pure biodiesel.

1.4 Expected Benefits

1.4.1 To fully understand the impacts of biodiesel on engine, focusing on metal parts.

1.4.2 To suggest the lifetime of metal parts when using pure biodiesel.

This material is reserved for educational use only, not allowed for commercial use.
Forbidden to modify the content, and cite the document when use.

CHAPTER 2

THEORY AND LITERATURE REVIEW

Biodiesel has many advantages over petroleum diesel fuels. It is reliable, renewable, and its use can strengthen local economy. Engines running on biodiesel can provide significant emission reduction such as for carbon monoxide, particulates and hydrocarbons.

2.1 Transesterification of Vegetable Oils

Transesterification is the general term used to describe the important class of organic reactions where an ester is transformed in to another through interchange of the alkoxy moiety. When the original ester is reacted with an alcohol, the transesterification process is called alcoholysis (Figure 2.1). In this review, transesterification will be used as synonymous for alcoholysis of carboxylic ester, in agreement with most publications this field. The transesterification is an equilibrium reaction and the transformation occurs essentially by mixing the reactants, vegetable oil, alcohol and catalyst. However, in order to achieve a high yield of the ester.

In the transesterifation of vegetable oils, a triglyceride reacts with an alcohol in the presence of strong acid or base, producing a mixture of fatty acids alkyl esters and glycerol. The overall process is a sequence of three consecutive and reversible reactions, in which di-and monoglycerides are formed as intermediates. The stoichiometric reaction requires 1 mol of a triglyceride and 3 mol of the alcohol.

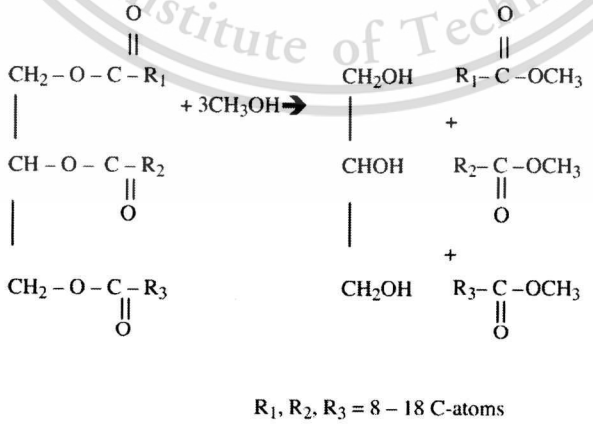

Figure 2.1 Transesterifications of vegetable oils.

This material is reserved for educational use only, not allowed for commercial use.
Forbidden to modify the content, and cite the document when use.

Several aspects, including the type of catalyst (alkaline or acid), alcohol/vegetable oil molar ratio, temperature, purity of the reactants (mainly water content) and free fatty acid content, have an influence on the course of the transesterification and will be discussed below, based on the catalyst used.

2.1.1 Vegetable oil as renewable fuel for diesel replacement

With exception of hydroelectricity and nuclear energy, the major part of all energy consumed worldwide comes from petroleum, charcoal and natural gas. However, these sources are limited, and will be exhausted by the end of the next century. Thus, looking for alternative sources of energy is of importance.

Vegetable oils are a renewable and potentially inexhaustible source of energy with and energy content closed to diesel fuel. Historically, it is believed that Rudolf Diesel himself started research with respect to the use of vegetable oils as fuel for diesel engines.

In the following decades, the studies became more systematic and, nowadays, much is known about its use as fuel. Despite energetically favorable, the direct use of vegetable oils in fuel engines is problematic. Due to their high viscosity (about 11 to 17 times higher than diesel fuel) and low volatility, they do not burn completely and form deposits in the fuel injector of diesel engines. Furthermore, acrolein (a highly toxic substance) is formed through thermal decomposition of glycerol. Different ways have been considered to reduce the high viscosity of vegetable oils:

- dilution of 25 parts of vegetable oil with 75 parts of diesel fuel;
- microemulsion with short chain alcohols (e.g. ethanol or methanol);
- thermal decomposition, which produced alkanes, alkenes, carboxylic acids and aromatic compounds (pyrolisis).
- catalytic cracking, which produces alkanes, cycloalkanes and alkylbenzenes, and
- transesterification with ethanol or methanol.

Among all these alternatives, the transesterification seems to be the best choice, as the physical characteristics of fatty acid esters (biodiesel) are very close to those of diesel fuel and the process is relatively simple. Furthermore, the methyl or ethyl esters of fatty acids can be burned directly in unmodified diesel engines, with very low deposit formation.

Several types of vegetable oils, with a diversified in the fatty acids, can be used for the preparation of biodiesel. Soybean, rapeseed, sunflower and palm oils are most studied. However, there

This material is reserved for educational use only, not allowed for commercial use.
Forbidden to modify the content, and cite the document when use.

are no technical restrictions to the use of other types of vegetable oils. Consideration the type of the alcohol, the use of methanol is advantageous as it allows the separation of glycerol. The same reaction using ethanol is more complicated as it requires a water-free alcohol, as well as an oil with a lower water content, in order to obtain glycerol separation.

Normally, methanol is used as it is the cheapest alcohol in most countries. However, in Brazil it is advantageous to use anhydrous ethanol, which is already produced in large quantity to be mixed with gasoline.

2.2 Biodiesel

Biodiesel is a diesel fuel substitute produced from renewable sources such as vegetable oil, animal fat, and recycled cooking oils. Chemically, it is defined as the mono alkyl ethers of long chain fatty acids derived from the renewable liquid sources. Biodiesel is typically produced through the reaction of a vegetable oil or animal fat with methanol or ethanol in the presence of a catalyst to yield glycerin and biodiesel (chemically called fatty acid methyl or ethyl esters). Biodiesel can be used in neat form, or blended with petroleum diesel for use in diesel engines. Its physical and chemical properties are similar to petroleum based diesel fuel yet, non-hazardous and biodegradable.

2.2.1 Biodiesel's Attributes

Across the global environmental concerns and energy security issues have prompted legislation and regulatory actions spurring demand for alternative fuel such as biodiesel. However, the greatest driving force for the use of biodiesel and biodiesel blends is the need to have a fuel that fulfills all of the environmental and energy security needs, previously mentioned, which does not sacrifice operating performance. One of the largest roadblock to the use of altetnative fuel is the change of performace noticed by users. Biodiesel has many positive attributes associated with its use, but by far the most noted attribute highlighted by fleet managers is the similar operating performance to conventional diesel fuel and the lack of change requied in facilities and maintenance procedures. Other attributes and biodiesel and biodiesel blends are detailed below:

2.2.2 Biodegradability

Biodiesel has desirable degradation attributes which male it the fuel of choice by environmentally conscious boaters. Studies at the University of Idaho compared the biodegradation of biodiesel in an aqueous solution to diesel fuel and dextrose (sugar). Biodiesel samples degraded more

This material is reserved for educational use only, not allowed for commercial use.
Forbidden to modify the content, and cite the document when use.

rapidly than dexstrose, and were 95 percent degraded at the end of 28 days. The diesel fuel was approximately 40 percent degraded after 28 days.

Its should also be noted that blending biodiesel with diesel fuel accelerates its biodegradability. For example blends of 20% biodiesel and 80% diesel fuel degrade twice as fast as diesel. Thus, biodiesel use has demonstrated bilodegradability benefits at levels lower than 100%. Simply stated, neat biodiesel degrades as fast as sugar and a B20 blend will degrade twice as fast as petroleum based diesel fuel.

2.2.3 Flash Point

The flash point of a fuel is defined as the temperature at which the fuel becomes a mixture that will ignite when exposed to a spark of flame. The flash point of biodiesel has been tested and reported by various sources. Specific testing at Southwest Research Institute concluded that the flash point of biodiesel blendes increases as the percentage of biodiesel increases. Therefore pure biodiesel and blends of biodiesel with petroleum diesel are safer to store, handle, and use than conventional diesel fuel. Neat biodiesel has a flash point over 300 Fahrenheit, well above the flash point of petroleum based diesel fuel.

2.2.4 Toxicity

The impact on human health is a significant criteria when considering the suitability of a fuel for commercial applications. Health effects can be measured in terms of the fuel's toxicity to the human body of health impacts due to exhaust emissions. Tests conducted by Wil Research Laboratories, Inc. investigated the acute oral toxicity or pure biodiesel fuel as well as B20, was found to be greater than 5000 mg/kg. The acute dermal toxicity of neat biodiesel was evaluated in a single dose study involving rabbits. The LD50 of neat biodiesel was found to be greater than 2000 mg/kg and the 2000 mg/kg dose level was found to be a no observable effect level (NOEL) for systematic toxicity. There were no deaths, remarkable body weight changes or gross necropsy findings for the LD50 dose levels for each of the studies.

Acute aquatic toxicity tests with Daphnia Magna have also been conducted. Table salt (NaCl), diesel, and biodiesel were compared to each other. The LC50 count (the concentration where 50 percent of the daphnia Magna have died and 50 percent were still alive) for table salt was 3.7 parts per million

This material is reserved for educational use only, not allowed for commercial use.
Forbidden to modify the content, and cite the document when use.

(ppm), 1.43 ppm for diesel fuel, and 23-332 ppm for biodiesel. Therefore, biodiesel is less toxic than diesel fuel and table salt.

2.2.5 Emission Reductions

The use of biodiesel in a conventional diesel engine results in substantial reduction of unburned hydrocarbons, carbon monoxide, and particulate matters. Emissions of nitrogen oxides are slightly reduced or slightly increased depending on the duty cycle of the engine and testing methods employed.

The use of biodiesel decreases the solid carbon fraction of particulate matter (since the oxygen in biodiesel enables more complete combustion to CO_2), eliminates the sulfate fraction (as there is no sulfur in the fuel), while the soluble, or hydrocarbon, fraction stays the same or is increased. Therefore, biodiesel works well with new technologies such as catalysts (which reduce the soluble fraction of diesel particulate but not the solid carbon fraction), particulate traps, and exhaust gas recirculation.

2.2.6 Health Effects

Evidence does exist which indicates that diesel particulate matter is a potential carcinogen. In 1988, the National Institute for Occupational Safety and Health (NIOSH) recommended that whole diesel exhaust be regarded as "a potential occupational carcinogen," as defined in the Cancer Policy of the occupational Safety and Health Administration. The use of biodiesel decreases most regulated emissions. Research results indicate that particulate matter (specifically the carbon or insoluble fraction), hydrocarbons, and carbon monoxide are significantly reduced.

In addition to reducing the overall levels of pollutants and carbon, the compounds that are prevalent in biodiesel and diesel fuel exhaust are different. Research conducted by Southwest Research Institute on a Cummins N14 engine indicates that biodiesel exhaust has a less harmful impact on human health than petrodiesel. Biodiesel emissions have decreased levels of all target polycyclic aromatic hydrocarbons (PAHs) and nitrited PAHs compounds, as compared to petroleum diesel exhaust. PAHs and nPAHs compounds have been identified as potential cancer causing compounds. All of the PAH compounds were reduced by 75 to 85 percent, with the exception of benzo(a)anthracene, which was reduced by roughly 50 percent. The target nPAH compounds were also reduced dramatically with biodiesel fuel, with 2-nitrofluorene and 1-nitropyrene reduced by 90 percent, and the rest of the nPAH compounds reduced to only trace levels. All of these reductions are due to the fact that biodiesel fuel contains no aromatic compounds of any kind, including PAHs.

This material is reserved for educational use only, not allowed for commercial use.
Forbidden to modify the content, and cite the document when use.

In addition, the total speciated hydrocarbon mass of biodiesel is nearly 50 percent less than that measured from conventional diesel fuel, and the associated ozone potential is reduced by the same amount. Significant reductions in most aldehyde compounds were also observed with biodiesel, with formaldehyde and acetaldehyde 30 percent lower than the levels observed for conventional diesel fuel.

2.2.7 Lubricity

In the United States the sulfur level of diesel fuel that is used for on-road purposes is limited to 0.05% by weight. This limit was mandated in October 1993 as a method to decrease particulate matter emitted from diesel powered vehicles. With the introduction of mandated Environmental Protection Agency (EPA) low-sulfur diesel fuel, fleet operators began to encounter premature wear and/or failure of injector pumps in increasing numbers. Pump manufacturers such as Stanadyne and Bosch began recommending the use of lubricity additives to alleviate the serious damage that the reduced sulphur content of low sulfur diesel was causing to their injection pumps. Many petroleum distributors are only marketing low-sulfur diesel even though it remains legal to sell high-sulfur diesel in off-road markets. Testing at labs such as Southwest Research Institute, Stanadyne Automotive, and Engineering Testing Services have demonstrated that biodiesel provides significant lubricity improvement over petroleum diesel fuel. Lubricity results of biodiesel and petroleum diesel using the High Frequency Reciprocating Rig test indicate that there is a marked improvements in lubricity when biodiesel is added to conventional diesel fuel, even at blend levels below 1%.

2.2.8 Stability

Oxidative stability is major industry issue for diesel and biodiesel fuels. Some biodiesel are more stable than others. The tendency of a fuel to be unstable can be predicted by the Iodine number (ASTM D 1510) but the test method may not pick up the presence of stability additives. Iodine number actually measure the presence of C=C bonds that are prone to oxidation. The general rule of thumb is that instability increases by a factor of 1 for every C=C bond on the fatty acid chain; thus 18:3 are three times more reactive than 18:0. Stability can be predicted from knowledge of feedstock only if you know the proportion of C18:2 and C18:3 fatty acids present in the fuel and know whether or not the fuel has been treated for stability. High fractions of those two types of fatty acids can adversely affect fuel stability if additives are not used.

This material is reserved for educational use only, not allowed for commercial use.
Forbidden to modify the content, and cite the document when use.

Poor stability can be lead to increasingly high acid numbers, increasing viscosity, and formation of gums and sediment that can clog filters. Long - term storage in the presence of diesel fuel, diesel additive, water, sediments, heat, and air has not been adequately documented in the field. Biodiesel and blends of biodiesel and diesel fuel should not be stored for longer than 6 months either storage tanks or vehicles until better field data is available.

2.2.9 Infrastructure

In general, the standard storage and handling procedure used for petroleum diesel can be used for biodiesel. The fuel should be stored in a clean, dry, dark environment. Temperature extremes should be avoided. Acceptable storage tank materials include stainless steel, fluorinated polyethylene, and fluorinated polypropylene. Biodiesel has a solvent effect which may release deposits accumulated on tank walls and pipes from previous fuel storage. The release of deposits may clog filters initially and precautions should be taken.

2.3 Properties of Diesel Fuels

Although diesel engines vary widely in size, power, speed output, and mechanical design, their fuel requirement are quite similar in many respects. Performance features desired of all diesel fuels, and physical properties most directly related to them are summarized below. Fuels properties are presented in the order in which they are seen by the engine as the fuel flows from the storage tank, through the fuel system, to the combustion chamber. No attempt is made in the table to indicate relative importance.

Performance Feature Desired	Indicated By
1. Safety in handling	Flash point
2. Pumpability at low temperature	Pour or cloud point, Viscosity
3. Freedom from all suspended matter	Storage stability
4. Readily atomized	Viscosity
5. Readily ignitable	Cetane No.
6. Clean burning	Volatility, Cetane No.
7. Good fuel economy	API Gravity
8. Major effect on engine wear and deposits	Sulfur, Aromatics

This material is reserved for educational use only, not allowed for commercial use.
Forbidden to modify the content, and cite the document when use.

Except for the calorific value or energy content, the required properties of hydrocarbon in fuels for diesel engines differ significantly from those in gasoline engines. Cetane number, density, viscosity, low-temperature property, sulfur content, aromatic content, volatility and boiling range make up the essential characteristics of diesel fuels necessary for satisfactory operation of the diesel engine.

2.3.1 Cetane number (CN). is a measured ignition quality or ignition delay , and is related to the time required for a liquid fuel to ignite after injection into a compression ignition engine. A high cetane number is representative of a short ignition delay. This properties is related to the fuel composition. The two standards, cetane (n-hexadecane) and 1-methylnaphthalene (1-MN) are assigned CN value of 100 and 0, respectively. The operating definition of CN represents the volume percentage of cetane which must be mixed with 1-MN to give the same ignition performance as s given real diesel fuel. Due to the difficulty to obtain large supplied of pure 1-MN (partly due to oxidative degradation during storage), there is now a secondary standard in use, heptamethylnonane (2, 2, 4, 4, 6, 8, 8-heptamethylnonane), which is assigned a CN = 15, and the corresponding equation for CN is as follows:

CN = vol.% of cetane+ 0.15 (vol% of heptamethylnonane)

The auto-ignition phenomenon is the basis of the physical meaning for cetane number. In the compression stroke, the air is precompressed until its temperature exceeds that necessary for auto-ignition or spontaneous combustion of the fuel. Near the end of compression stroke, the diesel fuel is injected into the cylinder in atomized form and is vaporized in the air. Auto-ignition temperature (AIT) is defined as the lowest temperature at which a substance will ignite in the absence of a spark of flame. Auto-ignition is initiated at elevated temperature where the oxygen in the air can begin to interact with the hydrocarbon, the resulting in an exothermic oxidation reaction. When the rate of heat production exceeds the rate at which the heat can be dissipated to the surrounding, auto-ignition occurs. Auto – ignition is believed to proceed through a free radical mechanism. The ease of auto-ignition generally increases, and thus AIT decreases in the order of aromatics< branched alkanes< cycloalkanes<n-alkane

2.3.2 Cetane Index (CI). Cetane index is a calculated value, derived from fuel density (see below) and volatility. Cetane index usually gives a reasonably close approximation to real cetane number, which is derived from measurement in a rail engine. Cetane index is wildly used for routine

This material is reserved for educational use only, not allowed for commercial use.
Forbidden to modify the content, and cite the document when use.

monitoring of diesel fuel ignition quality. The calculated cetane index has mainly served as an alternative method of determining the ignition quality of diesel fuel to minimize the need for engine tests. The method D4737-1998 by ASTM (American society for Testing and Materials) gives the relatively new equation for calculating the cetane index that used density and three distillation points are shown below:

$$CI = 45.2 + 0.0892(T10 - 215) + 0.131\ (T50 - 260) + 0.0523\ (T90 - 310) + 0.901\ B(T50 - 260) - 0.420\ B(T90 - 310) + 0.0049\ (T10 - 215)^2 - 0.0049\ (T90 - 310)^2\ 107.0\ B + 60.0\ B^2$$

Where T10, T50 and T90 are the 10%, 50%, and 90% recovery temperatures in °C. respectively, according to the distillation curve, correct to standard barometric pressure, and D the dendity in kg/l at 15 °C and

$$B = e^{[-3.5(D-0.85)]} - 1$$

2.3.3 Heating value. Heating value is defined as the amount of heat released per unit mass of fuel from its complete combustion. This property is also referred to as calorific value or energy content. Although cetane number determines the combustion performance, it is the heating value along with thermodynamic criteria that sets the maximum possible output of power. Heating value can be measure by ASTM D4809 method for transportation diesel fuels and by ASTM D 4868 for plant diesel fuels. Typical heating values for diesel fuels are in the range of 134,000 Btu/gal (19,700 Btu/lb) to 148,000 Btu/gal.

2.3.4 Density. Density is the mass per unit volume of diesel at given temperature. It can provide useful indication about a fuel's composition and performance-related characteristics. Density has an importance in diesel engine performance, since fuel injection operates on a volume metering system. A change in density will influence engine output due to different mass of fuel injected, and a higher density fuel will tend to produce more smoke as well as more power. The densities of fuels obtained by different refining processes are approximately as follows:

Straight-run distillates 0.805-0.870 g/ml

This material is reserved for educational use only, not allowed for commercial use.
Forbidden to modify the content, and cite the document when use.

Hydrocracked gas oil 0.815-0.840 g/ml

Thermally cracked gas oil 0.835-0.870 g/ml

Catalytically cracked gas oil 0.930-0.965 g/ml

A limit to maximum density is set to avoid smoke formation at full load. Therefore, the density of diesel fuels should be in the range of 0.80-0.86 g/ml (800-860 kg/m3). A related unit is API gravity by the American Petroleum institute.

API gravity (°) = [141.5/(specific gravity at 60 °F(15.6 °C))] – 131.5

It may be note that water has a specific gravity of 1.0 g/ml an API gravity of 10.0°. API gravity is a useful measure of density for liquids lighter than water. Diesel fuels have API gravity of 33-45°. Density differs from API gravity in that the higher the number in degree API, the lighter is the fuel.

2.3.5 Viscosity. Viscosity is a measure of the internal fluid friction, which tends to oppose any dynamic change in the fluid motion. It reflects on the extent of intermolecular (attractive) forces and decreases with increasing temperature. Therefore, the viscosity of a fluid indicates its resistance to flow; the higher the viscosity, the greater the resistance to flow. The viscosity of diesel fuels is important for fuel flow and engine operation. The unit of viscosity is the poise, which is the force required to move an area of 1 cm^2 at a speed of 1 cm/sec past two parallel surfaces that are separated by the fluid. The kinematic viscosity is the ratio of the viscosity to the density. The unit of kinematic viscosity is the Stoke (St), measured in cm^2/s but often reported in centistokes (cSt).

For convenience, the two figures as often expressed in centipoises (cP) and centistokes (cSt), and the two are related in that cP = cSt x density of the liquid. The term centistokes is being replaced by the preferred SI (System International) unit mm^2/s. A widely used laboratory method for determining the kinematic viscosity of diesel fuels is ASTM D445, which measures the time taken for a fixed volume of the fuel to flow under gravity through a capillary tube viscometer immersed in a thermostatically controlled bath.

Viscosity is an important property of diesel fuel because of its relevance to the performance of the fuel injection equipment, particularly at low temperature when the increase in viscosity affects the

This material is reserved for educational use only, not allowed for commercial use.
Forbidden to modify the content, and cite the document when use.

fluidity of the fuel. Increasing viscosity reduces the injector spay cone angle and fuel distribution and penetration while increasing the droplet size.

If viscosity is too high, poor atomizations of fuel spray a result, which leads to poor combustion and loss of power, and thus poor fuel economy. If the viscosity is too low, the lack of lubricity leads to injector pump wear. Very low viscosity can also result in significant leakage of fuel from pumping elements, particularly at low pumping speeds.

2.3.6 Boiling Range. Boiling range is defined by the initial boiling point (IBP) and final boiling point (FBP) in the distillation curve. Most diesel fuels contain hydrocarbon with boiling points within the range of 150 to 380 °C. For typical transportation diesel fuels in the U.S., boiling range is between 177 °C (350 °F) to 343 °C (650 °F).

2.3.7 Distillation Curve. It is necessary to obtain values for T10, T50, and T90 to meet fuel specification and to calculate the cetane index. The development of simulated distillation gas chromatography (Sim Dis Gc) has resulted in a never and simpler method for determining the distillation cure in addition to the boiling rage of the hydrocarbon fuels. AST M D2887 method can be used for measuring the boiling rage of diesel duels with GC. ASTM D 2887 method is much more efficient than the old distillation method ASTM D86. SimDis GC can be used for evaluating boiling range of light oils, heavy oils and even residual oils and their upgrading products. SimDis GC method generally uses a non-polar stationary phase (such as polymethylsiloxane) for GC column where the compounds are separated base on their different in boiling points. Thus the retention times of fuel components give their equivalent boiling points after calibration with standards. Fuels oils used for low- and medium-speed engines have higher boiling components that uses to require high- temp of vacuum distillation for analysis, but they all can be easily analyzed now by using 1 µl injection of the sample into SimDis GC. The extent of deviation from true boiling points depends on the contents of different compound classes in fuels as well as the polarity of GC column.

2.3.8 Volatility. Volatility of the fuel influences many other properties including density, auto-ignition temperature, cold-ignition temperature, flash point, viscosity, and cetane number. Volatility depends on the boiling range and the content of light fractions, which can be measures by distillation with SimDis GC. Increasing the contents of lower boiling fractions increases the volatility of fuels.

This material is reserved for educational use only, not allowed for commercial use.
Forbidden to modify the content, and cite the document when use.

2.3.9 Flash point. Flash point is the temperature to which fuel must be heated to produced a vapor-air mixture (above the liquid) that will ignite and spread over the liquid surface when a small flame is applied. It can be measured by ASTM D93 method using a Pensky-Martens closed cup tester, where the lowest temperature at which a small flame of a specified size causes the vapor above the sample to ignite and be self sustaining is recorded as the flash point. Flash point is roughly proportional to boiling range and volatility, and relates to the front-end volatility of the fuel. Typical minimum values of flash points for automotive diesel fuels range from 38-52 °C in the U.S. to 56 in some European counties. As far as performance in an engine is concerned, the flash point of a diesel fuel has no significance. It is solely concerned with fuel storage safety.

2.3.10 Pour point. Pour point is the temperature at which the amount of wax precipitated out of the solution is sufficient to gel the fuel. It is the lowest temperature at which the fuel is observed to flow. Definition from ASTM is the temperature at which a measured volume of fluid does not flow for 5 seconds when tilted horizontally. It is usually the lowest temperature at which a fuel can be pumped. The pour point is generally 5-11°C below could point. No wax precipitation problems are encountered above the cloud point. Pour points for most automotive diesel fuels are usually between -15 and -35 °C.

2.3.11 Cloud point. Cloud point is the temperature which wax is first precipitated, thus fuel begins to appear "cloudy". By the ASTM method D2500, it is the temperature at which wax first becomes visible to the observer when the fuel is cooled in a glass vessel at a specified rate. Cloud point depends on boiling range and paraffin content of fuel. Heavy n – alkanes are first components to come out as wax. Unfortunately the better the ignition quality of the fuel components, the less desirable their low temperature propertied are. One of the drawbacks of cloud point measurement is its dependence on the tester's judgment. Usually the cloud point of diesel is in the range between 10 and -20 °C depending upon location and season.

2.3.12 Low Temperature Filterability. Cold filter plugging point (CFPP) is the lowest temperature at which a given volume of diesel fuel passes through a well defined filter in a limited time interval. By European standard method EN116, this is the lowest temperature at which 20 ml of fuel will pass through a 45 um fine wire mesh screen in less than 60 seconds. However, CFPP does not correlate well with vehicle performance in the US where the fuel blends, quality, and weather

This material is reserved for educational use only, not allowed for commercial use.
Forbidden to modify the content, and cite the document when use.

conditions are different. Consequently, the low temperature flow test (LTFT) has been developed in the U.S. as ASTM D4539. it differs from the European CFPP test in that it requires a fixed volume of fuel to be cooled and filtered through a 17 um mesh screen. The LTFT pass temperature is the lowest point at which a fixed volume of fuel (180 mL) of fuel passes through the screen in less than 60 sec.

The cloud point is the highest temperature used for characterizing cold flow, and the pour point is the lowest. The CFPP and LTFT temperatures will be somewhere between the cloud and pour points.

2.3.13 Stability. storage stability can be an issue for diesel fuels. Some insoluble materials can be formed to oxidative degradation of fuel during storage. Excessive amounts of insoluble material can clog the screen and engine filters and cause malfunction. ASTM D4625 method measures the quantity insoluble material formed during storage of diesel fuels under air over periods of 0, 4, 8, 12, 18, and 24 weeks. This method is not suitable for quality control testing because of long storage periods. There are two accelerated oxidation tests adopted by ASTM. In ASTM D2274, a fixed volume of fuel is bubbled with oxygen for a given period of time at a specific rate and temperature. The total amounts of filterable and adhesive insoluble formed during the test are measured as mg per 100 mL. ASTM D5304 uses oxygen overpressure (100 psig) for a fixed volume of fuel (100 mL), without or with stabilizer additives, placed in a borosilicate container that is placed inside a pressure vessel at 90 °C for 16 hours. At the end of the test, the sample is cooled and the amount of insoluble determined. This method achieves acceleration of oxidation without resorting to higher temperature.

2.3.14 Color. Color is another property of diesel fuel. It is viewed as a qualitative indication of diesel fuel quality. By ASTM D1500 test, which employs a standard light source and a comparison of colored glass disks, a scale ranging from 0.5 to 8.0 is used. A variation outside the established range may indicate degradation or contamination of the fuel with other products. Some hydrotreated light oils also have color, but they can be rendered colorless by a low – temperature hydrogenation.

2.3.15 Diesel Index. is also used to represent the quality of diesel fuels. Diesel index can be derived from API gravity and aniline point, but the result can be misleading, especially when applied to blended fuels. To determine aniline point, a specific volume of aniline is mixed with the fuel, as described in the ASTM D611 method. The mixture is cooled at controlled rate. The temperature at which two phases separate is defined as aniline point. Aniline points are high for paraffins and low for

This material is reserved for educational use only, not allowed for commercial use.
Forbidden to modify the content, and cite the document when use.

aromatics, with cycloalkanes and olefins in between; aniline number has been found to correlate with cetane number of diesel fuels. Aniline point could be used to estimate aromatics content of a fuel, but the quantitative determination method.

2.4 Diesel engine [6]

Type diesel engines and gasoline engines are reciprocating engines that operate with four stroke of the piston in the cylinder:

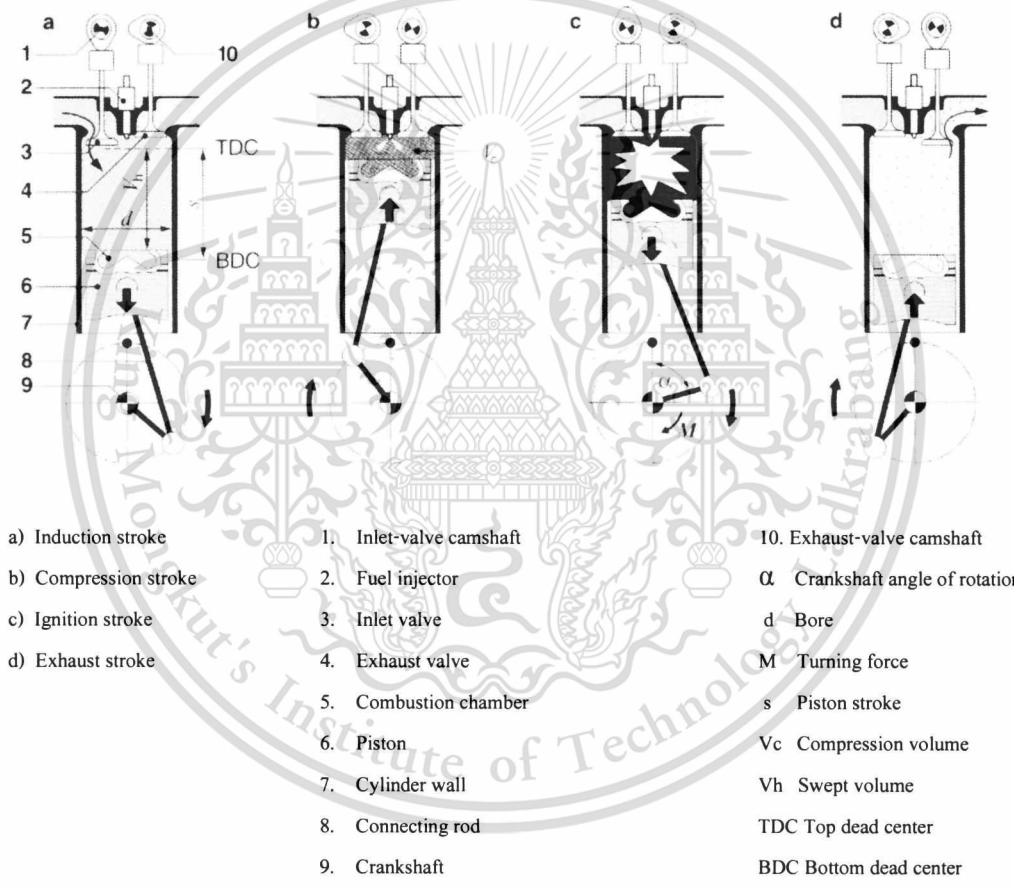

a) Induction stroke
b) Compression stroke
c) Ignition stroke
d) Exhaust stroke

1. Inlet-valve camshaft
2. Fuel injector
3. Inlet valve
4. Exhaust valve
5. Combustion chamber
6. Piston
7. Cylinder wall
8. Connecting rod
9. Crankshaft

10. Exhaust-valve camshaft
α Crankshaft angle of rotation
d Bore
M Turning force
s Piston stroke
Vc Compression volume
Vh Swept volume
TDC Top dead center
BDC Bottom dead center

Figure 2.2 Operating cycle of a four-stroke diesel engine

The gasoline engines draw in a pre- mixed combustible charge of air and fuel, whereas the diesel unit is supplied with air and fuel separately. Power control over gasoline engine is effected by throttling the flow of the air/fuel mixture into the injected per induction stroke into the cylinders.

This material is reserved for educational use only, not allowed for commercial use.
Forbidden to modify the content, and cite the document when use.

สำนักหอสมุดกลาง พระจอมเกล้าลาดกระบัง

Specifically, the diesel engine takes in and compresses air. The air compression increases the pressure and temperature inside the cylinder to values in the rage of 3-5 MPA and 500-600 °C, respectively. Shortly before the end of the of the compression stroke, one or more of fuel are injected into the cylinder. The fuel droplets absorb heat from the compressed air and vaporize, and then ignition of the fuel begins by auto-ignition in one or several zones in the marginal operating conditions such as cold starting, a high compression ratio is necessary, generally between 14 and 25. The delay time between injection (vaporization) and ignition must be kept short. If the ignition delay of the large quantity of fuel can causes diesel knock, which is noisy and can cause damage to the engine.

In a high-speed diesel engine, the delay time between fuel ignition and ignition is only about 0.5-0.6 ms. After ignition, fuel ignition continues for a portion of the power stroke; the addition fuel burns as a diffusion flame (almost instantly) as it mixed with the remaining air and combustion products in the cylinder. Fuel injection is terminated partway through the power stroke. The rate of injection is carefully controlled during fuel injection to provide smooth engine operation. The temperature and pressures of gases inside cylinder of diesel engines during combustion can reach as high as 1600-2000 °C. Power output is controlled, not by adjusting the quantity of air/fuel mixture as in the case of spark ignition engines, but by changing the mass (flow) of diesel fuel introduced into a fixed volume of air.

By the concept, the diesel engine operates at variable fuel-air ratios. It is not possible to attain the stiochiometric ratio because the fuel does not diffuse in an ideal manner into the air. A large part of combustion occurs (after the auto-ignition) in a diffusion-type flame. The equivalence ratio is defined as the actual fuel-air ratio divided by the stoichiometric fuel air ratio. For an average equivalence fuel-air ratio of 1.00, the combustion accompanied by smoke and soot formation. Finally, at full load, the overall equivalence ratio in a diesel engine is between 0.7 and 0.85.

For the gasoline engine, auto-ignition is highly undesirable and is minimized as much as possible by design and by fuel formation, to avoid engine nock. It seems surprising at first glance that auto-ignition should be so highly desirable and preferred in the diesel engine. This is because auto-ignition in diesel engine occurs in very localized zones and concerns only a small fraction of the total amount of fuel introduced. Thus there are one or more ignition centers instead of auto-ignition of one massive homogeneous system which characterizes knocking. Furthermore, the study the structure of the diesel engine provides good residence to damage which might be caused by a rapid release of energy at the moment of auto-ignition.

This material is reserved for educational use only, not allowed for commercial use.
Forbidden to modify the content and cite the document when use.
077727

2.5 The Diesel Combustion Process

The diesel combustion process in diesel engines is a complex sequence of events consisting of 3 phases. The first phase is the ignition delay period during which the fuel must vaporize, mix with air, and undergo pre-flame chemical reaction that produce the chemical species necessary for spontaneous combustion. The second is the premixed burning phase (chemically controlled), which is spontaneous combustion regions of fuel-air mixtures formed (prepared) during the ignition delay period. The rapidly rising temperature and pressure in the cylinder accelerate the combustion in an uncontrolled manner until the backlog is depleted. The third phase is the diffusion burning phase (controlled by mixing rate). After the second phase, the fuel in the spray core is too rich to burn, and the fuel in the periphery of the spray is too burn. As a result, combustion slows down and is controlled by the rate at which the air is entrained and a combustible mixture formed.

The rates of burning during the mixing-controlled phase depend on the air motion and fuel spray momentum. The burning rates start quite high because there is considerable excess air and the fuel spray entrains air rapidly. After the end of ignition, particularly at high loads when there is not as much excess air as with light loads, the burning rates decrease gradually.

2.6 Combustion of Diesel Fuel Oils

Both physical and chemical processes are involved to any combustion process. In the diesel engine, the physical processes include transportation of the fuel and air into the combustion chamber, mixing of fuel and air, and provision of environmental conditions favorable to chemical reaction. The chemical processes involve self-ignition or auto-ignition of the fuel and finally extensive chemical reaction that liberates the potential energy in the fuel.

2.7 Combustion Type of Diesel Engines

Diesel engines are durable and efficient. Most of the diesel engines in commercial vehicles are direct injection (DI) engines and indirect injection (IDI) which each type of engine are describe:

2.7.1 Direct injection (DI) systems [9]

In the large – size engines, where mixing rate requirements are least stringent, quiescent direct – injection systems of the type shown in Fig 2.2 are used. The momentum and energy of the injected fuel jets are sufficient to achieve adequate fuel distribution and rates of mixing with the air. Additional

This material is reserved for educational use only, not allowed for commercial use.
Forbidden to modify the content, and cite the document when use.

organized air motion is not required. The combustion chamber shape is usually a shallow bowl in the crow of the piston, and a center multihole injector is used.

As engine size decreases, increasing amount of air are used to achieve faster fuel – air mixing rates. Air swirl is generated by suitable design of the inlet port, the swirl rate can be increase as the piston approaches TC by forcing the air toward the cylinder axis, into a bowl- in – piston type of combustion chamber

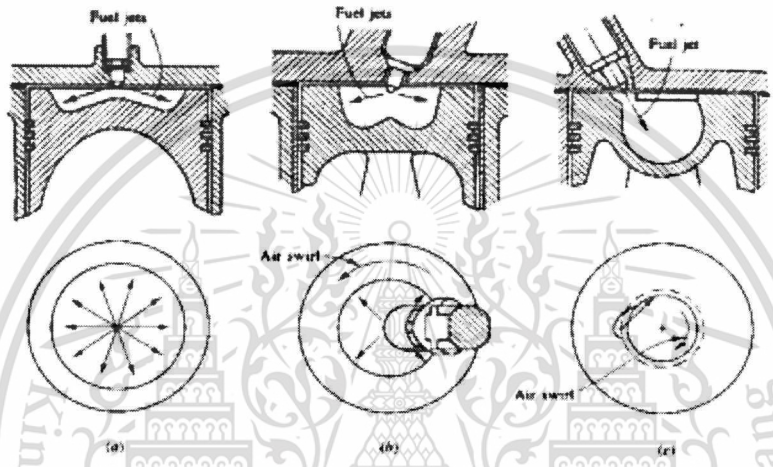

Figure 2.3 Direct injection engine (DI) systems **[9]**

2.7.2 Indirect-Injection System [9]

Inlet generated air swirl, despite amplification in the piston cup, has not provided sufficiently high fuel – air ratio mixing rates for small high – speed diesels such as those used in automobile. Indirect – injection or divided – chamber engine systems have been used instead, where the vigorous charge motion required during fuel injection is generated during the compression stroke. Two broad classes of IDI systems can be defined:

1) Swirl chamber systems

2) Prechamber systems, as illustrated in Fig. 2.4a and b

During compression, air is forced from the main chamber above the piston into the auxiliary chamber, through the nozzle or orifice. Thus, toward the end of compression, a vigorous flow in the auxiliary chamber is set up; in swirl chamber systems the connecting passage and chamber are shape so that this flow within the auxiliary chamber rotates rapidly.

This material is reserved for educational use only, not allowed for commercial use.
Forbidden to modify the content, and cite the document when use.

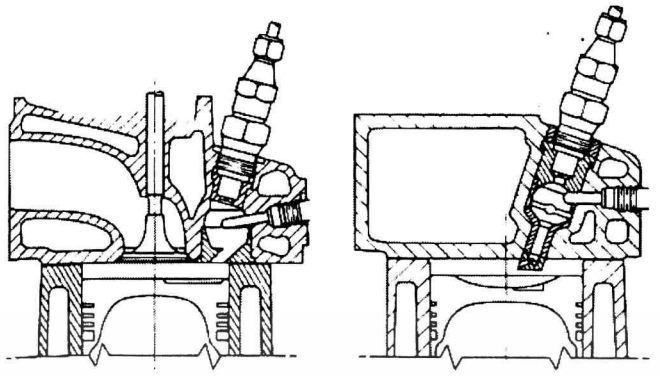

Figure 2.4 Indirect injection engine (IDI) systems **[9]**

2.8 Thermal Efficiency of Diesel Engine

Thermal efficiencies for gasoline engines are the order of 24%, whereas diesel engines can reach as high as 43% thermal efficiency. The high compression ratio and reduction of air pumping (the decrease of energy required to aspirate the air) along with thermodynamic considerations such as average specific heat of gases present in the cylinder generally explain the higher efficiency of the diesel engine.

In general, the IDI engine has a lower thermal efficiency than DI engine. It has been reported that the DI engine has up to 20% fuel efficiency than the IDI engine. The reasons for the lower thermal efficiency of IDI engine (compared to DI engine) include

1) The higher ratio of surface area to volume of combustion chamber (in the cylinder head) and thus a larger loss of heat;
2) Thermodynamic losses due to the late combustion process that occurs as the rich pre – chamber mixture expands into the main chamber;
3) The higher friction losses in the small engine operating at higher compression ratios and with heavy mechanical loading.

However the thermal efficiency if IDI engine is small better than of a SI (gasoline) engine.

In the last few decades, Europe and Japan have seen a significant growth in the number of passenger cars fitted with diesel engines, most of which have indirect injection systems. For example, among all the new cars registered in France, diesel – powered cars increased from less than 8% in 1980 to over 28% in 1990; in the UK diesel cars accounted for well over 12% of all registrations in 1992, and the increase in demand for diesel fuel for cars was about 22% in comparison to 7% for gasoline. In

This material is reserved for educational use only, not allowed for commercial use.
Forbidden to modify the content, and cite the document when use.

Japan, diesel cars accounted for over 20% of all registrations today. For passenger cars in the U.S., the gasoline engine is still supreme, with less than 1% of the market taken by diesel cars in 1998. This is due larger to the fact that low – price gasoline reduces the incentive to adopt the more economical diesel engine for road transportation of passenger (in addition to the environmental regulations on exhaust emissions) in the U.S.

2.9 Fuel system of diesel engine [6]

The fuel injection system comprises a fuel injection pump, injection nozzles, a fuel filter, and a fuel tank. The fuel that is drawn from the fuel tank by the feed pump is filtered through the fuel filter, and is delivered to the injection pump.

The fuel that is delivered to the injection pump is pressurized into a highly compressed state, and is delivered via the injection steel pipe to the nozzle. The fuel is then injected in an atomized state into the combustion chamber, where combustion takes place.

A portion of the fuel that is delivered to the nozzle lubricates the sliding portion of the nozzle and returns to the fuel tank via the overflow pipe. To prevent the fuel delivered to the injection pump from becoming excessively pressurized, an overflow valve is provided in the fuel filter or in the injection pump itself. If the feed pressure from the feed pump exceeds a prescribed value, the overflow valve opens to allow excess fuel to return to the fuel tank via the overflow pipe.

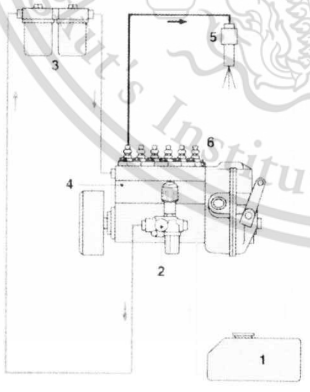

1. Fuel tank
2. Supply pump
3. Fuel filter
4. In-line fuel-injection pump
5. Nozzle-and-holder assembly

----- Supply line

- - - Return line

Figure 2.5 Fuel system of diesel engine [6]

2.9.1 Injection pump

An Injection Pump is the device that pumps fuel into the cylinders of a diesel engine or less typically, a gasoline engine. Traditionally, the pump is driven indirectly from the crankshaft by gears, chains or a toothed belt (often the timing belt) that also drives the camshaft on overhead-cam engines

This material is reserved for educational use only, not allowed for commercial use.
Forbidden to modify the content, and cite the document when use.

(OHC). It rotates at half crankshaft speed in a conventional four-stroke engine. Its timing is such that the fuel is injected only very slightly before top dead-centre of that cylinder's compression stroke. It is also common for the pump belt on gasoline engines to be driven directly from the camshaft. In some system injection pressures can be as high as 200Mpa.

Because of the need for positive injection into a very high-pressure environment, the pump develops great pressure typically 15,000 psi (100 MPa) or more on newer systems. This is a good reason to take great care when working on diesel systems; escaping fuel at this sort of pressure can easily penetrate skin and clothes, and be injected into body tissues with serious consequences serious enough to warrant amputation.

Earlier diesel pumps used an in-line layout with a series of cam-operated injection cylinders in a line, rather like a miniature inline engine. The pistons have a constant stroke volume, and injection volume (ie, throttling) is controlled by rotating the cylinders against a cut-off port that aligns with a helical slot in the cylinder. When all the cylinders are rotated at once, they simultaneously vary their injection volume to produce more or less power from the engine. Inline pumps still find favour on large multi-cylinder engines such as those on trucks, construction plant, static engines and agricultural vehicles.

For use on cars and light trucks, the rotary pump or distributor pump was developed. It uses a single injection cylinder driven from an axial cam plate, which injects into the individual fuel lines via a rotary distribution valve. Later incarnations such as the Bosch VE pump vary the injection timing with crank speed to allow greater power at high crank speeds, and smoother, more economical running at slower revs. Some VE variants have a pressure-based system that allows the injection volume to increase over normal to allow a turbocharger or supercharger equipped engine to develop more power under boost conditions.

All injection pumps incorporate a governor to cut fuel supply if the crank speed endangers the engine - the heavy moving parts of diesel engines do not tolerate over speeding well, and catastrophic damage can occur if they are over-revved.

Mechanical pumps are gradually being phased out in order to comply with international emissions directives, and to increase performance and economy. Alternatives include common rail diesel systems and electronic unit direct injection systems. These allow for higher pressures to be developed, and for much finer control of injection volumes compared to mechanical systems.

This material is reserved for educational use only, not allowed for commercial use.
Forbidden to modify the content, and cite the document when use.

2.9.2 In-line fuel-injection pump [6]

In-line fuel-injection pumps have one pump element for each engine cylinder. These are arranged in a row. The camshaft of the in-line fuel-injection pump is driven by the gear wheels or chains of the combustion engine. The in-line fuel-injection pump runs at half the speed of the engine and always synchronously to the piston movements of the diesel engine. The fuel reaches the nozzle-holder assemblies with the injection nozzles via high-pressure lines.

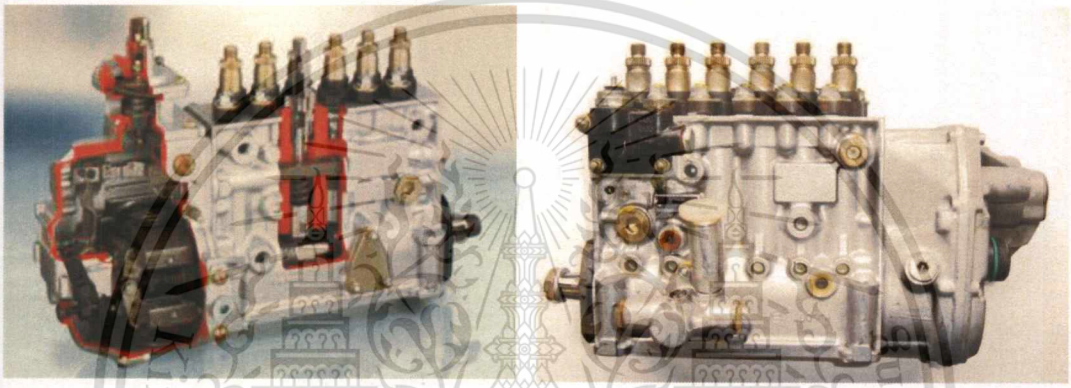

Figure 2.6 in-line fuel-injection pumps

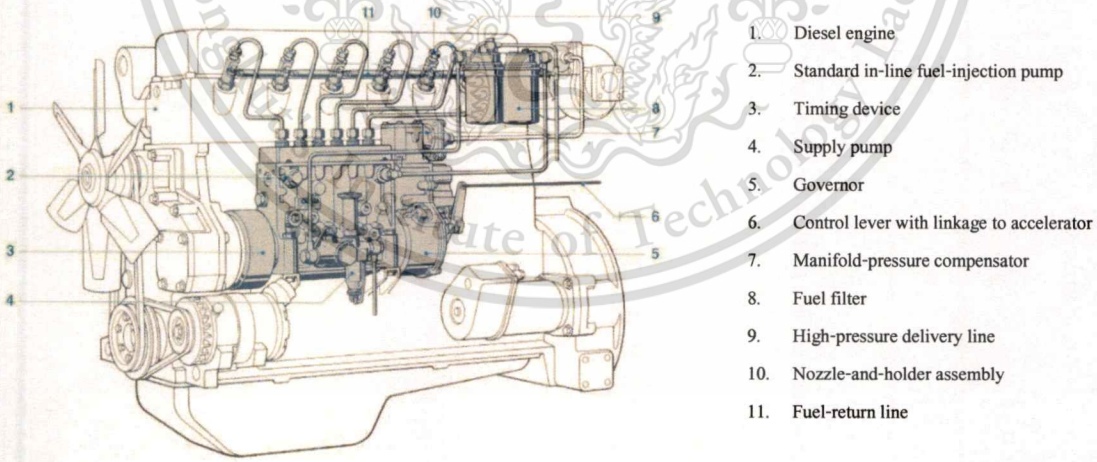

Figure 2.7 in-line fuel-injection pumps on 6-cylinder diesel engine

This material is reserved for educational use only, not allowed for commercial use.
Forbidden to modify the content, and cite the document when use.

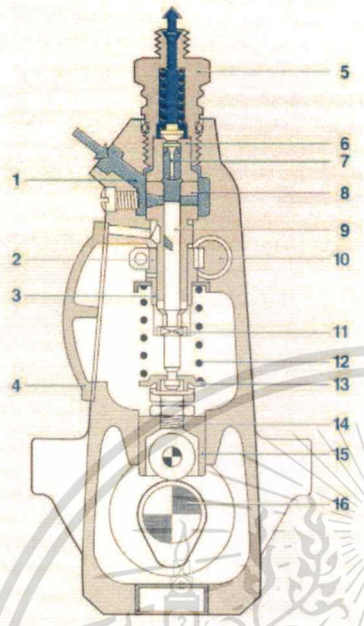

1. Fuel gallery
2. Control-sleeve gear
3. Control sleeve
4. Cover plate
5. Pressure-valve holder
6. Pressure-valve body
7. Delivery-valve cone
8. Pump barrel
9. Pump plunger
10. Control rack
11. Plunger control arm
12. Plunger spring
13. Spring seat
14. Adjusting screw
15. Roller tappet
16. Camshaft

Figure 2.8 in-line fuel-injection pump (sectional view)

The pump housing is made of cast aluminum and provides support and protection for inner part.

The camshaft is supported by two taper roller bearings and driven by the engine, to work the feed pump and plungers. The pump element, which is the most important part, consists of a plunger and cylinder, one element for each engine cylinder.

The control rack is connected to the linkage of the governor and meshed with each pinion which rotates the plunger to control the fuel delivery quantity and in the case of a special plunger, the injection timing also. The delivery valve prevents reverse flow of fuel in the high pressure pipe and dribbles from nozzle after injection.

2.10 Electrochemical mechanisms

2.10.1 The dry-cell analogy and Faraday's law

Corrosion processes are most often electro chemical. In aqueous media, the action a similar to that taking place in a flashlight cell made up of a center carbon electrode and a zinc cup electrode separated by an electrolyte consisting essentially of NH_4Cl solution (Fig. 2.9). An incandescent light bulb connected to both electrodes glows continuously, the electrical energy being supplied by chemical reactions at both electrodes. At the carbon electrode (positive pole), chemical reduction occurs, and at

This material is reserved for educational use only, not allowed for commercial use.
Forbidden to modify the content, and cite the document when use.

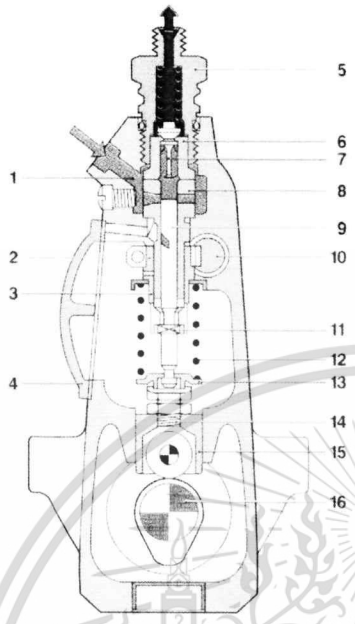

1. Fuel gallery
2. Control-sleeve gear
3. Control sleeve
4. Cover plate
5. Pressure-valve holder
6. Pressure-valve body
7. Delivery-valve cone
8. Pump barrel
9. Pump plunger
10. Control rack
11. Plunger control arm
12. Plunger spring
13. Spring seat
14. Adjusting screw
15. Roller tappet
16. Camshaft

Figure 2.8 in-line fuel-injection pump (sectional view)

The pump housing is made of cast aluminum and provides support and protection for inner part.

The camshaft is supported by two taper roller bearings and driven by the engine, to work the feed pump and plungers. The pump element, which is the most important part, consists of a plunger and cylinder, one element for each engine cylinder.

The control rack is connected to the linkage of the governor and meshed with each pinion which rotates the plunger to control the fuel delivery quantity and in the case of a special plunger, the injection timing also. The delivery valve prevents reverse flow of fuel in the high pressure pipe and dribbles from nozzle after injection.

2.10 Electrochemical mechanisms

2.10.1 The dry-cell analogy and Faraday's law

Corrosion processes are most often electro chemical. In aqueous media, the action a similar to that taking place in a flashlight cell made up of a center carbon electrode and a zinc cup electrode separated by an electrolyte consisting essentially of NH_4Cl solution (Fig. 2.9). An incandescent light bulb connected to both electrodes glows continuously, the electrical energy being supplied by chemical reactions at both electrodes. At the carbon electrode (positive pole), chemical reduction occurs, and at

This material is reserved for educational use only, not allowed for commercial use.
Forbidden to modify the content, and cite the document when use.

the zinc electrode (negative pole) oxidation occurs, metallic zinc being converted into hydrated zinc ions, $Zn^{2+} \cdot nH_2O$.T The greater the flow of electricity through the cell, the greater is the amount of zinc that corrodes. The relationship is quantitative, as Michael Faraday showed in the early nineteenth century (Faraday's law):

$$\text{Weight of metal reacting} = kIt \qquad (1)$$

Where I is the current in amperes (A), t is in seconds (s), and k is a constant called the electrochemical equivalent. The value of k in the case of zinc is 3.39×10^{-4} g/C (gram per coulomb), the coulomb being defined as the amount of electricity represented by 1 A flowing for 1 s. On short-circuiting the cell with a low-resistance metallic connector, the zinc cup perforates by corrosion within a matter of hours; but when the cell is left disconnected (open circuit), the zinc may remain intact for years. The slow consumption of zinc occurring on open circuit is accounted for largely by activity of minute impurities, like iron, embedded in the surface of zinc; these impurities assume the same role as carbon and allow the flow of electricity accompanied by corrosion of zinc. Current of this kind is called local-action current, and the corresponding cells are called local-action cells. Local-action current, of course, produces no useful energy, but acts only to heat up the surroundings.

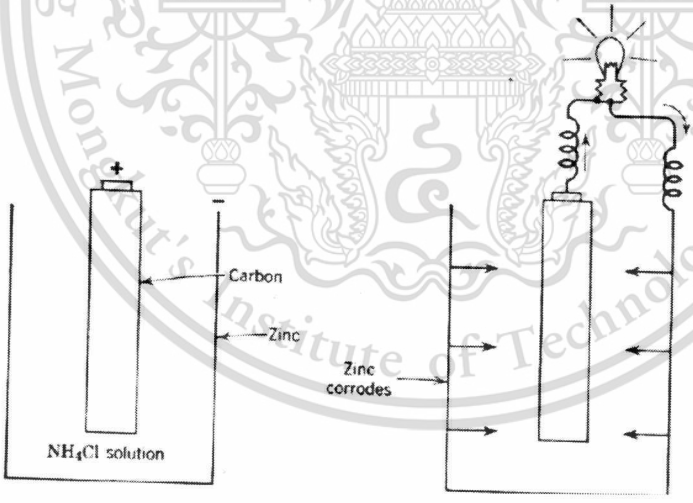

Figure 2.9 Dry cell.

Any metal surface, similar to the situation for zinc, is a composite of electrodes electrically short-circuited through the body of the metal itself (Fig.2.10). So long as the metal remains dry, local-action current and corrosion are not observed. But on exposure of the metal to water or aqueous solutions, local-action cells are able to function and are accompanied by chemical conversion of the

This material is reserved for educational use only, not allowed for commercial use.
Forbidden to modify the content, and cite the document when use.

metal to corrosion products. Local-action currents, in other words, may account for the corrosion of metals exposed to water, salt solutions, acids, or alkalies.

Whenever impurities in a metal constitute the electrodes of local-action cells, their removal, as might be expected, appreciably improves corrosion resistance. Accordingly, purdingly, purified aluminum and magnesium are much more resistant to corrosion in seawater or in acids than are the commercial varieties of these metals, and high-purity zinc resists dilute hydrochloric acid much better than does commercial zinc. However, it is not correct to assume, as was done many years ago when the electrochemical theory was first proposed, that pure metals do not corrode at all. As we see later, local-action cells are also set up when there are variations in the environment or in temperature. With iron or steel in aerated water, for example, the negative electrodes are commonly portions of the from surface itself covered perhaps by porous rust (iron oxides), and positive electrodes are areas exposed to oxygen, the positive and negative electrode areas interchanging and shifting from place to place as the corrosion reaction proceeds. Accordingly, high-purity iron in air-saturated water corrodes at essentially the same rate as impure or commercial iron. A difference in rates is observed in acids, however, because impurities now enter predominantly as electrodes of local-action cells.

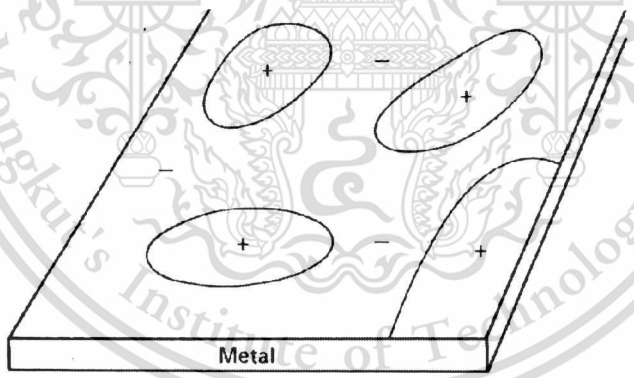

Figure 2.10 Metal surface enlarged, showing schematic arrangement of local-action cells.

2.10.2 Definition of anode and cathode

A combination of two electrical conductors (electrodes) immersed in an electrolyte is called a galvanic cell in honor of Luigi Galvani, a physician in Bologna, Italy, who published him studies of electrochemical action in 1971. A galvanic cell converts chemical energy into electrical energy. On short-circuiting such a cell (attaching a low-resistance wire to each electrode), positive current flows through the metallic path from positive electrode to negative electrode. This direction of current flow

This material is reserved for educational use only, not allowed for commercial use.
Forbidden to modify the content, and cite the document when use.

follows an arbitrary convention, established before anything was known about the nature of electricity, and is employed today despite contemporary knowledge that only negative carriers or electrons move in a metal. Electrons, of course, go from negative to carriers or electrons move in a metal. Electrons, of course, go from negative to positive pole, opposite to the imaginary flow of positive carriers. Whenever current is said to flow, however, without designating the sign of the carrier, positive current is always implied.

Within the electrolyte, current is carried by both negative and positive carriers know as ions (electrically charged atoms or groups of atoms). The current carried by each ion depends on its mobility and electric charge. The total of positive and negative current in the electrolyte of a cell is always exactly equivalent to the current carried in the metallic path by electrons alone. Ohm's law, that is, I = EIR where I is the current in amperes, E the potential difference in volts, and R the resistance in ohms, applies precisely, under conditions with which we are presently concerned, to current flow in electrolytes as well as in metals.

The electrode at which chemical reduction occurs (or + current enters the electrode from the electrolyte) is called the cathode. Examples of cathodic reactions are:

$$H^{+} \rightarrow \frac{1}{2}H^{2} - e^{-}$$

$$Cu^{2+} \rightarrow Cu - 2e^{-}$$

$$Fe^{3+} \rightarrow Fe^{2+} - e^{-}$$

All of which represent reduction in the chemical sense.

The electrode at which chemical oxidation occurs for + electricity leaves the electrode and enters the electrolyte) is called the anode. Examples of anodic reactions are:

$$Zn \rightarrow Zn^{2+} + 2e^{-}$$

$$Al \rightarrow Al^{3+} + 3e^{-}$$

$$Fe^{2+} \rightarrow Fe^{3+} + e^{-}$$

These represent oxidation in the chemical sense. Corrosion of metals usually occurs at the anode.

In galvanic cells, the cathode is the positive pole and the anode is the negative pole. However, when current is impressed on a cell form a generator or an external battery, for example as in electroplating, reduction occurs at the electrode connected to the negative pole of the external current source, and this electrode, consequently, is the cathode. Similarly, the electrode connected to the positive pole of the generator is the anode. It is perhaps best, therefore, not to remember anode and

This material is reserved for educational use only, not allowed for commercial use.
Forbidden to modify the content, and cite the document when use.

cathode as negative and positive electrodes, or vice versa, but instead to remember the cathode as the electrode at which current enters from the electrolyte, and the anode as the electrode at which current leaves to return to the electrolyte. This situation is true whether current is impressed on or drawn from the cell.

Captions are ions that migrate toward the cathode when electricity flows through the cell (e.g., H+, Fe2+) and are always positively charged whether current is drawn from or supplied to the cell. Similarly, anions are always negatively charged (e.g., Cl^-, OH^-, So_4^{2-}).

2.10.3 Types of cells

There are three main types of cells that take part in corrosion reactions.

1. Dissimilar Electrode Cells. These are illustrated by the dry cell, discussed earlier. A metal containing electrically conducting impurities on the surface as a separate phase, a copper pipe connected to an iron pipe, and a bronze propeller in contact with the steel hull of a ship are examples of this type of corrosion cell. These cells also include cold-worked metal in contact with the same metal annealed, grain-boundary metal in contact with grains, and a single metal crystal of definite orientation in contact with another crystal of differing orientation

2. Concentration Cells. These are cells having two identical electrodes each in contact with solution of differing composition. There are two kinds of concentration cells. The first is called a salt concentration cell. For example, if one copper electrode is exposed to a concentrated copper sulfate solution and another to a dilute copper sulfate solution (Fig. 2.11), on short-circuiting such a cell, copper dissolves from the electrode in contact with the dilute solution (anode) and plates out on the other electrode (cathode). Both reactions tend to bring the solutions to the same concentration.

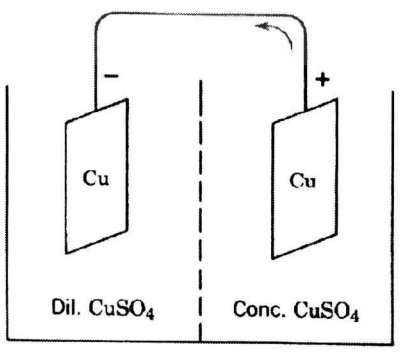

Figure 2.11 Salt concentration cell

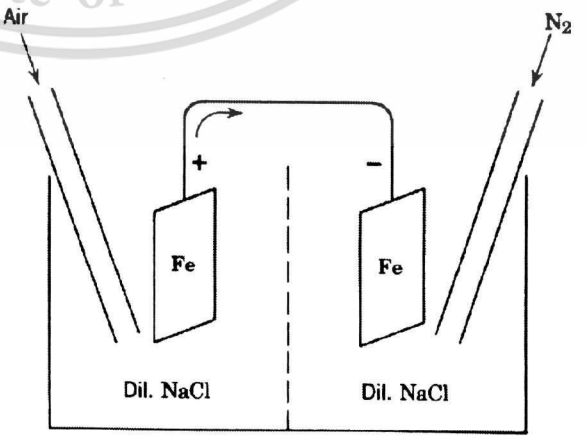

Figure 2.12 Differential aeration

This material is reserved for educational use only, not allowed for commercial use.
Forbidden to modify the content, and cite the document when use.

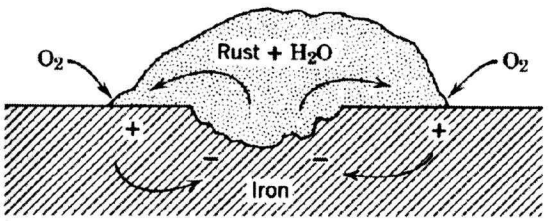

Figure 2.13 Differential aeration cell formed by rust on iron.

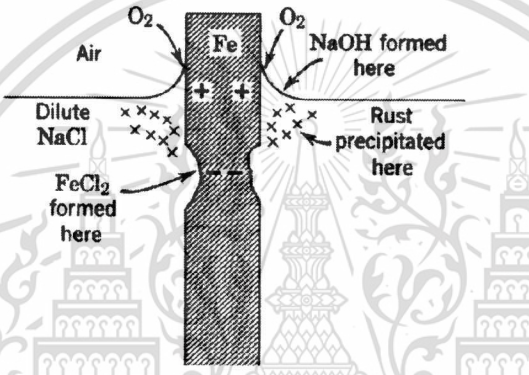

Figure 2.14 Differential aeration cell illustrated by water-line corrosion.

The second kind of concentration cell, which in practice is the more important, is called a differential aeration cell. This may include two iron electrodes in dilute sodium chloride solution, the electrolyte around one electrode being thoroughly aerated (cathode), and the other desecrated (anode), brought about, for example, by bubbling through nitrogen. The (anode), brought about, for example, by bubbling through nitrogen. The difference in oxygen concentration produces a potential difference and causes current to flow (Fig. 2.12). This type of cell accounts for pronounced damage at crevices (crevice corrosion) such as is formed at the interface of two coupled pipes or at threaded connections, because the oxygen concentration is lower within the crevice or at the threads than elsewhere. It also accounts for pitting damage under rust (Fig.2.13) or at the water line (water-air interface) (Fig. 2.14). The amount of oxygen reaching the metal that is covered by rust or other insoluble reaction products in less than the amount that contacts other portions where the permeable coating is thinner or absent.

Differential aeration cells also usually initiate pits (crevice corrosion) in the stainless steels, aluminum, nickel, and other so-called passive metals when they are exposed to aqueous environments, such as seawater.

This material is reserved for educational use only, not allowed for commercial use.
Forbidden to modify the content, and cite the document when use.

3. Differential Temperature Cells. Components of these cells are electrodes of the same metal, each of which is at a different temperature, immersed in an electrolyte of the same initial composition. Less is known about the practical importance and fundamental theory of differential temperature cells than for the cells previously described. They are found in heat exchangers, boilers, immersion heaters, and similar equipment.

In copper sulfate solution the copper electrode at the higher temperature is cathode and the copper electrode at the lower temperature is anode. On short-circuiting the cell, copper deposits on the hot electrode and dissolves from the cold electrode. Lead acts similarly, but for silver the polarity is reversed.

For iron immersed in dilute aerated sodium chloride solutions, the hot electrode is anodic to colder metal of the same composition; but after a matter of hours, depending on aeration, stirring rate, and whether the two metals are short-circuited, the polarity may reverse.

In practice, cells responsible for corrosion may be a combination of these three types.

2.10.4 Types of corrosion damage

Corrosion is often thought of only in terms of rusting of rusting and tarnishing. However, corrosion damage also occurs in other ways, resulting, for example, in failure by cracking or in loss of strength or ductility. In general, most types, with some exceptions, occur by an electrochemical mechanism, but corrosion products are not necessarily observable and metal weight loss need not be appreciable. The five main types of corrosion classified with respect to outward appearance or altered physical properties are:

1. Uniform Attack. This includes the commonly recognized rusting of iron or tarnishing of silver. "Fogging" of nickel and high-temperature oxidation of metals are also examples of uniform attack.

Rate of uniform attack is reported in various units, an accepted terminology being millimeters penetration per year (mm/y) and grams per square meter per day (gmd). The units inches penetration per year (ipy), mils (1 mil = 0.001 in.) per year, and milligrams per square decimeter per day (mdd) are also frequently cited. These units refer to metal penetration or to weight loss of metal, excluding any adherent or nonadherent corrosion products on the surface, Steel, for example, corrodes at a relatively uniform rate in sea-water equal to about 0.13 mm/y, 2.5 gmd, 25 mdd, or 0.005 ipy. These represent time-averaged values. Generally, for uniform attack, the initial corrosion rate is greater than subsequent

This material is reserved for educational use only, not allowed for commercial use.
Forbidden to modify the content, and cite the document when use.

rates. Hence duration of exposure should always be given when corrosion rates are reported, for it is often not safe to extrapolate a reported rate to times of exposure far exceeding the test period.

Conversion of mm/y to gmd or vice versa requires knowledge of the metal density. A given weight loss per unit area for a light metal (e.g., aluminum) represents a greater actual loss of metal thickness than the same weight loss for a heavy metal (e.g., lead).

For handling chemical media whenever attack is uniform, metals are classified into three groups according to their corrosion rates and intended application. These classifications are:

1. <0.15 mm/y (<0.005 ipy) Metals in this category have good corrosion resistance to the extent that they are suitable for critical parts, for example, valve seats, pump shafts and impellors, springs.

2. 0.15 to 1.5 mm/y (0.005 to 0.05 ipy) Metals in this group are satisfactory if a higher rate of corrosion can be tolerated, for example, for tanks, piping, valve bodies, bolt heads.

3. >1.5 mm/y (>0.05 ipy) Usually not satisfactory.

2. Pitting. This is a localized type of attack, the rate of corrosion being reater at some areas than at others. If appreciable attack is confined to a relatively small fixed area of metal, acting as anode, the resultant pits are described as deep. If the area of attack it relatively larger and not so deep, the pits are called shallow. Depth of pitting is sometimes expressed by the term pitting factor. This is the ratio of deepest metal penetration to average metal metal penetration as determined by weight loss of the specimen. A pitting factor of unity represents uniform attack (Fig. 2.15).

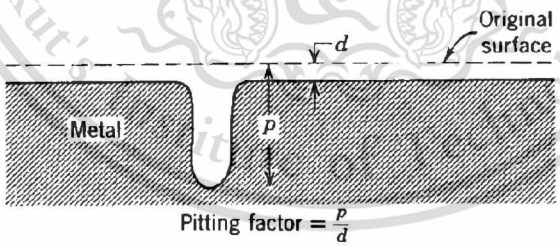

Figure 2.15 Sketch of deepest pit with relation to average metal penetration and the pitting factor

Iron buried in the soil corrodes with formation of shallow pits, whereas stainless steels immersed in seawater characteristically corrode with formation of deep pits. Many metals, when subjected to high-velocity liquids, undergo a pitting type of corrosion called impingement attack, or sometimes corrosion-erosion. Copper and brass condenser tubes, for example, are subject to this type of attack.

This material is reserved for educational use only, not allowed for commercial use.
Forbidden to modify the content, and cite the document when use.

Fretting corrosion, which results from slight relative motion (as in vibration) of two substances in contact, one or both being metals, usually leads to a series of pits at the metal interface. Metal-oxide debris usually fills the pits so that only after the corrosion products are removed do the pits become visible.

Capitation-erosion resulting from formation and collapse of vapor bubbles at a dynamic metal-liquid interface (as in rotors of pumps or on trailing faces of propellers) causes a sequence of pits, sometimes appearing as a honey-comb of small relatively deep.

3. Dezincification and Parting. Dezincification is a type of attack occurring with zinc alloys (e.g., yellow brass) in which zinc corrode preferentially, leaving a porous residue of copper and corrosion products. The alloy so corroded often retains its original shape, and may appear undamaged except for surface tarnish, but its tensile strength and especially ductility are seriously reduced. Dezincified brass pipe may retain sufficient strength to resist internal water pressures until an attempt is made to un-couple the pipe, or a water hammer occurs, causing the pipe to split open.

Parting is similar to dezincification in that one or more reactive components of the alloy corrode preferentially, leaving a porous residue that may retain the original shape of the alloy. Parting is usually restricted to such noble metal alloys as gold-copper or gold-silver and is made use of practically in refining of gold. For example, an alloy of Au-Ag containing more than 65% gold resists concentrated nitric acid as well as does gold itself. However, on addition of silver to form an alloy of approximately 25% Au-75% Ag, reaction with concentrated HNO_3 forms silver nitrate and a porous residue or powder of pure gold.

Copper-base alloys that contain aluminum are subject to a form of corrosion resembling dezincification, with aluminum corroding preferentially.

4. Intergranular Corrosion. This is a localized typed of attack at the grain boundaries of a metal, resulting in loss of strength and ductility. Grain-areas of grains acting as cathode. The attack is often rapid, penetrating deeply into the metal, and sometimes causing catastrophic failures. Im-properly heat-treated 18-8 stainless steels or Duralumin-type alloys (4% Cu-Al) are among the alloys subject to intergranular corrosion. An example of nonelectrochemical grain-boundary attack is provided by nickel heated in a sulfer-bearing atmosphere which fails because sulfur penetrates along the grain boundaries.

5. Cracking. If a metal cracks when subjected to repeated or alternate tensile stresses in a corrosive environment, it is said to fail by corrosion fatigue. In absence of a corrosive environment, the metal stressed similarly but at values below a critical stress, called the fatigue limit or endurance limit, will not fail by fatigue even after a very large or infinite number of cycles. A true endurance limit does

This material is reserved for educational use only, not allowed for commercial use.
Forbidden to modify the content, and cite the document when use.

not commonly exist in a corrosive environment the metal fails after a prescribed number of stress cycles no matter how low the stress. The types of environment causing corrosion fatigue are many and are not specific.

If a metal, subject to a constant tensile stress and exposed simultaneously to a specific corrosive environment, cracks immediately or after a given time, the failure is called stress-corrosion cracking. The stress may be residual in the metal, as from cold working or heat treatment, or it may be externally applied. The observed cracks are intergranular or transgranular, depending on the metal and the damaging environment. Failures of this kind differ basically from intergranular corrosion defined earlier, which proceeds without regard to whether the metal is stressed.

Almost all structural metals (e.g., carbon- and low-alloy steels, brass, stainless steels, Duralumin, magnesium alloys, titanium alloys, nickel alloys, and many others) are subject to stress-corrosion cracking in some environments. Fortunately, either the damaging environments are often restricted to a few chemical species, or the necessary stresses are sufficiently high to limit observed failures of this kind in practice. As knowledge accumulates regarding the specific media that cause cracking and regarding the limiting stresses necessary to avoid failure within a given time period, it will be possible to design metal structures without incidence of stress corrosion cracking. Unfortunately, not all highly stressed metal structures are designed today with adequate assurance that stress-corrosion cracking will not occur.

2.10.5 Iron and steel

The electrochemical theory of corrosion as described earlier relates corrosion to a network of short-circuited galvanic cells on the metal surface. Metal ions go into solution at anodic areas in an amount chemically equivalent to the reaction at cathodic areas. At anodic areas the following reaction takes place:

$$Fe \longrightarrow Fe^{2+} + 2e^{-} \qquad (1)$$

This reaction is rapid in most media, as shown by lack of pronounced polarization when iron is made anode employing an external current. When iron corrodes, the rate is usually controlled by the cathodic reaction, which in general is much slower (cathodic control). In desecrated solutions, the cathodic reaction is

$$H^{+} \longrightarrow \frac{1}{2}H_2 - e^{-} \qquad (2)$$

This material is reserved for educational use only, not allowed for commercial use.
Forbidden to modify the content, and cite the document when use.

This reaction proceeds rapidly in acids, but only slowly in alkaline or neutral aqueous media. The corrosion rate of iron in dearated water at room temperature, for example, is less than 0.005 mm/y (0.1 gmd). The rate of hydrogen evolution at a specific pH depends on presence or absence of low hydrogen overvoltage impurities in the metal. For pure iron, the metal surface itself provides sites for H_2 evolution; hence, high-purity iron continues to corrode in acids but at a measurably lower rate than does commercial iron.

The cathodic reaction can be accelerated by dissolved oxygen in accord with the following reaction, a process called depolarization:

$$2H^+ + \frac{1}{2}O_2 \longrightarrow H_2O - 2e^- \qquad (3)$$

Dissolved oxygen reacts with hydrogen atoms adsorbed at random on the iron surface, independent of the presence or absence of impurities in the metal. The oxidation reaction proceeds as rapidly as oxygen reaches the metal surface.

Adding (1) and (3), making use of the reaction $H_2O \longrightarrow H^+ + OH^-$,

$$Fe + H_2O + \frac{1}{2}O_2 \longrightarrow Fe(OH)_2 \qquad (4)$$

Hydrous ferrous oxide ($FeO + n\ H_2O$) or ferrous hydroxide [$Fe(OH)_2$] composes the diffusion-barrier layer next to the iron surface through which O_2 must diffuse. The pH of saturated $Fe(OH)_2$ is about 9.5, so that the surface of iron corroding in aerated pure water is always alkaline. The color of $Fe(OH)_2$, although white when the substance is pure, is normally green to greenish black because of incipient oxidation by air. At the outer surface of the oxide film, access to dissolved oxygen converts ferrous oxide to hydrous ferric oxide or ferric hydroxide, in accord with

$$Fe(OH)_2 + \frac{1}{2}H_2O + \frac{1}{2}O_2 \longrightarrow Fe(OH)_2 \qquad (5)$$

Hydrous ferric oxide is orange to red brown in color and comprises most of ordinary rust. It exists as nonmagnetic αFe_2O_3 (hematite) or as magnetic γ Fe_2O_3, the α form having the greater negative free energy of formation (greater stability). Saturated $Fe(OH)_3$ is nearly neutral in pH. A magnetic hydrous ferrous ferrite, $Fe_3O_4 \cdot nH_2O$, often forms a black intermediate layer between hydrous Fe_2O_3 and FeO. Hence rust films normally consist of three layers of iron oxides in different states of oxidation.

This material is reserved for educational use only, not allowed for commercial use.
Forbidden to modify the content, and cite the document when use.

2.10.6 Aqueous environments

2.10.6.1 Effect of Dissolved Oxygen

Air-Saturated Water. At ordinary temperatures in neutral or near-neutral water, dissolved oxygen is necessary for appreciable corrosion of iron. In air-saturated water, the initial corrosion rate may reach a value of about 10 gmd. This rate diminishes over a period of days as the iron oxide (rust) rilm is formed and acts as a barrier to oxygen diffusion. The steady-state corrosion rate may be 1.0-2.5 gmd, tending to be higher the greater the relative motion of water with respect to iron. Since the diffusion rate at steady state is proportional to oxygen concentration, it follows from (3) that the corrosion rate of iron is also proportional to oxygen concentration. Typical data are shown in Fig. 2.16. In the absence of dissolved oxygen, the corrosion rate at room temperature is negligible both for pure iron and for steel.

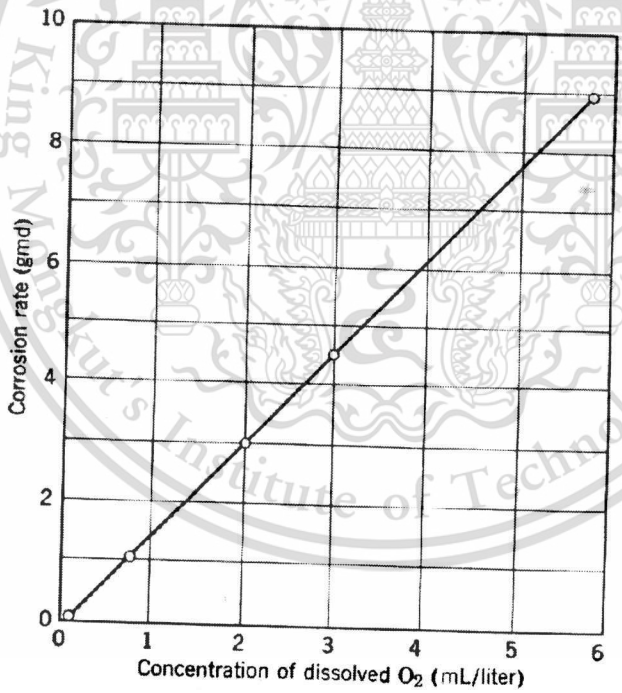

Figure 2.16 Effect of oxygen concentration on corrosion of mild steel in slowly moving water containing 165 ppm $CaCl_2$, 48-h test, 25°C

2.10.6.2 Higher Partial Pressures of Oxygen. Although increase in oxygen concentration at first accelerates corrosion of iron, it is found that beyond a critical concentration the corrosion rate

This material is reserved for educational use only, not allowed for commercial use.
Forbidden to modify the content, and cite the document when use.

drops again to a low value. Deviations from the linear relation between corrosion rate and oxygen concentration occur sooner in distilled water than when Cl^- ions are present as in Fig. 1. In distilled water, the critical concentration of oxygen above which corrosion decreases again, is about 12 ml. O_2/liter (Fig. 2.17). This value increases with dissolved salts and with temperature, and decreases with increase in velocity and pH. At pH of about 10, the critical oxygen concentration reaches the value for air-saturated water (6ml. O_2/liter) and is still less for more alkaline solutions.

The decrease of corrosion rate is caused by passivation of iron by oxygen as shown by potentials of iron in air-saturated H_2O (28 mL O_2/liter). Apparently, at higher partial pressures, more oxygen reaches the metal surface than can be reduced by the corrosion reaction—the excess therefore is available to form the passive film. On the basis of the oxide-film theory of passivity, the excess oxygen supposedly oxidizes the ferrous oxide film to one having greater protective value as a diffusion barrier. According to the adsorption theory, the excess oxygen is available to chemisorbs on the iron surface forming an adsorbed passive film.

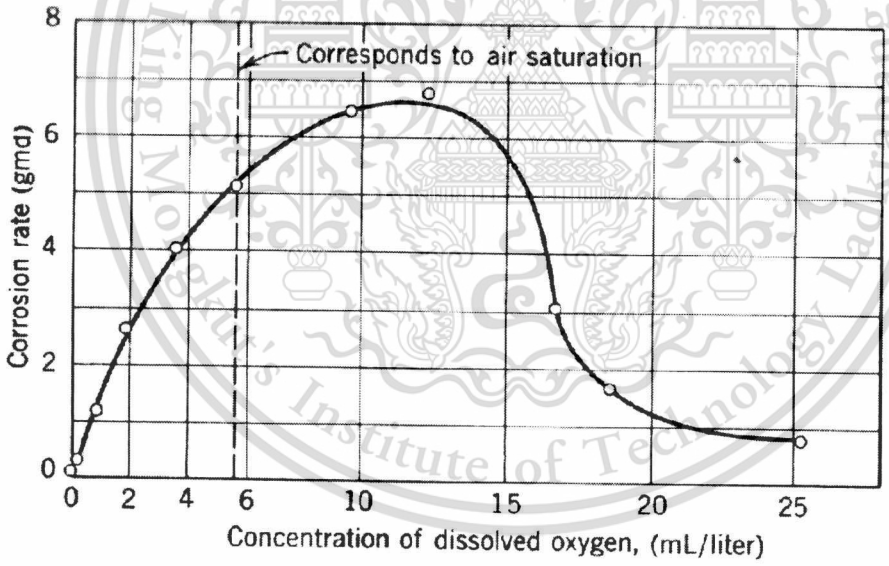

Figure 2.17 Effect of oxygen concentration on corrosion of mild steel in slowly moving distilled water. 48-h test, 25°C

Because passivity accompanies higher oxygen pressures, passive-active cells are established in the event passivity breaks down locally (e.g., at crevices). Such breakdown is accompanied by severe pitting, particularity at higher temperatures, in the presence of halide ions, or at a critical pressure of

This material is reserved for educational use only, not allowed for commercial use.
Forbidden to modify the content, and cite the document when use.

oxygen where passivity is on the verge of either forming or breaking down. This behavior limits the practical use of high partial oxygen pressures as a means of reducing corrosion of steel. In appreciable concentrations of chlorides (e.g., seawater) passivity of iron is not established at all, and in such media increased oxygen pressure results only in an increased corrosion rate.

2.10.6.3 Action of Anaerobic Bacteria. Although in dilacerated water does not corrode appreciably, the corrosion rate in some natural deacrated environments is found to be abnormally high. These high rates have been traced to the presence of sulfate-reducing bacteria, for example, Desulfovibrio desulfuricans. Their relation to an observed accelerated corrosion rate in soils low in dissolved oxygen was first observed in Holland by von Wolzogen Kühr. The bacteria are curved, measuring about 1×4 μm, and are found widespread in many waters and soils. They thrive only under anaerobic conditions in the pH range of about 5.5-8.5. Certain varieties multiply in fresh waters and in soils containing sulfates, others in brackish waters and seawater, and still others are stated to exist in deep soils at temperatures as high as 60-80°C (140-175°F).

Sulfate-reducing bacteria easily reduce inorganic sulfates to sulfides in presence of hydrogen or organic matter, and a aided in this process by the presence of an iron surface. The aid which iron provides in this reduction is probably to supply hydrogen which is normally adsorbed on the metal surface, and which the bacteria make use of in the reduction of SO_4. For each equivalent of hydrogen atoms they consume, one equivalent of Fe^{2+} enters solution to form rust and FeS. The bacteria, therefore, probably act essentially as depolarizers.

The reaction sequence can be outlined as follows:

Anode: $4Fe \longrightarrow 4Fe^{2+} + 8e^-$

Cathode: $8H_2O \longrightarrow 8H_{ads\ on}\ Fe + 8OH^- - 8e^-$

$8H_{ads} + Na_2SO_4 \xrightarrow{\text{bacteria}} 4H_2O + Na_2S$

$Na_2S + 2H_2CO_3 \longrightarrow 2NaHCO_3 + H_2S$

Summary: $4Fe + 2H_2O + Na_2SO4 + 2H_2CO_3 \longrightarrow 3Fe(OH)_2 + FeS + 2NaHCO_3$

Note that ferrous hydroxide and ferrous sulfide are formed in the relation of 3 moles to 1 mole. Analysis of given rust in which sulfate-reducing bacteria were active shows this approximate ratio of oxide to sulfide. In the event corrosion was caused instead by dissolved hydrogen sulfide or soluble sulfides, it is not likely that a similar ratio of oxide to sulfide would be found, and furthermore the corrosion rate would be lower. Qualitatively, the action of sulfate-reducing bacteria as the cause of

This material is reserved for educational use only, not allowed for commercial use.
Forbidden to modify the content, and cite the document when use.

corrosion in a water initially free of sulfides can be detected by adding a few drops of hydrochloric acid to the rust and noting the smell of hydrogen sulfide.

King and Miller have proposed that the hydrogen evolution reaction occurs on the ferrous sulfide which is produced by the reaction of ferrous ion with bacterially produced sulfide ion. They also propose that the bacteria increase the amount of active iron sulfide on which the hydrogen evolution reaction may occur.

Severe damage by sulfate-reducing bacteria has been observed particularly in oil-well casing, buried pipelines, water-cooled rolling mills, or in pipe from deep water wells. A well water in the U.S. Middle West caused failure within 2 years of a galvanized water pipe 50 mm (2 in.) in diameter by action of sulfate-reducing bacteria, where as municipal water employing similar wells, but which was chlorinated beforehand, was much less corrosive.

Chlorination is one way to reduce the damage caused by these bacteria, but it is apparently not always effective according to some reports. Aeration of water reduces activity of the bacteria since they are unable to thrive in presence of dissolved O_2. Addition of certain bactericides can also be beneficial. Streptomycin has no effect, but it is reported that tannates, potassium tellurite, cetyl pyridinium bromide, o-nitrophenol, or inorganic selenates are effective.

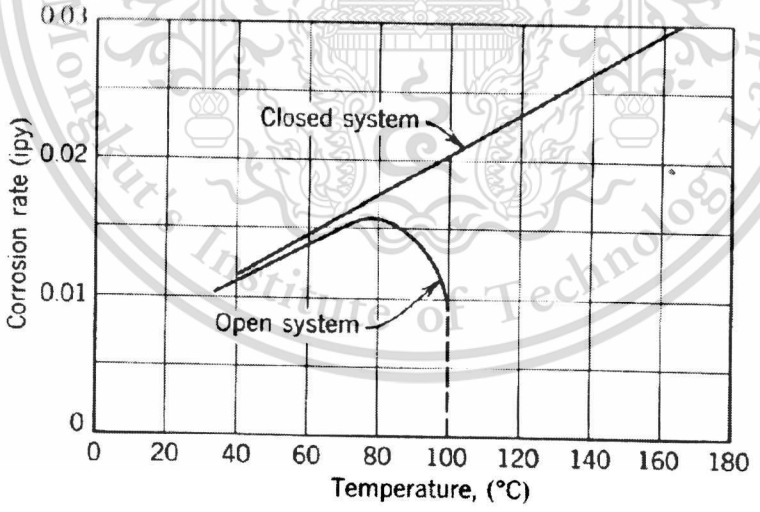

Figure 2.18 Effect of temperature on corrosion of iron in water containing dissolved oxygen

2.10.6.4 Effect of Temperature

When corrosion is controlled by diffusion of oxygen, the corrosion rate at a given oxygen concentration approximately doubles for every 30°C (55°F) rise in temperature. In an open vessel,

This material is reserved for educational use only, not allowed for commercial use.
Forbidden to modify the content, and cite the document when use.

allowing dissolved oxygen to escape, the rate increases with temperature to about 80°C (175°F) and then falls to a very low value at the boiling point (Fig.2.18). The falling off of corrosion above 80°C is related to a marked decrease of oxygen solubility in water as the temperature is raised, and this effect eventually overshadows the accelerating effect of temperature alone. In a closed system, on the other hand, oxygen cannot escape and the corrosion rate continues to increase with temperature until all the oxygen is consumed.

When corrosion is attended by hydrogen evolution, the rate increase is more than double for every 30°C rise in temperature. The rate for iron corroding in hydrochloric acid, for example, approximately doubles for every 10° rise in temperature.

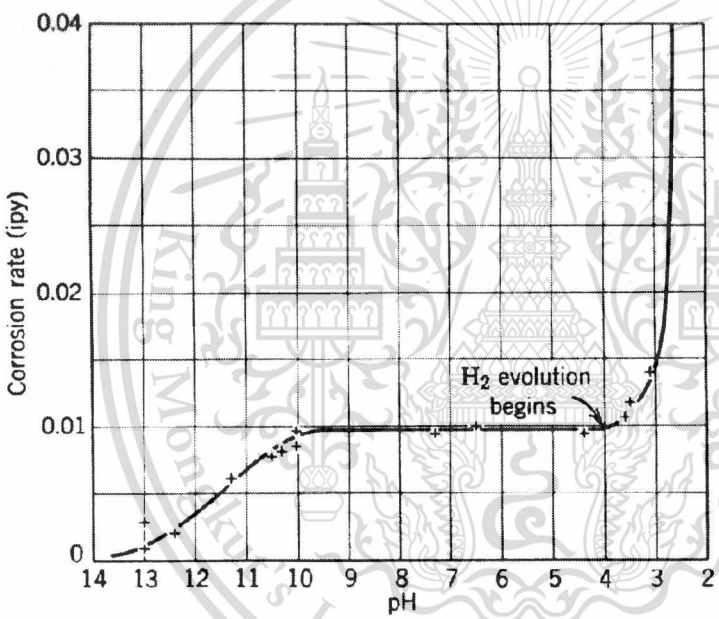

Figure 2.19 Effect of pH on corrosion of iron in aerated soft water, room temperature

2.10.6.5 Effect of pH

The effect of pH of aerated pure (or soft) water on corrosion of iron at room temperature is shown in Fig 2.19. Sodium hydroxide and hydrochloric acid were used to adjust pH in the alkaline and acid ranges.

Within the range of about pH 4-10, the corrosion rate is independent of pH, and depends only on how rapidly oxygen diffuses to the metal surface. The major diffusion barrier of hydrous ferrous oxide is continuously renewed by the corrosion process. Regardless of the observed pH of water within

This material is reserved for educational use only, not allowed for commercial use.
Forbidden to modify the content, and cite the document when use.

this range, the surface of iron is always in contact with an alkaline solution of saturated hydrous ferrous oxide, the observed pH of which is about 9.5.

Within the acid region (pH < 4), the ferrous oxide film is dissolved, the surface pH falls, and iron is more or less in direct contact with the aqueous environment. The increased rate of reaction is then the sum of both as appreciable rate of hydrogen evolution and oxygen depolarization.

Above pH 10, increase in alkalinity of the environment raises the pH of the iron surface. The corrosion rate correspondingly decreases because iron becomes increasingly passive in the presence of alkalies and dissolved 0xygen, as explained in the section "Higher Partial Pressures of Oxygen" in this chapter. Confirming the occurrence of passivity by Def. 1 in Chapter 5, the potential of iron in water of pH < 10 changes from an active value 5, the potential of iron in water of pH < 10 changes from an active value of – 0.4 to – 0.5, to a noble value of 0.1 V in 1N NaOH, with an accompanying decrease in the corrosion rate. If the alkalinity is markedly increased, for example, to 16N NaOH (43%), passivity is disrupted and the potential achieves the very active value of – 0.9 V. The corrosion rate correspondingly increases slightly to 0.003-0.1 mm/y 0.05-2.0 gmd), but that is still a relatively low rate. In this region, iron corrodes with formation of soluble sodium ferrite ($NaFeO_2$). In absence of dissolved oxygen, the reaction proceeds with hydrogen evolution forming sodium hypoferrite, Na_2FeO_2. The fact that Fe^{2+} is complexes by OH^- in strong alkalies to form FeO_2^- with accompanying reduction in activity of Fe^{2+} accounts for the observed active potential of iron. Although the rate of formation of FeO_2^- in concentrated alkalies at room temperature is low, caused by marked polarization of probably both anodic and cathodic areas, the rate becomes excessively high at boiler temperatures.

As noted previously, in the region of pH 4-10 the corrosion rate depends only on the rate of diffusion of oxygen to the available cathodic surface. The extent of the cathodic surface is apparently not important. This was made clear by an experiment of Whitman and Russell, who exposed to Camb5ridge tap water, steel specimens that were copper-plated over three-quarters of the surface. The total weight loss of these specimens compared to control specimens not plated was found to be the same. All oxygen reaching the copper surface, acting as cathode, was reduced in accord with the reaction

$$H_2O + \frac{1}{2}O_2 \longrightarrow 2OH^- - 2e^-$$

And an equivalent amount of Fe2+ was formed at the iron surface acting as anode. In addition, all oxygen reaching cathodic areas of the iron surface itself produced an equivalent amount of Fe^{2+}. The total amount of iron corroding, therefore, was the same regardless of whether copper was plated over

This material is reserved for educational use only, not allowed for commercial use.
Forbidden to modify the content, and cite the document when use.

part of the specimens. However, penetration of iron in the case of the plated specimens was four times that of the bare specimens.

It follows, therefore, that so long as oxygen diffusion through the oxide layer is controlling, which is the case within pH 4-10, any small variation in composition of a steel and its heat treatment, or whether it is cold worked or annealed, has no bearing on corrosion properties provided the diffusion-barrier layer remains essentially unchanged. Oxygen concentration, temperature, and velocity of the water alone determine the reaction rate. These facts are important because almost all natural waters fall within the pH range 4-10. This means that whether a high- or low-carbon steel, or similarly a low-alloy steel (e.g., 1-2% Ni, Mn, Mo, etc.), wrought iron, cast iron, or

Table 2.1 Corrosion Rates of Various Steels When Oxygen Diffusion is controlling

% Carbon	Treatment	Environment	Temperature of Test	Corrosion (ipy)	Rate (mm/y)
		Effect of Heat Treatment			
0.39	Cold drawn, annealed 500°C (930°F)	Distilled water	65°C (150°F)	0.0036	0.091
0.39	Normalized 20 min. at 90 0°C (1650°F)	Distilled water	65°C (150°F)	0.0034	0.086
0.39	Quenched 850°C (1650°F) Various specimens tempered 300°C (570°F) - 800°C (1470°F)	Distilled water	65°C (150°F)	0.0033	0.084
		Effect of Carbon			
0.05	Not stated	3% NaCl	Room	0.0014	0.036
0.11	Not stated	3% NaCl	Room	0.0015	0.038
0.32	Not stated	3% NaCl	Room	0.0016	0.041
		Effect of Alloying			

This material is reserved for educational use only, not allowed for commercial use.
Forbidden to modify the content, and cite the document when use.

0.13	Not stated	Seawater	0.004	0.10
0.10, 0.34% Cu	Not stated	Seawater	0.005	0.13
0.6, 2.2% Ni	Not stated	Seawater	0.005	0.13
Wrought iron	Not stated	Seawater	0.005	0.13

Cold-rolled mild steel is exposed to fresh water or seawater, all the observed corrosion rates in a given environment are essentially the same. Many laboratory and service data obtained with a variety of irons and steels support the validity of this conclusion. A few typical data are summarized in Table 2.1 These observations answer the once vociferous argument that wrought iron, for example, is supposedly more corrosion resistant than steel.

In the acid range (pH < 4) oxygen diffusion is no longer controlling, and the corrosion reaction is established in part by the rate of hydrogen evolution. The latter, in turn, depends on the hydrogen over voltage of various impurities or phases present in specific steels or irons. The rate becomes sufficiently high in this pH range to make anodic polarization a possible contributing factor (mixed control). Because cementite (Fe_3C) is a phase of low hydrogen over voltage, a low-carbon steel corrodes in acids at a lower rate than does a high-carbon steel. Similarly, heat treatment affecting the presence and size of cementite particles can appreciably alter the corrosion rate. Furthermore, cold-rolled steel corrodes more rapidly in acids than does an annealed or stress-relieved steel because cold working produces finely dispersed low-over voltage areas originating largely from interstitial nitrogen and carbon.

Since iron is not commonly used in strongly acid environments, the factors governing its corrosion in media of low pH are less important than those in natural waters and in soils. Nevertheless, there are certain applications where such factors must be considered, for example, in steam-return lines containing carbonic acid, or in food cans where fruit and vegetable acids corrode the container with accompanying hydrogen evolution.

Less is known about the effect of impurities and metallurgical factors on the corrosion rate in the very alkaline region (pH =14) where corrosion is again accompanied by hydrogen evolution. In the passive region, approximately pH 10-13, the effect on passivity by impurities in their usual concentrations, or the effect of metallurgical factors, are not expected to be pronounced. In general, any

This material is reserved for educational use only, not allowed for commercial use.
Forbidden to modify the content, and cite the document when use.

condition producing a large cathode-to-anode ratio facilitates achievement of passivity and increases the stability of the passive state once it is achieved.

2.10.5.6 Corrosion of Iron in Acids. We have seen that in strong acids (e.g., hydrochloric, sulfuric) the diffusion-barrier oxide film on the surface of iron is dissolved below pH 4. In weaker acids (e.g., acetic or carbonic) dissolution of the oxide occurs at a higher pH, hence the corrosion rate of iron increases accompanied by hydrogen evolution at pH 5 or 6. This difference is explained[8] by the higher total acidity or neutralizing capacity of a partially dissociated acid compared with a totally dissociated acid at a given pH. In other words, at a given pH there is more available H+ to react with and dissolve the barrier oxide film using a weak acid compared to a strong acid.

The increased corrosion rate of iron as pH decreases is not caused alone by increased hydrogen evolution; in fact, greater accessibility of oxygen to the metal surface on dissolution of the surface oxide favors oxygen depolarization which is often the more important reason. The sensitivity of the corrosion rate of iron or steel in nonoxidizing acids to dissolved oxygen concentration is shown by data of Table 2.2 In 6^ acetic acid at room temperature the ratio of corrosion rate with oxygen present, to corrosion rate with oxygen absent, is 87. In oxidizing acids (e.g., nitric acid), which act as depolarizers and for which the corrosion rate is therefore independent of dissolved oxygen, the ratio is almost unity. In general, the ratios are larger the more dilute the acid. In more concentrated acids, the rate of hydrogen evolution is so pronounced that oxygen has difficulty in reaching the metal surface. Hence depolarization in more concentrated acids contributes less to the overall corrosion rate than in dilute acids in which diffusion of oxygen is impeded to a lesser extent.

Table 2.2 Effect of Dissolved Oxygen on Corrosion of Mild Steel in Acids

	Corrosion Rate, mm/y		
Acid	Under O_2	Under H_2	Ratio
6% acetic	13.9	0.16	87
6% H_2SO_4	9.1	0.79	12
4% HCl	12.2	0.79	15
0.04% HCl	9.9	0.14	71
1.2% HNO_3	46	40	1.2

This material is reserved for educational use only, not allowed for commercial use.
Forbidden to modify the content, and cite the document when use.

2.11 Literature review

In this section, the author has carefully reviewed literatures from many researchers who are interested in alternative fuel, especially biodiesel and material compatibility, in order to use it as an alternative fuel in a vehicle and the importance of their works can be summarized as follow;

Savita Kaul *et al.* (2006) [2] have studied the corrosion behavior of biodiesel from seed oils of Indian origin on diesel engine parts. Studies for the synthesis and characterization of biodiesel from non-edible oils like *Jatropha curcas*, *Pongamia glabra* (Karanja), *Madhuca indica* (Mahua) and *Salvadora oleoides* (Pilu) have already been carried out in theirs laborotary. Corrosion characteristics of biodiesel are important for long term durability of engine parts. Using long duration static immersion test method was carried out for a period of 300 days at ambient temperature. During the test period the temperature variation was observed between 15 and 40 °C due to climatic changes. The test metal specimens were evaluated after 300 days for qualitative and quantitative estimation of corrosion. Corrosion studies on engine parts like piston metal and piston liner were carried out with neat diesel procured from one of the Indian refineries and biodiesel was synthesised from these non-edible oils. Biodiesel from Salvadora marked corrosion on both metal parts (piston and piston liner) of diesel engine due to high sulphur compounds (sulphur 1600 ppm): such as thioglycosides, glucotropaeolin, dibenzylthiourea and diben- zylurea indicated that this oil was not suitable for biodiesel production whereas biodiesel from other oils showed little or/no corrosion as comparing to neat diesel. An increase in Total acid number (TAN) after test duration indicated oxidization of biodiesel samples due to metal. However there was no gum formation observed on the test metals.

Wimonrat Trakarnpruk *et al.* (2007) [3] have studied the palm oil biodiesel synthesized with potassium loaded calcined hydrotalcite and effect of biodiesel blend on elastomer properties. Biodiesel was prepared from palm oil by transesterification with methanol in the presence of 1.5%K loaded–calcined Mg-Al hydrotalcite. Fatty acid methyl esters content of 96.9%and methyl ester yield of 86.6%were achieved using a 30:1 methanol to oil molar ratio at 100 °C for 6 h and 7wt% catalyst. The biodiesel was characterized and its impact on elastomer properties was evaluated. The compatibility of B10 diesel blend (10% biodiesel) with six types of elastomers commonly found in fuel systems (NBR, HNBR, NBR/PVC, acrylic rubber, co-polymer FKM, and terpolymer FKM) were investigated. The physical properties of elastomers after immersion in tested fuels (for 22, 670, and 1008 h at 100 °C) were measured according to American Society of Testing and Materials (ASTM). These included swelling (mass change and volume change), hardness, tensile and elongation, as well as the dynamic

This material is reserved for educational use only, not allowed for commercial use.
Forbidden to modify the content, and cite the document when use.

mechanical property. The results showed that properties of NBR, NBR/PVC and acrylic rubber were affected more than other elastomers. This is due to the absorption and dissolving of biodiesel by rubber in these samples. Co-polymer FKM and terpolymer FKM which are fluoroelastomers show little property change. The study of elastomer compatibility with B10 demonstrated little impact on the properties of elastomers. The results obtained from this work can assure consumer confidence in using B10.

Koji Yamane *et al.* (2003) [9] presented two interests. One was the effects of refining process of biodiesel fuel on fuel properties, diesel engine performance and exhaust emissions and another was the influences of plant oil plants for biodiesel production on combustion and emission characteristics. Plant oils and used cooking oils were reacted with methanol and a lye catalyst: KOH, to produce fatty acid methyl ester: unwashed-biodiesel. Washing the unwashed-biodiesel by water and dying processes were necessary in order to improve its fuel properties. Experiments were carried out on a single-cylinder, 4-stroke-cycle, DI diesel engine and various unwashed-, washed-and refined-biodiesel fuels derived from new or used cooking oil. From the results, it was found that the unwashed-biodiesel caused unstable engine operation and there was not much difference in engine performance and emissions comparing biodiesel fuel derived from new and used cooking oil of the same oil plant.

Mongkol Jampamee *et al.* (2004) [10] have studied the effect of biodiesel blended fuels on exhaust emissions of diesel engines. The test fuels were 2%, 5%, 20% of rapeseed methyl ester blended with diesel, pure rapeseed methyl ester, 2%, 5%, 20% of palm stearin methyl ester blended with diesel, pure palm strearin methyl ester and 20%, 30%, 40% of used cooking oil methyl ester blended with diesel. Two kinds of vehicle-tested were Toyota D4D 2.5L and Isuzu DMAX 2.5L. The exhaust emissions analysis was carried out by running on chassis dynamometer. The results showed that the blends of 2%, 5% of palm strearin methyl ester and rapeseed methyl ester were not significant different in exhaust emissions and fuel consumption compared to based diesel. On the other hand, the blends of 5% showed tendency of THC and PM emission reduction. For blends 20% of all kind methyl esters, the THC and PM emissions were decreased 10 – 34% and 6 – 34%, respectively while the fuel consumption was increased 2 – 5%. Used cooking oil methyl ester blended with diesel in the ratio of 30 and 40 percent could decrease THC and PM emissions for 18 – 27% and 16 – 36%, consecutively NOX emissions and fuel consumption were increased 7% and 5 - 6%. Pure palm strearin methyl ester and rapeseed methyl ester provided a greater reduction of all exhaust emissions. On the contrary, NOX emission and fuel consumption were increased.

This material is reserved for educational use only, not allowed for commercial use.
Forbidden to modify the content, and cite the document when use.

B Terry *et al.* (2005) [11] have studied the impact of biodiesel on fuel system component durability. In this study, physical properties of five candidate elastomers commonly used in automotive fuel systems were examined before and after immersion in six biodiesel blends (B5 RME, B5 SME, B5 SME oxidized, B20 RME, B20 SME, B20 SME oxidized) and base fuel under controlled conditions. The properties such as hardness, tensile strength, volume change and compression set were compared. Of the five materials tested, two elastomers emerged as being most compatible with the test blends. Injector wear tests were conducted on the base fuel and three B20 biodiesel blends using a 500-hour test method. Detailed metrology measurements were taken on fuel injector sets before and after testing to quantify injector wear. This study has concluded that there was no increase in 'out-of-roundness' of the injector needles for any of the test fuels and hence the lubricity values of the test fuels were adequate for the protection of the injector components running under conditions similar to the test method. The injector wear test on the B20 oxidized soy biodiesel was terminated after only twelve hours of running because of separation of the fuel into two phases. Fuel pump wear tests were conducted using a 500-hour test method based on the CEC F-32-X-99 test procedure. Bosch VE in-line pumps were evaluated for wear before and after testing on the base fuel, B5 and B20 test fuels. The rating measurements from the pump lubricity tests could be concluded that the fuels property were within the range which would normally be expected for commercial automotive diesel fuels. The rotary pump test conducted on the B20 blend of oxidized soy biodiesel failed to reach full duration due to blockage of the fuel filter. This was found to be due to separation of the fuel blend into two phases. To conclude this AVFL-2a study, a common rail test rig was built to mimic the real life operation of a common rail passenger car system. A test procedure was developed to accelerate wear conditions on common rail pumps using a 500-hour protocol. Pumps from tests conducted on the base fuel, B5 and B20 fuels were examined and the components visually rated for abrasion, fretting, corrosion and wear and polishing steps. Examination of the pump following the test on the B20 blend containing highly oxidized soy biodiesel revealed a hard lacquer accumulation on one of the pump components and significant seal swell. This candidate fuel concluded without operational failure but significant fuel separation was noted. A further common rail test on a less highly oxidized B20 blend was concluded without operational failure and without evidence of fuel separation or signs of lacquering. Swelling of one of the seals in the test pump was again noted. No unusual wear was found on any of the common rail test pumps used in the study. The rating measurements from the common rail pump lubricity tests concluded that the fuels were within the range which would normally be expected for commercial automotive diesel fuels. The evidence indicated that phase separation of B20 blends prepared from

This material is reserved for educational use only, not allowed for commercial use.
Forbidden to modify the content, and cite the document when use.

oxidized biodiesel did not occur in storage. Decomposition reactions occurring under the conditions of test probably accelerated fuel separation in the more highly oxidized B20 test fuel containing very high levels of water and sediment. Phase separation did not take place in the B20 fuel containing biodiesel oxidized to a lesser extent and which contained lower water and sediment. The main factor therefore affecting the different behavior of the oxidized fuels is thought to be the extent of oxidation.

This material is reserved for educational use only, not allowed for commercial use.
Forbidden to modify the content, and cite the document when use.

CHAPTER 3

EXPERIMENTAL PROCEDURES

3.1 Methodology

The methodology is divided into 2 parts. One was mechanical simulation of fuel supply line and another is fuel immersion test. As shown in Fig.3.1.

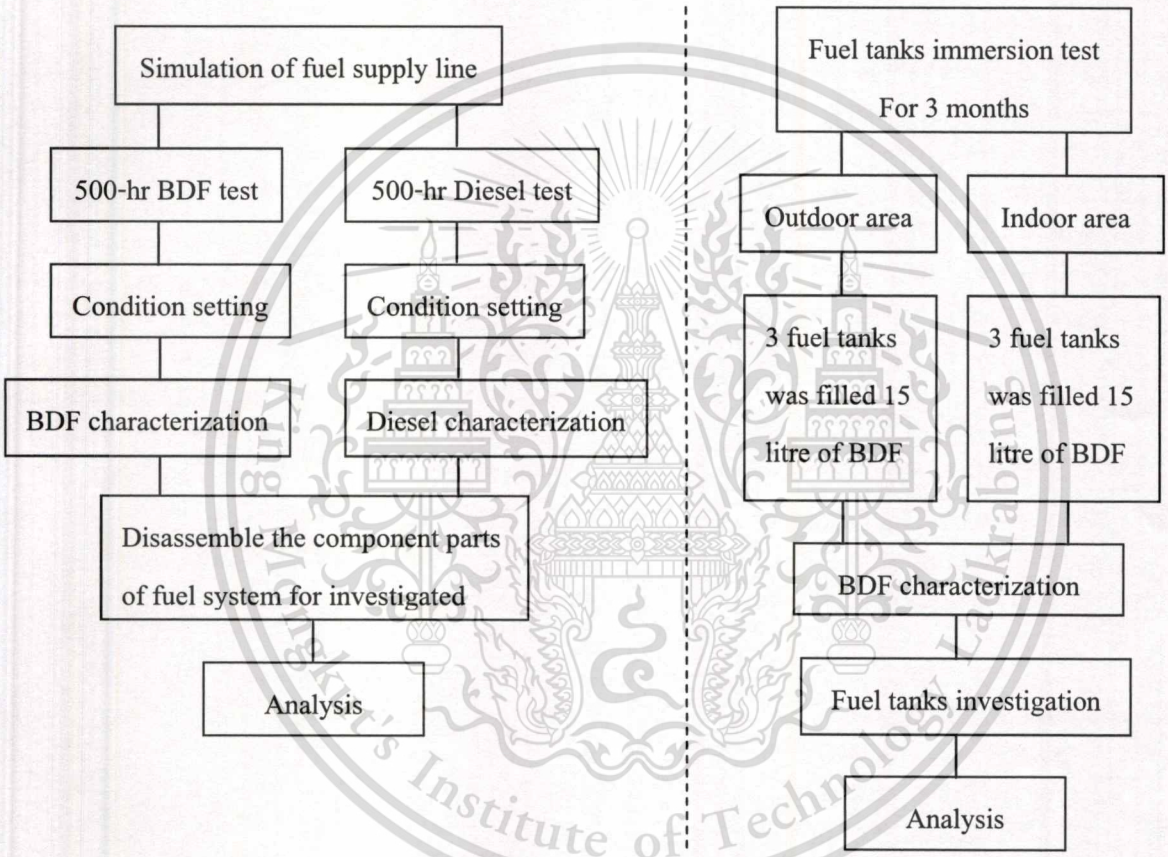

Figure 3.1 Methodology diagram

3.2 Tested Fuels

The Ministry of Energy has issued biodiesel standard in Thailand based on ASTM (American Society of Testing and Materials International) and EN (European Committee for Standardization) which were derived from soybean and rapeseed oil whereas raw material for Thai biodiesel fuel is palm or jatropha oil. In Thailand, the use of biodiesel fuel in agriculture sector has been promoted but there are no automobile manufacturer accepts B100 (100%biodiesel). Only B5 (5% biodiesel blended with diesel) can be used to ensure the fuel quality will not much different from diesel there are some arguments regarding to the

Forbidden to modify the content, and cite the document when use.

CHAPTER 3

EXPERIMENTAL PROCEDURES

3.1 Methodology

The methodology is divided into 2 parts. One was mechanical simulation of fuel supply line and another is fuel immersion test. As shown in Fig.3.1.

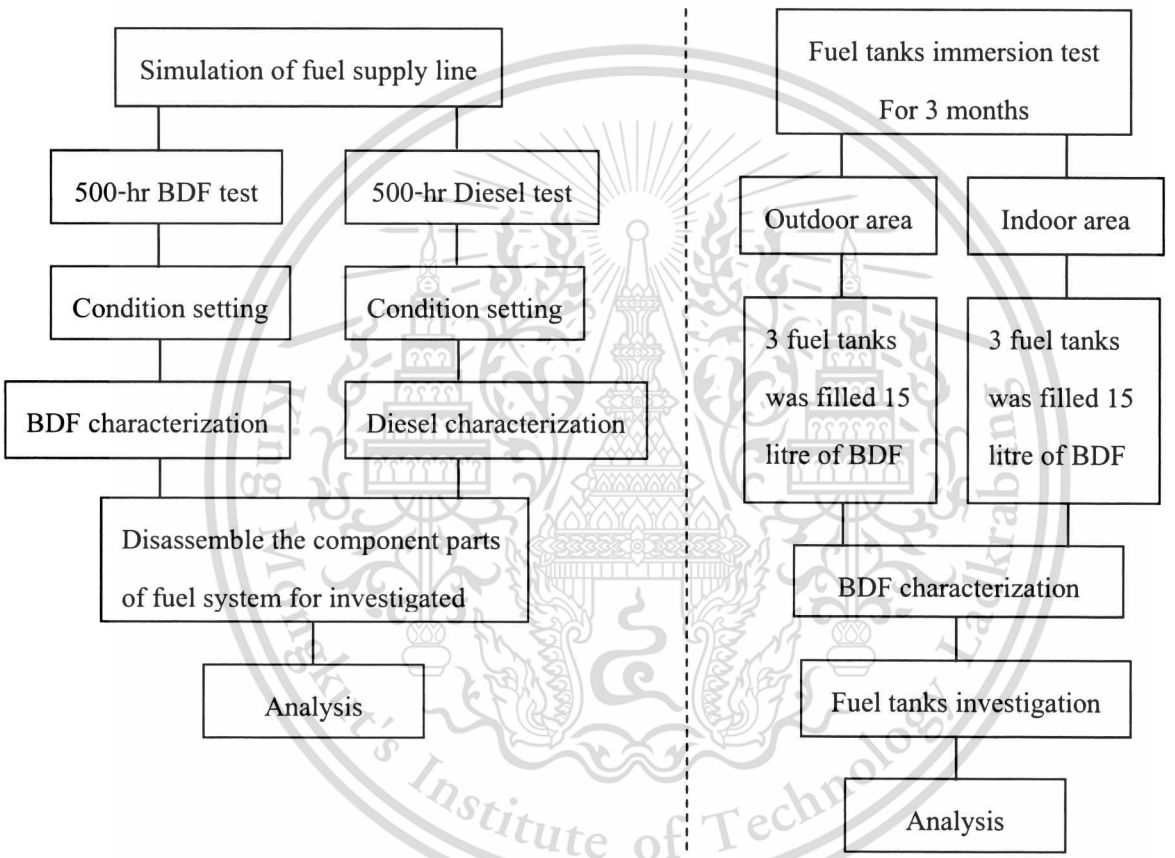

Figure 3.1 Methodology diagram

3.2 Tested Fuels

The Ministry of Energy has issued biodiesel standard in Thailand based on ASTM (American Society of Testing and Materials International) and EN (European Committee for Standardization) which were derived from soybean and rapeseed oil whereas raw material for Thai biodiesel fuel is palm or jatropha oil. In Thailand, the use of biodiesel fuel in agriculture sector has been promoted but there are no automobile manufacturer accepts B100 (100%biodiesel). Only B5 (5% biodiesel blended with diesel) can be used to ensure the fuel quality will not much different from diesel there are some arguments regarding to the

This material is protected by copyright and was for non-profit educational use only, not allowed for commercial use.
Forbidden to modify the content, and cite the document when use.

compatibility of biodiesel and diesel engine. In other words, palm stearin methyl ester (PSME) and diesel were taken from commercial plants that meet Thai standard (DOEB, 2007) [1]. The properties are shown in Table 3.1.

Table 3.1 Properties of PSME.

Properties	***Method***	***Value***	***Thailand Standard***
Density (g/cm^3)	ASTM D 4052	0.87	0.86 – 0.9
Kinematic viscosity @ 40 °C (mm^2/s)	ASTM D 445	4.45	3.5 - 5
Flash Point (°C)	ASTM D 93	162.00	> 120
Water Content (ppm)	ASTM D 6304	315.6	< 500
Oxidation Stability (Hour)	EN 14112	16.39	> 6
Acid Value (mg KOH/g)	ASTM D 664	0.17	< 0.5
Cloud Point (°C)	ASTM D 2500	15.80	N/A
Pour Point (°C)	ASTM D 97	12.00	N/A

3.3 Model of diesel engine

Figure 3.2 Diesel engine model 4100QB-2

This material is reserved for educational use only, not allowed for commercial use.
Forbidden to modify the content, and cite the document when use.

Table 3.2 Engine specification

Description	***Specification***
Type	4-stroke, vertical engine
Bore x Stroke	100 x 115 mm.
Number of Cylinder	4
Cylinder Type,	Waterish type
Combustion Type	Direct injection ω type
Displacement	3.612 liters
Compression Ratio	17.5:1
Firing Order	1-3-4-2
Idle Speed	750 rpm
Rated Power	66.2/3200 kW-hr
Max Torque	230/2000-2200 N.m/rpm
Fuel Consumption	≤238 g/kW-hr
Net weight	320 kg
Injection timing/pressure	12°/19.1±0.49MPa

Table 3.3 Quantity of fuel supplied by injection pump

Injection pump specification	***Value***
Piston diameter (mm)	9
Rated fuel amount (ml/400times/rpm)	28.4/1600
Max.torque fuel amount (ml/400times/rpm)	26/1100
Starting fuel amount (ml/400times/rpm)	>11/150
Fuel amount at idling steady speed (ml/400times/rpm)	2.4/350

This material is reserved for educational use only, not allowed for commercial use.
Forbidden to modify the content, and cite the document when use.

3.4 Apparatus

3.4.1 Measuring Instruments for Physical and Chemical Property Tests

During the experiment in order to monitor its degradation. As shown in Fig 3.2 some biodiesel properties such as acid value were measured by automatic titrator, oxidation stability were measured by oxidation stability measurement, water content stability measurement by Karl Fisher coulometer and kinematic viscosity were measured by viscosity measurement..

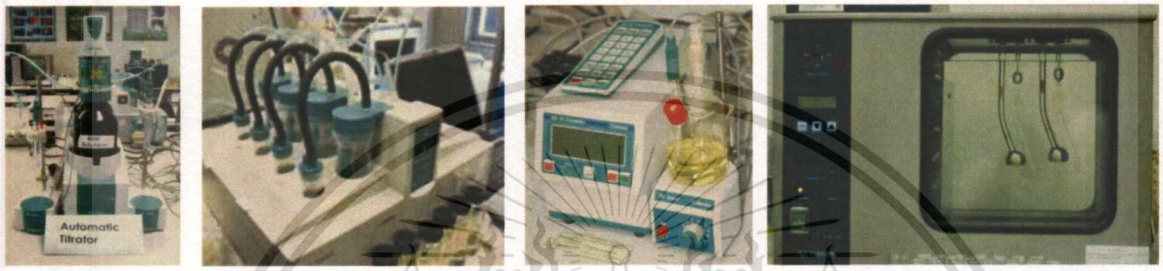

(a) (b) (c) (d)

Figure 3.3 Instruments for physical and chemical property tests (a) Automatic Titrator, (b) Oxidation stability measurement, (c) Karl Fisher coulometer, (d) Viscosity measurement

3.4.2 Equipment for analyzed component parts of fuel system.

Some component parts of fuel system such as inline pump, injector, and fuel tank were analyzed by using various equipments, as shown in Figure 3.3 (a) Surface Roughness Tester for investigated surface of metal parts such as pump plunger, (b) Injection Tester for investigated the injection pressure of injectors (8 injectors), (c) Mechanical pump Tester for investigated the fuel capacity of each cylinder following manual guideline, (d) Scanning Electron Microscope (SEM) for investigated the surface of metal part especially fuel tanks parts, (e) Optical Microscopy (OM) for investigated the cross section area of metal part especially fuel tanks parts and (f) Temperature and humidity sensor were installed around the fuel tanks for evaluated the ambient conditions.

This material is reserved for educational use only, not allowed for commercial use.
Forbidden to modify the content, and cite the document when use.

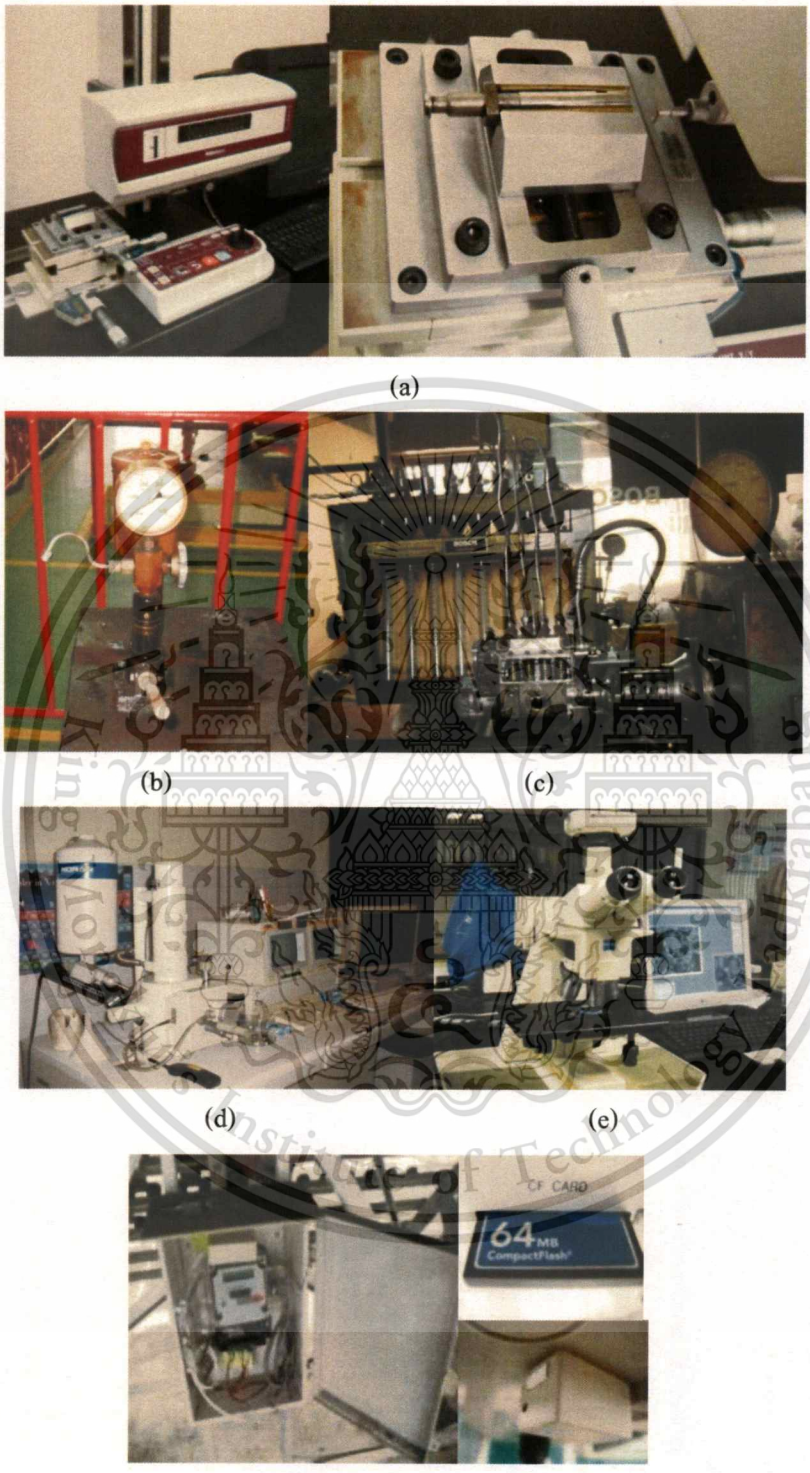

Figure 3.4 Equipment for analyzed component parts of fuel system (a) Surface Roughness Tester, (b) Injection Tester, (c) Mechanical pump Tester, (d) Scanning Electron Microscope (SEM), (e) Optical Microscopy (OM), (f) Temperature and humidity sensor

This material is reserved for educational use only, not allowed for commercial use.
Forbidden to modify the content, and cite the document when use.

3.5 Experiments

This study has been divided into two main parts. The first part is simulated the effect of B100 on fuel supply line whereas the second part is to study corrosion behaviour and compatibility of fuel tank when immersed with B100 for 3 months. Therefore, the experiment can be described as followings.

3.5.1 Simulation test apparatus and methodology

The experiments were taken on the simulation test apparatus as shown in Fig.3.4 – Fig 3.7. The pump rig tests were divided into two sets, one was for diesel and another was for biodiesel fuel (B100). In one set, a fuel tank was equipped with a hydraulic pump and heater to maintain the fuel temperature closeted to the operating condition of the engine. The tested fuel was then pumped through fuel filter to the injector. After that it was then sprayed via injector under designed pressure. The remaining tested fuel, also called spray fuel, was collected and returned to the fuel tank. Noted that the fuel was recirculate during the experiment (normally this fuel amount would be combusted in real engine running). Schematic drawing of fuel supply system simulation test apparatus is shown in Fig.3.4. During the trial, both heaters and hydraulic pumps of diesel and B100 could be adjusted to reach the similar temperature as the fuel in the engine operation. Thus, it could be assumed that fuel tank temperature could be adjusted to approach the actual condition as much as possible.

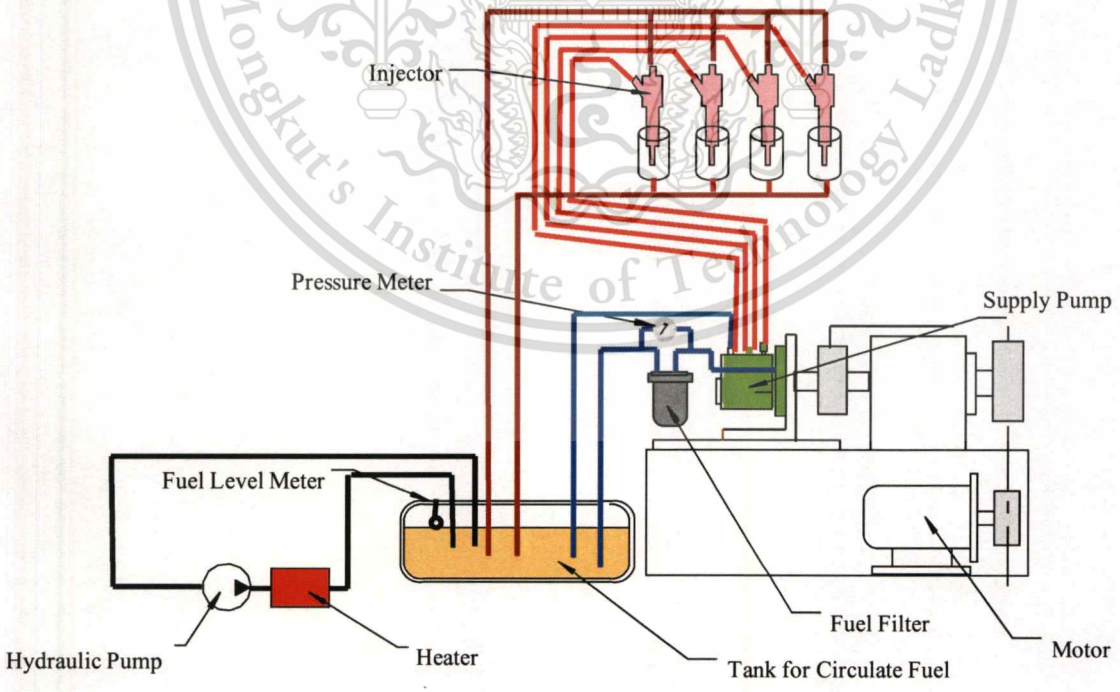

Figure 3.5 Schematic drawing of fuel supply system simulation test apparatus

This material is reserved for educational use only, not allowed for commercial use.
Forbidden to modify the content, and cite the document when use.

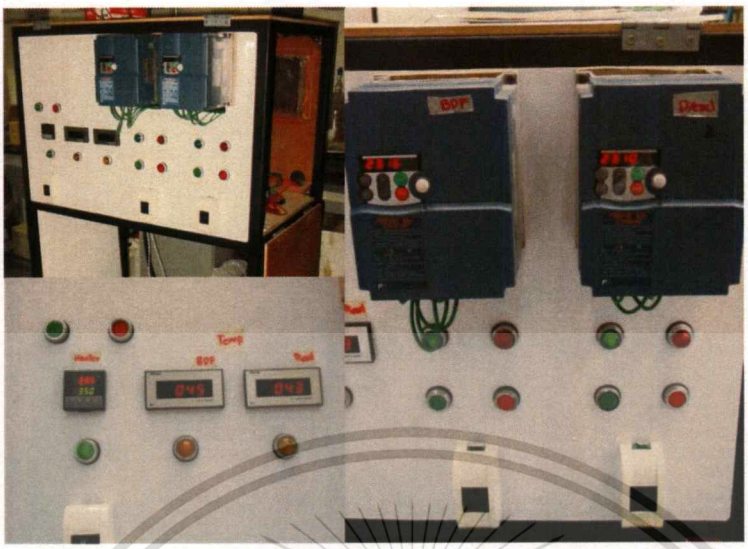

Figure 3.6 Controller

Figure 3.7 The pump rig test

The test cycle chosen for the study was based on the pump rig test cycle but limited to a 500 hours test duration. The key test conditions are as follows:

- The running speed of fuel system chosen was approximately speed 1,150 rpm which represented the speed of injection pump when this engine was running at the maximum load (torque) of 230 N.M. with the gear ratio 2:1 between injection pump and crankshaft, the engine speed of 2,300 rpm was reduced to 1,150 rpm

This material is reserved for educational use only, not allowed for commercial use.
Forbidden to modify the content, and cite the document when use.

- The pump was arranged to operate at the target pressure of 260 bar, which is typical for many vehicle applications. Throughout the test, the operating pressure was arranged to be between 250 bar and 270 bar.
- The fuel control lever was locked at the maximum fuel amount position so as to put the maximum load on the pumping element components.
- The test fuel was supplied to the pump at a flow rate and feed pressure matching the specifications of the vehicle system. This was arranged to be between 2.0 and 3.0 bar.
- The fuel inlet temperature was controlled at 40°C ± 5°C. Fuel heating units were employed to meet this condition.

3.5.2 Immersion test of fuel tank and methodology

The experiment is study the effect of 100% biodiesel on fuel tank that is normally used in heavy duty truck. It focuses on biodiesel and fuel tank degradation, including the study of problems occurring in practice.

Six 45-litre fuel tanks, normally used in 4-wheel truck, obtained from Sammitr Motor Co., Ltd were used in this experiment. This type of fuel tank is made of cold-rolled steel and may be corroded when contacting with moisture and degraded biodiesel.

Palm stearin methyl ester (PSME) was received from Veerasuwan Co., Ltd. conformed to the Department of Energy business standard (DOEB, 2007). Some biodiesel properties were measured during the experiment in order to monitor its degradation. To access the fuel acidity, pH meter and automatic tritrator were used while the water absorption behaviour was measured by Karl Fisher coulometer.

Optical Microscope (OM) and Scanning Electron Microscope (SEM) were used to evaluate the fuel tank corrosion. During the experiment, temperature and humidity sensors were also used to monitor the environment around the outdoor storage area. Note that on the average periodic sampling, indoor storage area has a 20% lower temperature and a 20% higher humidity (data not shown here).

As shown in Fig. 3.9, the fuel tank samples were divided into two sets, one was put indoor and another was left outside under the shade. These two sets represented two cases of vehicle that had been parked in garage and in open-air area for 3 months with some biodiesel left in their tanks. Instead of filling the whole tank with biodiesel, it was intended to fill those tanks with only 15 liter of biodiesel or 1/3 of the full tank capacity. This was in order to leave some air space inside the tank so the biodiesel could be reacted by oxygen and moisture, which depends on the environment condition. Since the tested fuel tanks did not have other accessories, such as returned/suction fuel lines, all openings were sealed with silicone

Forbidden to modify the content, and cite the document when use.

to minimize humidity fluctuation from the surrounding environment. The fuel tank lid was also tightly closed. Every week, the biodiesel in each tank was sampled to monitor the biodiesel and fuel tank degradation. Its properties consisting of pH value, conductivity value, acid value and water content were measured. At the end of each month, one tank from each sample set was taken and cut for investigation by SEM and OM.

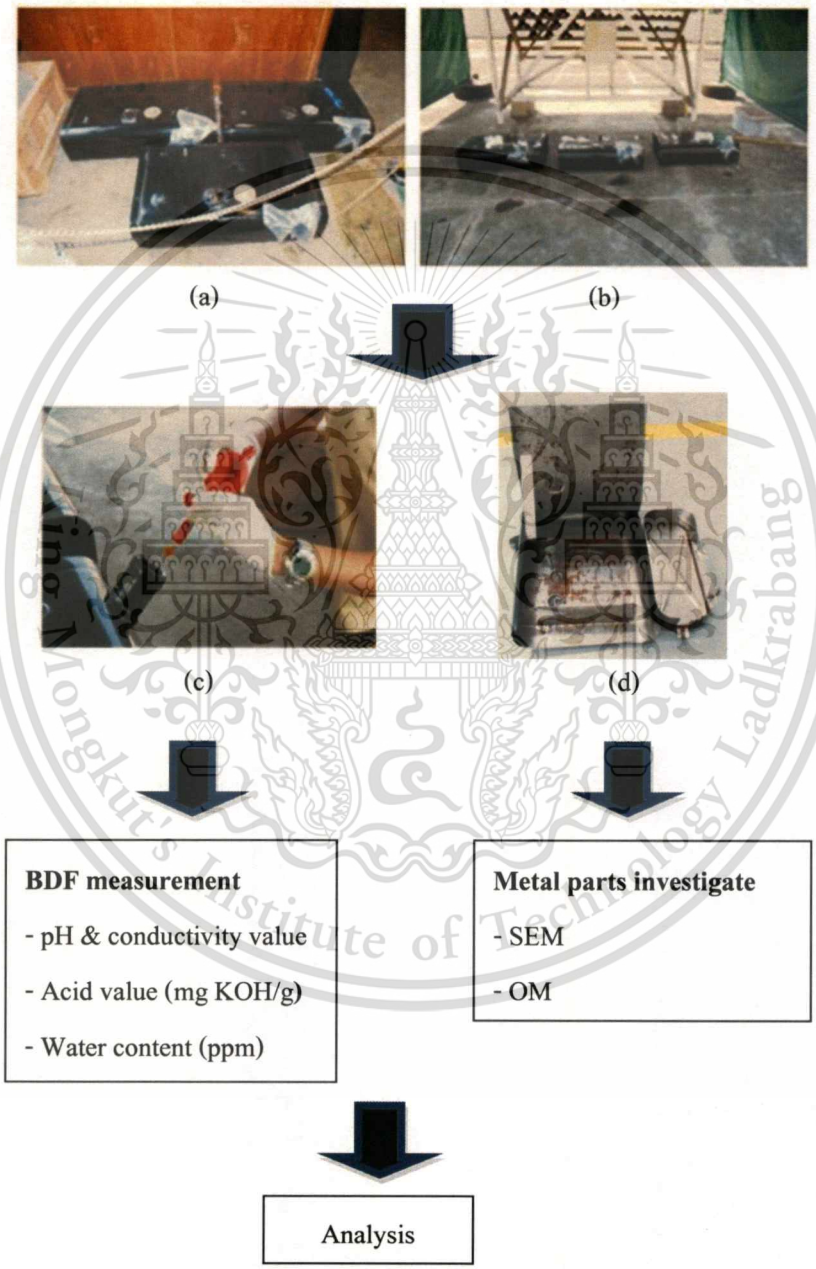

Figure 3.8 Test procedures for studying the effect of biodiesel on fuel tank (a) fuel tanks at indoor area, (b) fuel tanks at outdoor area, (c) sampling biodiesel from the fuel tank every week, (d) observation of fuel tank corrosion.

This material is reserved for educational use only, not allowed for commercial use.
Forbidden to modify the content, and cite the document when use.

CHAPTER 4

EFFECT OF B100 ON SIMULATION OF FUEL SUPPLY LINE

According to the experimental procedure from the previous chapter, the test results are separated into two chapters, chapter 4 and 5. This chapter is about the simulation of fuel supply line with B100 (PME), meanwhile chapter 5 is about the test results of effect of B100 on fuel tank.

A test rig was designed based on fuel system operation of the chosen diesel engine model. 500-hour simulation was the target to simulate BDF flow in the system. The pump rig tests were divided into two sets, one was the fuel system simulation of diesel fuel and another was fuel system simulation of biodiesel fuel (B100). During the test properties of B100 was controlled to meet Thailand biodiesel standard according to the Ministry of Energy's regulation. Furthermore, the main parts of fuel system were analyzed by various equipments.

4.1 Results of inline-pump

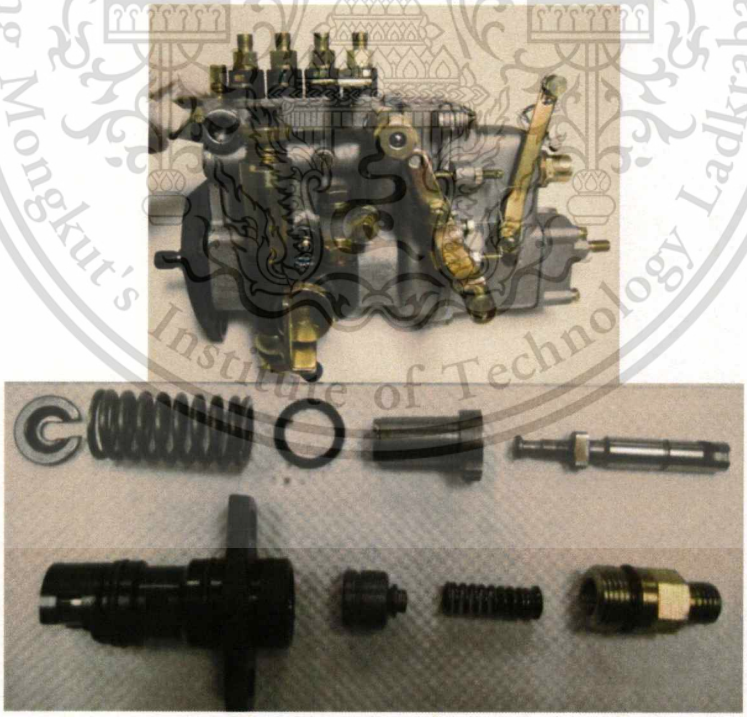

Figure 4.1 Dismantled Inline Pump

This material is reserved for educational use only, not allowed for commercial use.
Forbidden to modify the content, and cite the document when use.

4.1.1 Weight of inline pump parts

The metal parts of the inline pump, which mostly contact with fuel during pump operation, were holders, delivery valves and pump plunger. These parts hence were chosen to investigate as shown Fig.4.2 shows the metal which contact with fuel during test. All of the metal parts from inline pump which parallel running between biodiesel and diesel system. One set have 4 cylinders and 4 injectors.

(a) (b) (c)

Figure 4.2 Metal parts of inline pump (a) holder, (b) delivery valve, (c) pump plunger

Table 4.1 Weight of metal parts for inline pump (average of 10 values)

Metal parts	**Weight of metal parts from inline pump both of diesel and biodiesel system**							
	Metal parts of diesel system (4 cylinders)				Metal parts of biodiesel system (4 cylinders)			
	D1	D2	D3	D4	B1	B2	B3	B4
Holder	15.8506 g	15.5565 g	15.8976 g	15.6964 g	15.7620 g	15.7058 g	15.7153 g	15.6419 g
Delivery valve	2.7438 g	2.7063 g	2.7397 g	2.7392 g	2.6987 g	2.7843 g	2.7198 g	2.7430 g
Pump plunger	23.8079 g	23.7593 g	23.6624 g	23.6180 g	23.6657 g	23.6980 g	23.7271 g	23.6994 g

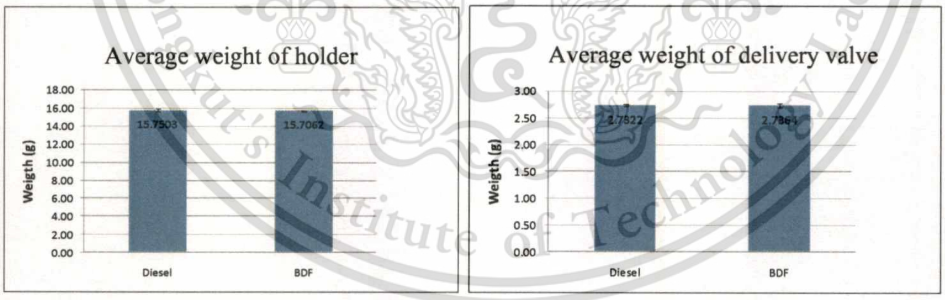

(a) (b)

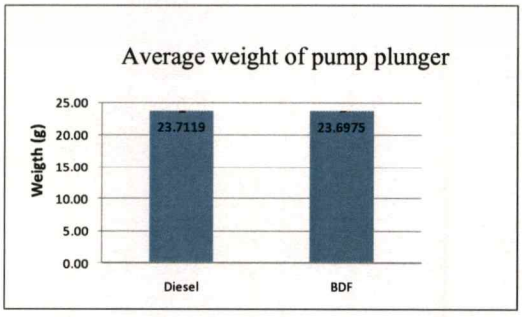

(c)

Figure 4.3 Weight of metal parts from inline pump (a) average weight of holder, (b) average weight of delivery valve, (c) average weight of pump plunger

This material is reserved for educational use only, not allowed for commercial use.
Forbidden to modify the content, and cite the document when use.

4.1.2 Delivery valve and holder investigation

The delivery valve is fitted between the plunger and barrel assembly and the high pressure delivery line. Its purpose is to isolate the high-pressure delivery line from the plunger and barrel assembly. It also reduces the pressure in the high-pressure delivery line and the nozzle chamber following fuel injection to a set static pressure. Pressure reduction causes rapid and precise closure of the nozzle and prevents undesirable fuel dribble into the combustion chamber. [6]

In the course of the delivery stroke, the increasing pressure in the plunger chamber lifts the delivery-valve cone from the valve seat in the delivery-valve body. Fuel then passes through the delivery-valve holder and into the high pressure delivery line to the nozzle. As soon as the helix of the pump plunger brings the injection process to an end, the pressure in the plunger chamber drops. The delivery-valve cone is then pressed back against the valve seat by the valve spring. This isolates the space above the pump plunger and the high-pressure side of the system from one another until the next delivery stroke.

The fuel system simulation had been parallel running on biodiesel and diesel fuel for a period of 510 hr. For the delivery-valve holder, it was focused on wear of valve seat which contacted with fuel directly diameter of the parts were measured by microscope as show in Fig 4.4 and Table 4.2.

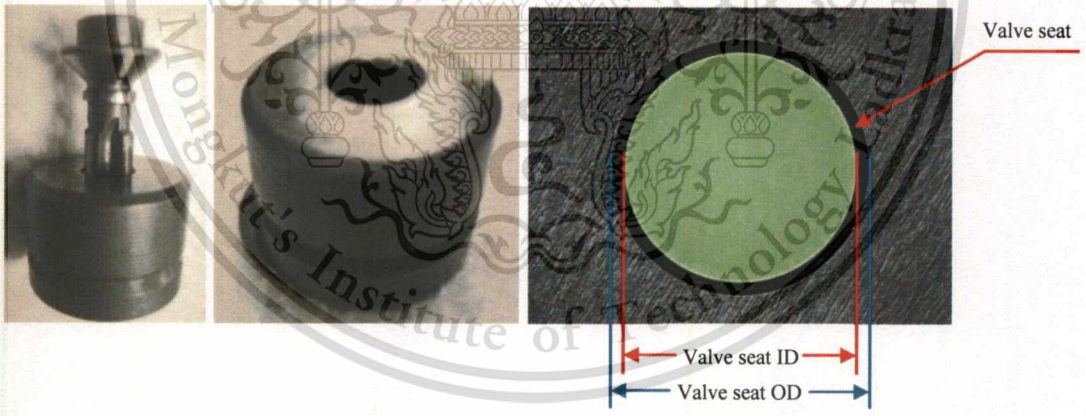

Figure 4.4 Delivery- valve holder

Table 4.2 Diameter of delivery-valve holder

Diameter	Diameter of delivery-valve holder							
	Delivery valve of diesel system (4 cylinders)				Delivery valve of biodiesel system (4 cylinders)			
	D1	D2	D3	D4	B1	B2	B3	B4
Inside	4.994 mm	4.987 mm	4.993 mm	4.967 mm	4.985 mm	4.984 mm	4.988 mm	4.988 mm
Outside	5.444 mm	5.485 mm	5.441 mm	5.424 mm	5.515 mm	5.480 mm	5.471 mm	5.471 mm

This material is reserved for educational use only, not allowed for commercial use.
Forbidden to modify the content, and cite the document when use.

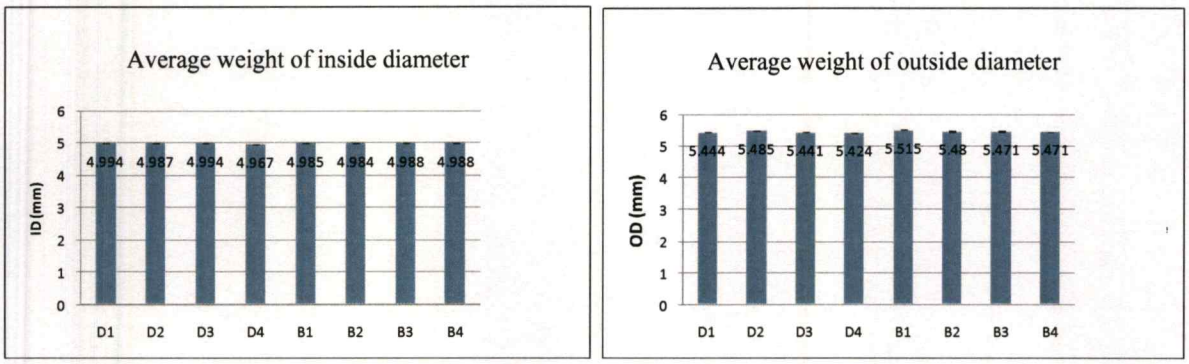

(a) (b)

Figure 4.5 Diameter of delivery-valve seat holder which is measured by using microscope (a) Average weight of inside diameter, (b) Average weight of outside diameter.

4.1.3 Pump plunger surface investigation

Pump unit with leakage return channel

If the fuel-injection pump is connected to the engine lube-oil circuit, leakage fuel can result in thinning of the engine oil under certain circumstance. Assemblies with a leakage return channel to the fuel gallery of the fuel-injection pump largely avoid this problem. There are two designs:

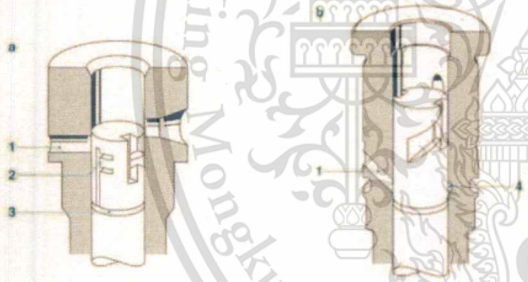

1. Leakage return bore
2. Leakage return slots
3. Ring groove in the pump plunger
4. Ring groove in the pump barrel

(a) (b)

Figure 4.6 Pump elements with leakage return channel; (a) A ring groove in the plunger collects the leakage fuel and returns it to the fuel gallery via other specially located grooves (2) in the piston, (b) Leakage fuel flows back to the fuel gallery via a ring groove in the pump barrel (4) and a hole (1).

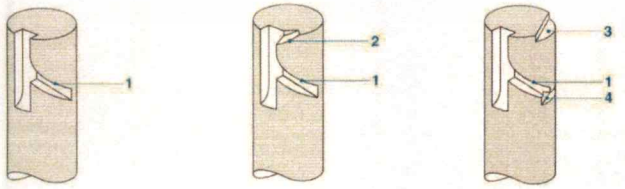

1. Bottom helix
2. Top helix
3. Starting groove
4. Start-quantity limitation groove

(a) (b) (c)

Figure 4.7 Pump plunger design variation (a) helix at bottom, (b) helix at top and bottom, (c) helix at bottom and starting groove.

This material is reserved for educational use only, not allowed for commercial use.
Forbidden to modify the content, and cite the document when use.

To determine the alterations on pump plunger surfaces due to usage of B100 and diesel fuels, the electron microscope is used. The surfaces have been examined before and after biodiesel usage. The fuel system simulation has been parallel running on biodiesel and diesel fuel for a period of 510 h.

To determine the influence of biodiesel usage on the roughness of the pump plunger active surface, some of the relevant roughness parameters have been determined. The arithmetic roughness average Ra.

The influence of biodiesel and diesel fuel on the pump plunger surface was presented in Fig. 4,9 and Fig 4.10. The surface area, positioned close to the top of the pump plunger, has been selected. It is known that this surface has a very important influence on the injection pressure. It turned out that under the microscope the surface looked always pretty the same, regardless of the fuel used.

One can see that the surface roughness at the pump plunger head increased by a factor of two when biodiesel was used for about 430 h. Luckily, for fuel leakage in the high pressure pump, the surface roughness at the pump plunger head is not as important as the roughness at the pump plunger skirt. For this reason, the obtained results are not alarming, although some further tribology investigations would be necessary to evaluate the situation more precisely.

In order to obtain the surface roughness parameters, the average of three measurements were performed on both, plunger skirt and head, for each parameter. It turned out that the influence of diesel and biodiesel usage is rather minor for the plunger skirt, Fig. 4.8. On the contrary, the roughness parameters Ra of the plunger skirt exhibited not significant changes after diesel and biodiesel usage, Fig. 4.11. In fact when analyzed with statistics it shows that effect of B100 and diesel fuel usage on pump plunger skirt surface is not significant different (0.0562% different).

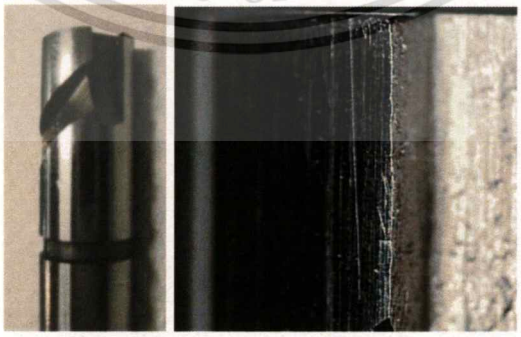

Figure 4.8 Pump plunger skirt surface

This material is reserved for educational use only, not allowed for commercial use.
Forbidden to modify the content, and cite the document when use.

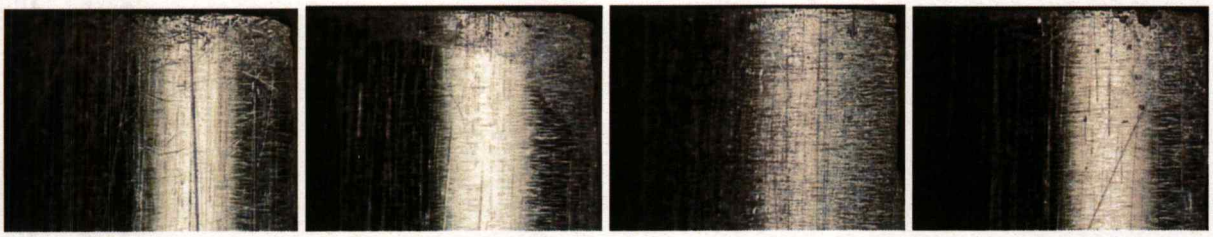

D1 D2 D3 D4

Figure 4.9 Pump plunger skirt surface after diesel fuel usage 510 hour

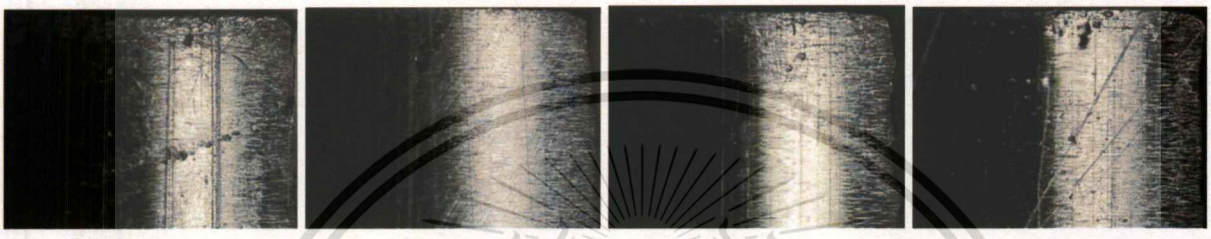

B1 B2 B3 B4

Figure 4.10 Pump plunger skirt surface after biodiesel usage 510 hour

Table 4.3 Surface Roughness, Ra (μm) of pump plunger skirt surface after diesel and biodiesel fuel usage.

Surface Roughness	**Pump plunger skirt surface**							
	Pump plunger of diesel system (4 cylinders)				Pump plunger of biodiesel system (4 cylinders)			
	D1	D2	D3	D4	B1	B2	B3	B4
Ra (μm)	0.043	0.043	0.049	0.043	0.055	0.040	0.037	0.047

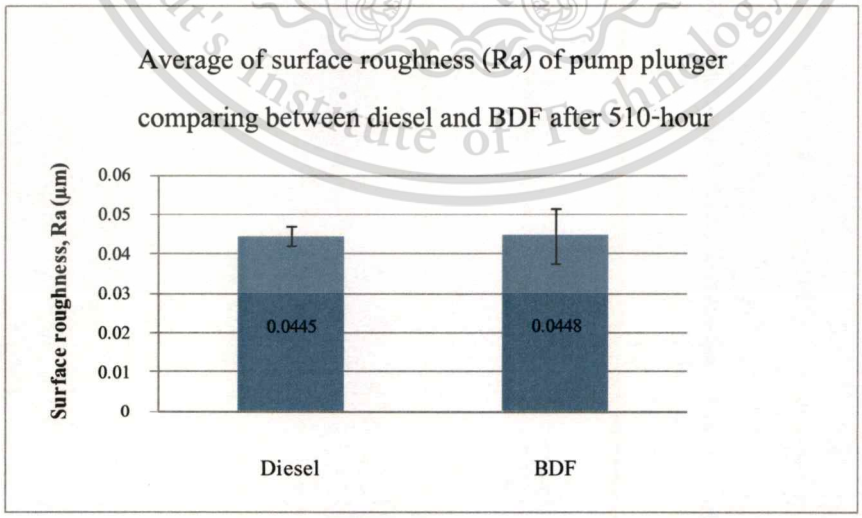

Figure 4.11 Average of surface roughness (Ra) of pump plunger comparing between diesel and BDF after 510-hour

This material is reserved for educational use only, not allowed for commercial use.
Forbidden to modify the content, and cite the document when use.

4.2 Injector investigation

The injection nozzle injects the fuel into the combustion chamber of the diesel engine. It is a determining factor in the efficiency of mixture formation and combustion and, therefore has a fundamental effect on engine performance, exhaust-gas behavior, and noise. In order that injection nozzles can perform their function as effectively as possible, they have to be designed to match the fuel-injection system and engine in which they are used.

Hole-type nozzles are used on engine that operate according to the Direct-Injection process (DI). The position in which the nozzles are fitted is generally determined by the engine design. The injection orifices are set at a variety of angles according to the requirements of the combustion chamber.

Fuel in the volume below the nozzle-needle seat evaporates after combustion. This produces a large part of the engine's hydrocarbon emissions. For this reason, it is important to keep the dead volume, or "detrimental" as small as possible.

In addition, the geometry of the needle seat and the shape of the nozzle cone have a decisive influence on the opening and closing characteristics of the nozzle. This, in turn, affects the soot and NO_x emissions produced by the engine.

The consideration of these various factors, in combination with the demands of the engine and the fuel-injection system, has resulted in a variety of nozzle designs. There are two basic designs, blind-hole nozzles and Sac-less (vco) nozzles, for this research is blind-hole type.

- **Heat shield**

  The maximum temperature capacity of hole-type nozzles is around 300°C (heat resistance of material). Thermal-protection sleeves are available for operation in especially difficult conditions, and there are even cooled nozzles for large-scale engines.

- **Effect on emissions**

  Nozzle geometry has a direct effect on the engine's exhaust-gas emission characteristics.

  - The spray-hole geometry influence particulate and NO_x emissions.
  - The needle-seat geometry affects engine noise due to its effect on the pilot volume, i.e. the volume injected at the beginning of the injection process. The aim of optimizing spray-hole and seat geometry is to produce a durable nozzle capable of mass production to very tight dimensional tolerances.

This material is reserved for educational use only, not allowed for commercial use.
Forbidden to modify the content, and cite the document when use.

- Blind-hole geometry affects HC emissions, as previously mentioned. The designer can select and combine the various nozzle characteristics to obtain the optimum design for a particular engine and vehicle concerned.

For this reason, it is important that the nozzles are designed specifically for the vehicle, engine and fuel-injection system in which they are to be used. When servicing is required, it is equally important to use genuine OEM parts in order to ensure that engine performance is not impaired and exhaust-gas emissions are not increased.

For the test rig, diesel fuel and biodiesel were supplied to the injectors and both fuels return back to fuel tanks. The test method was developed to determine diesel injector wear and biodiesel injector wear after 510-hour test procedure.

The injectors of the direct injection design with corresponding nozzles. During the test, every 100 hour, all injectors were checked for spray pattern, leaks and opening pressure at the start of each test. The opening pressures were set to 260 ±5 bar absolute.

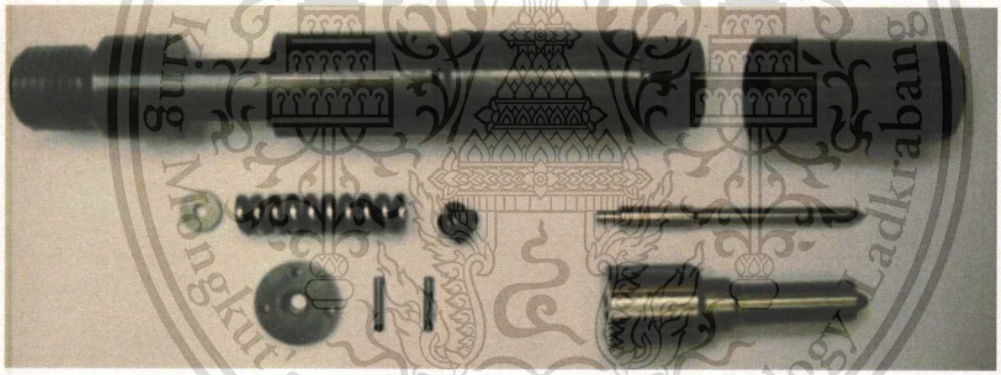

Figure 4.12 Dismantled Injector, the type is DSLA 154 P018, 6 holes

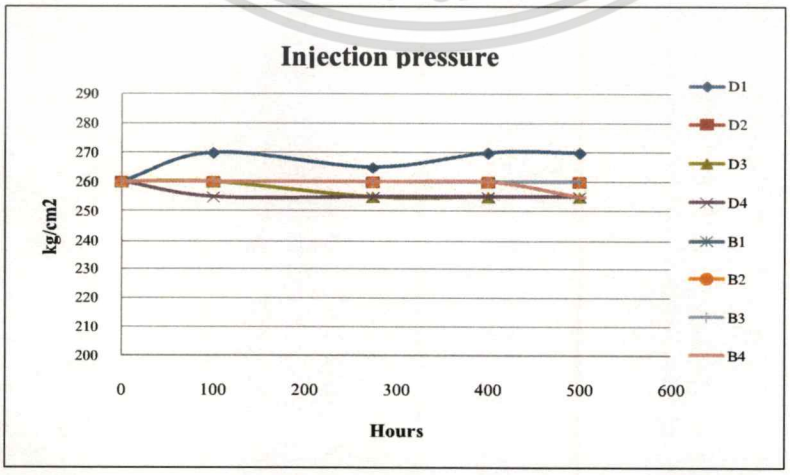

Figure 4.13 The injection pressure during the diesel fuel and B100 usage

This material is reserved for educational use only, not allowed for commercial use.
Forbidden to modify the content, and cite the document when use.

4.2.1 Weight of injector parts

The fuel system simulation has been parallel running on biodiesel and diesel fuel for a period of 510-hour. After that all injectors were dismantled and the main parts of injector were selected for analysis.

(a) (b) (c)

Figure 4.14 Parts of injector being investigated (a) injector housing, (b) needle, (c) spring

Table 4.4 Weight of injector parts (B100 and diesel) which is from the average of 10 values.

Parts of injectors	**Weight of injector parts**							
	Injectors of diesel system (4 injectors)				Injectors for biodiesel system (4 injectors)			
	D1	D2	D3	D4	B1	B2	B3	B4
Housing	23.0098 g	23.1020 g	22.8970 g	22.9273g	22.9671 g	23.0926 g	23.1471 g	23.0098 g
Needle	3.2198 g	3.2361 g	3.2182 g	3.2402 g	3.2104 g	3.2202 g	3.2262g	3.2251 g
Spring	4.3681 g	4.3728 g	4.3647g	4.4095 g	4.3988 g	4.3885 g	4.2998 g	4.4008 g

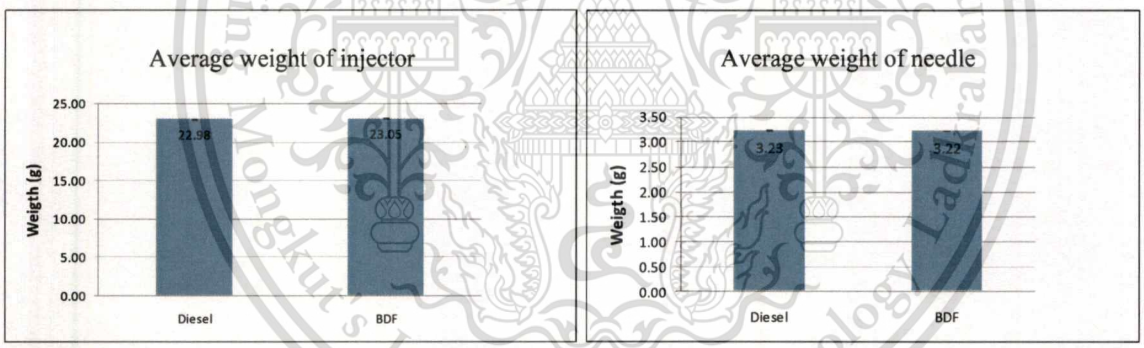

(a)

(b)

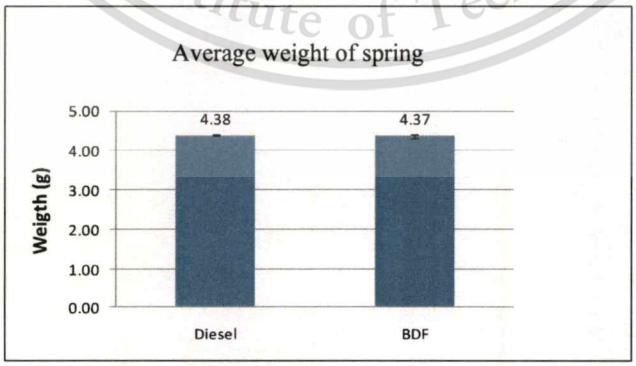

(c)

Figure 4.15 Weight of injector parts (a) average weight of injector, (b) average weight of needle, (c) average weight of spring

This material is reserved for educational use only, not allowed for commercial use.
Forbidden to modify the content, and cite the document when use.

4.2.2 Injector housing investigation

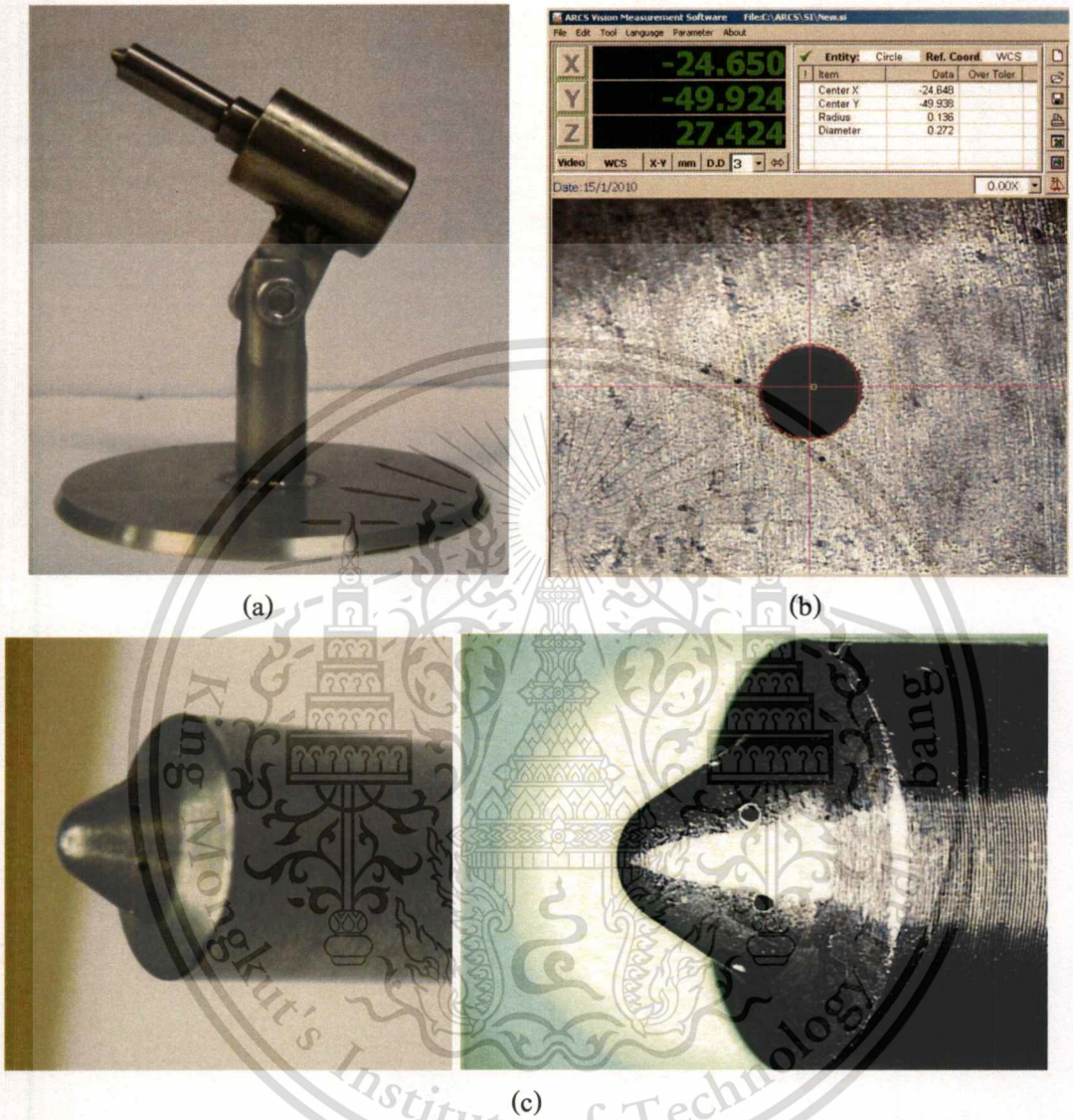

Figure 4.16 Injector orifice investigations (a) Injector housing is mounted at the jig which prepared for taking photo of orifice, (b) Orifice measurement, (c) Round tip.

Table 4.5 Injector orifice after diesel and biodiesel fuel usage

Injector housing	**Injection orifice after diesel and biodiesel fuel usage 510-hour**							
	Diesel system (4 injectors)				Biodiesel system (4 injectors)			
	D1	D2	D3	D4	B1	B2	B3	B4
Orifice (mm)	0.275	0.273	0.272	0.272	0.274	0.267	0.273	0.285

This material is reserved for educational use only, not allowed for commercial use.
Forbidden to modify the content, and cite the document when use.

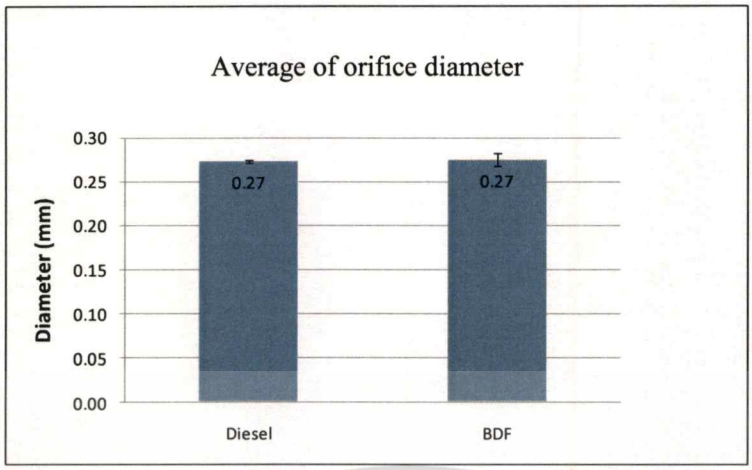

Figure 4.17 Average of orifice diameter

4.2.3 Needle investigation

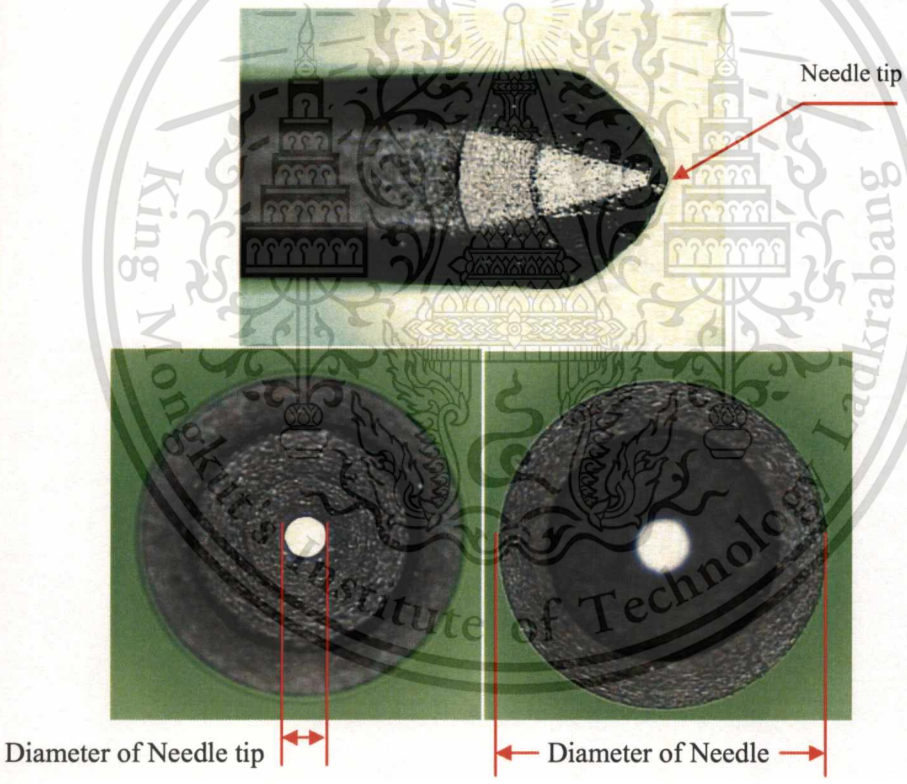

Figure 4.18 Needle investigations focusing on diameter of needle tip and diameter of needle after diesel and biodiesel fuel usage

This material is reserved for educational use only, not allowed for commercial use.
Forbidden to modify the content, and cite the document when use.

Table 4.6 Diameter of needle tip and diameter of needle after diesel and biodiesel fuel usage 510-hour

Needle	Diameter (mm)							
	Diesel system (4 injectors)				Biodiesel system (4 injectors)			
	D1	D2	D3	D4	B1	B2	B3	B4
Tip	0.392	0.424	0.434	0.419	0.414	0.431	0.404	0.429
Needle	3.213	3.204	3.208	3.208	3.208	3.213	3.206	3.210

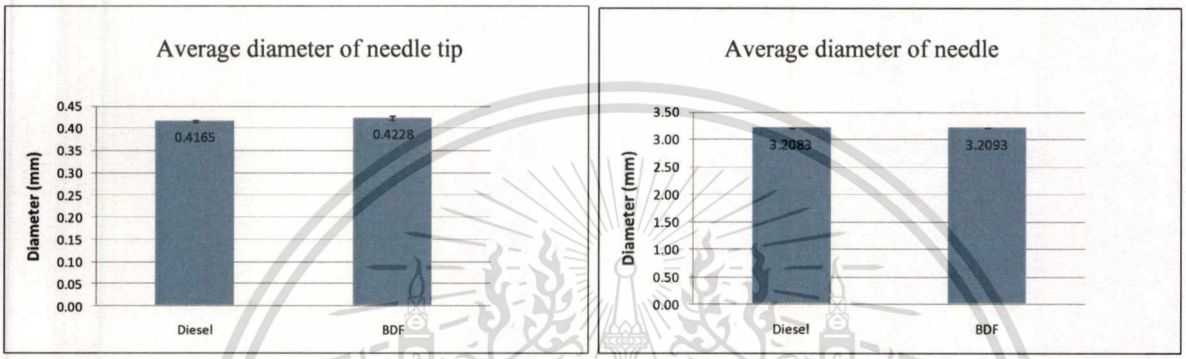

(a) (b)

Figure 4.19 Needle investigations

4.2.4 Spring investigation

Figure 4.20 Spring tester

This material is reserved for educational use only, not allowed for commercial use.
Forbidden to modify the content, and cite the document when use.

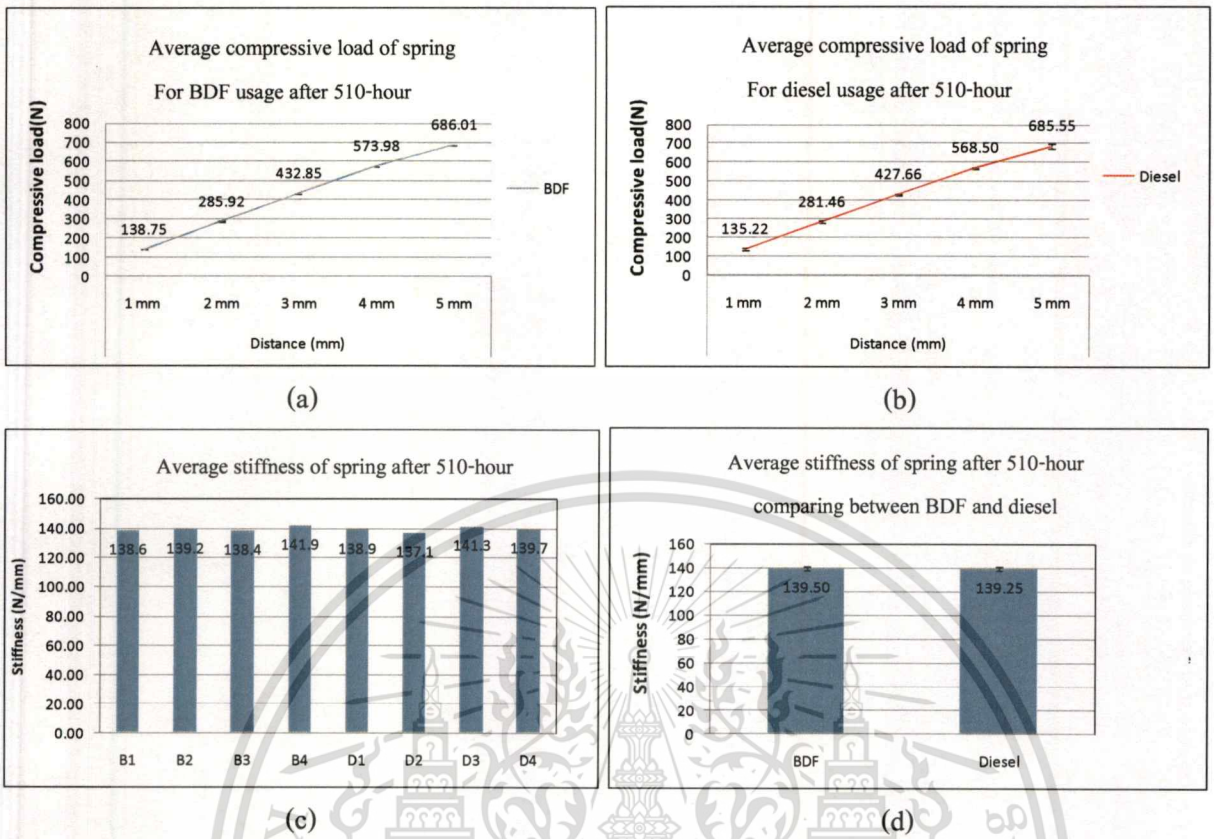

Figure 4.21 Spring results (a) Average compressive load of spring for BDF usage after 510-hour, (b) Average compressive load of spring for diesel usage after 510-hour, (c) Average stiffness of spring after 510-hour, (d) Average stiffness of spring after 510-hour comparing between BDF and diesel

4.3 Properties of B100 during 510 hour test.

This research had been target for 500 hours test equivalent to 50,000 kilometers for evaluation the durability of fuel system when use B100. Some biodiesel properties such as acid value, kinematic viscosity, oxidation stability and water content were measured during the experiment in order to monitor its degradation.

During the test biodiesel properties were investigated, the sample was collected every day, as shown in figure 4.22 (a) viscosity of B100 during test were meet standard ASTM D445 which must between 3.5-5 cSt/s, figure 4.22 (b) water content of B100 from initial to at 402 hours were meet standard ASTM 6304(< 500 ppm), figure 4.22 (c) oxidation stability of B100 from initial to at 402 hours were meet standard EN 14112 (> 10 hours), figure 4.22 (d) acid value of B100 from initial to at 402 hours were meet standard ASTM D 664 (<0.5 mg KOH/g) after at 402 hours B100 properties as show figure 4.22 (b) water content, figure (c) oxidation stability, figure (d) acid value were not meet standard because effect of humidity around the pump rig test which could collect water inside the fuel tanks, made B100 degrade.

This material is reserved for educational use only, not allowed for commercial use.
Forbidden to modify the content, and cite the document when use.

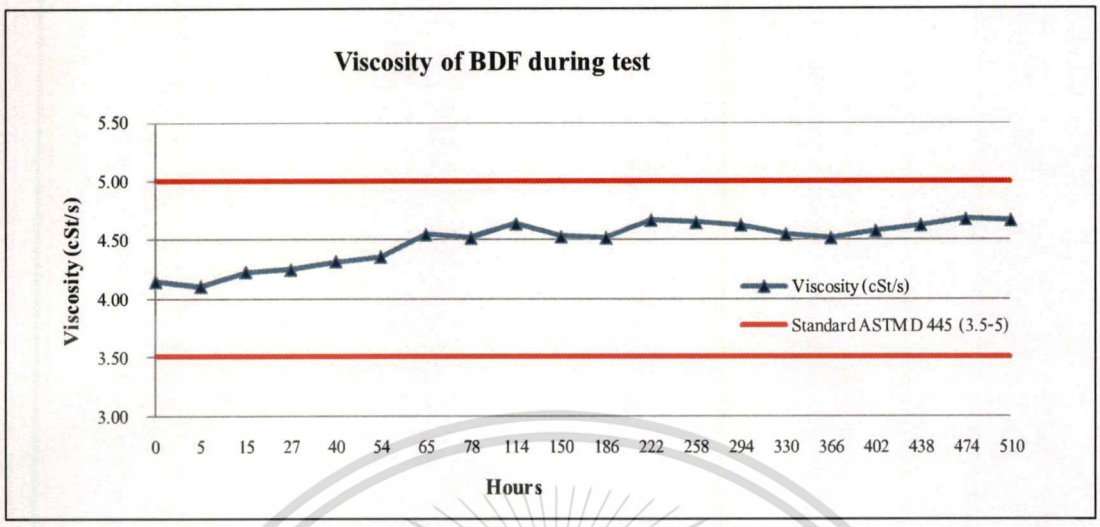

(a)

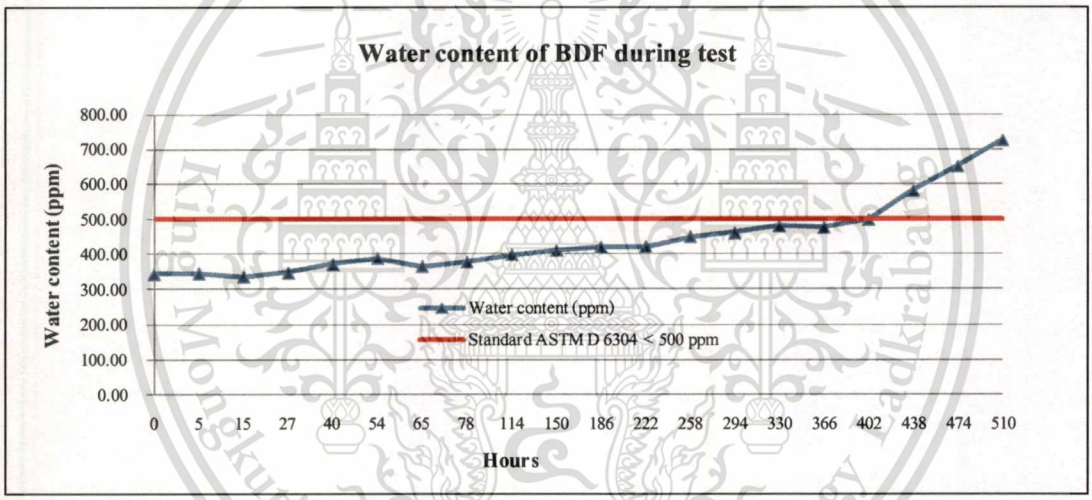

(b)

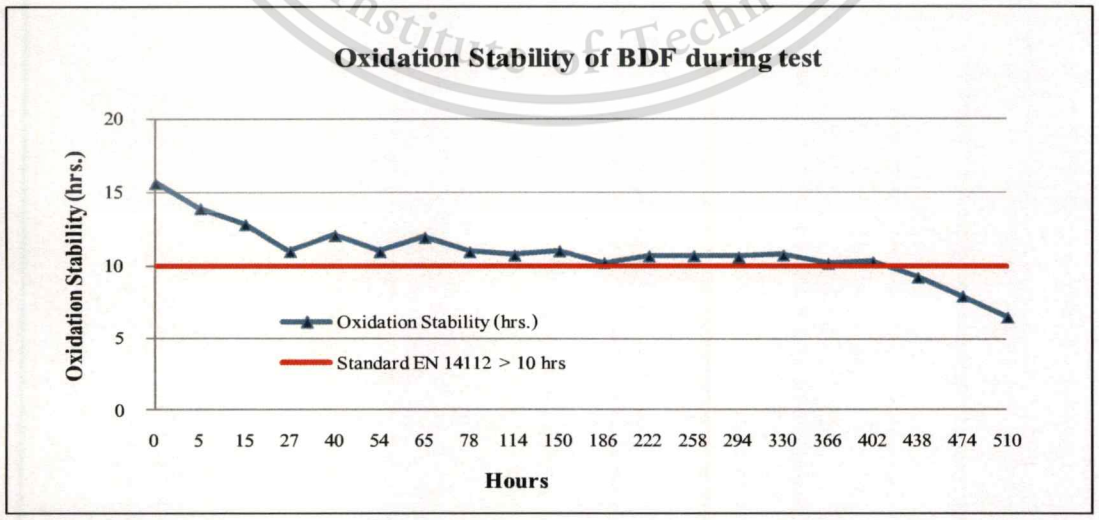

(c)

This material is reserved for educational use only, not allowed for commercial use.
Forbidden to modify the content, and cite the document when use.

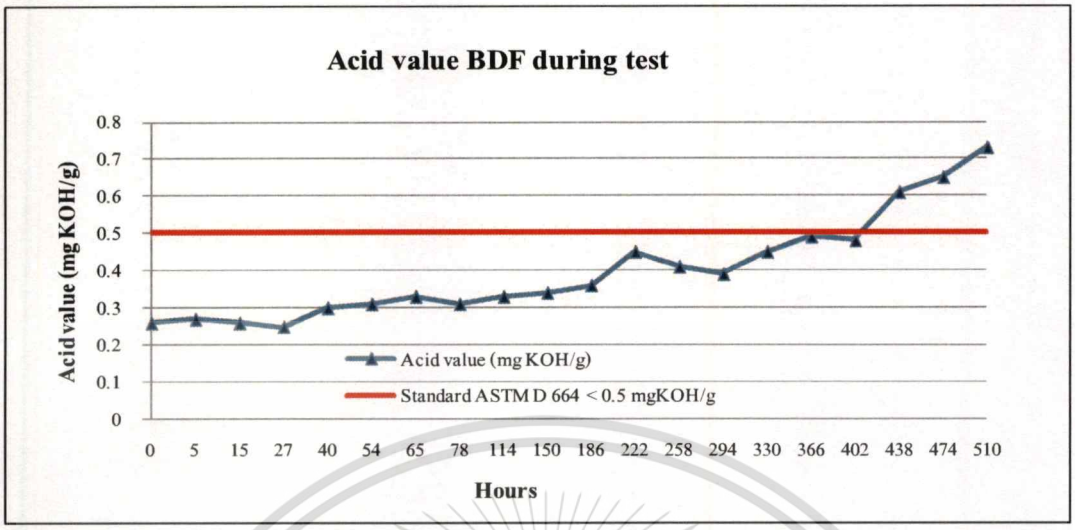

(d)

Figure 4.22 Properties of B100 during 510 hours test (a) water content of B100 during 510 hours test, (b) viscosity of B100 during 510 hours test, (c) oxidation stability of B100 during 510 hours test, (d) acid value of B100 during 510 hours test.

This material is reserved for educational use only, not allowed for commercial use.
Forbidden to modify the content, and cite the document when use.

CHAPTER 5

EFFECT OF B100 ON FUEL TANK

Immersion test of fuel tank and its methodology have been explained in Chapter 3. The fuel tank samples were divided into two sets, one was put indoor and another was left outside under the shade. These two sets represented two cases of vehicle that had been parked in garage and in open-air area for 3 months with some biodiesel left in their tanks. Instead of filling the whole tank with biodiesel, it was intended to fill those tanks with only 15 liter of biodiesel or 1/3 of the full tank capacity. This was in order to leave some air space inside the tank so the biodiesel could be reacted by oxygen and moisture, which depended on the environment condition. Since the tested fuel tanks did not have other accessories, such as returned/suction fuel lines, all openings were sealed with silicone to minimize humidity fluctuation from the surrounding environment. The fuel tank lid was also tightly closed. Every week, the biodiesel in each tank was sampled to monitor the biodiesel degradation. Its properties consisting of pH value, conductivity value, acid value and water content were measured. At the end of each month, one tank from each sample set was taken and cut for investigation by SEM and OM.

5.1 Testing Environment

The temperature and %relative humidity (%RH) around the outdoor storage area were measured by Temperature-Humidity sensor, as shown in Figure 5.1 (a) and (b), respectively. For the total time of 91 days covering the time of experiment, the temperature was around 30 degree Celsius, whereas the relative humidity was fluctuated between 30 to 60% with a maximum of 80% by the end of the first month. The temperature and %RH were monitored to ensure typical ambient environment in Thailand. Even though the fuel tank was closed-cap, the temperature outside the tank could affect the temperature of tested fuel via heat conduction.

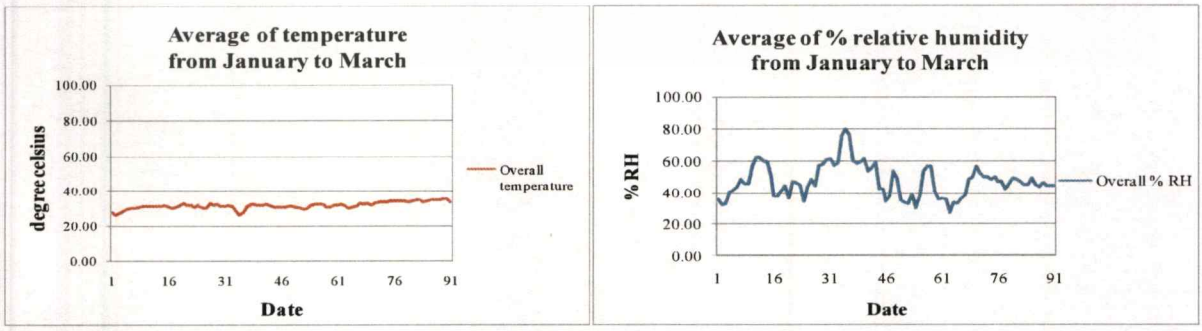

(a) (b)

Fig. 5.1: History plots of outdoor storage condition for 3 months showing: (a) temperature (degree Celsius); (b) %relative humidity.

This material is reserved for educational use only, not allowed for commercial use.
Forbidden to modify the content, and cite the document when use.

5.2 Biodiesel properties evaluation

Biodiesels from all tanks were sampled on a weekly basis for 12 weeks. The results are shown in Figure 5.2.

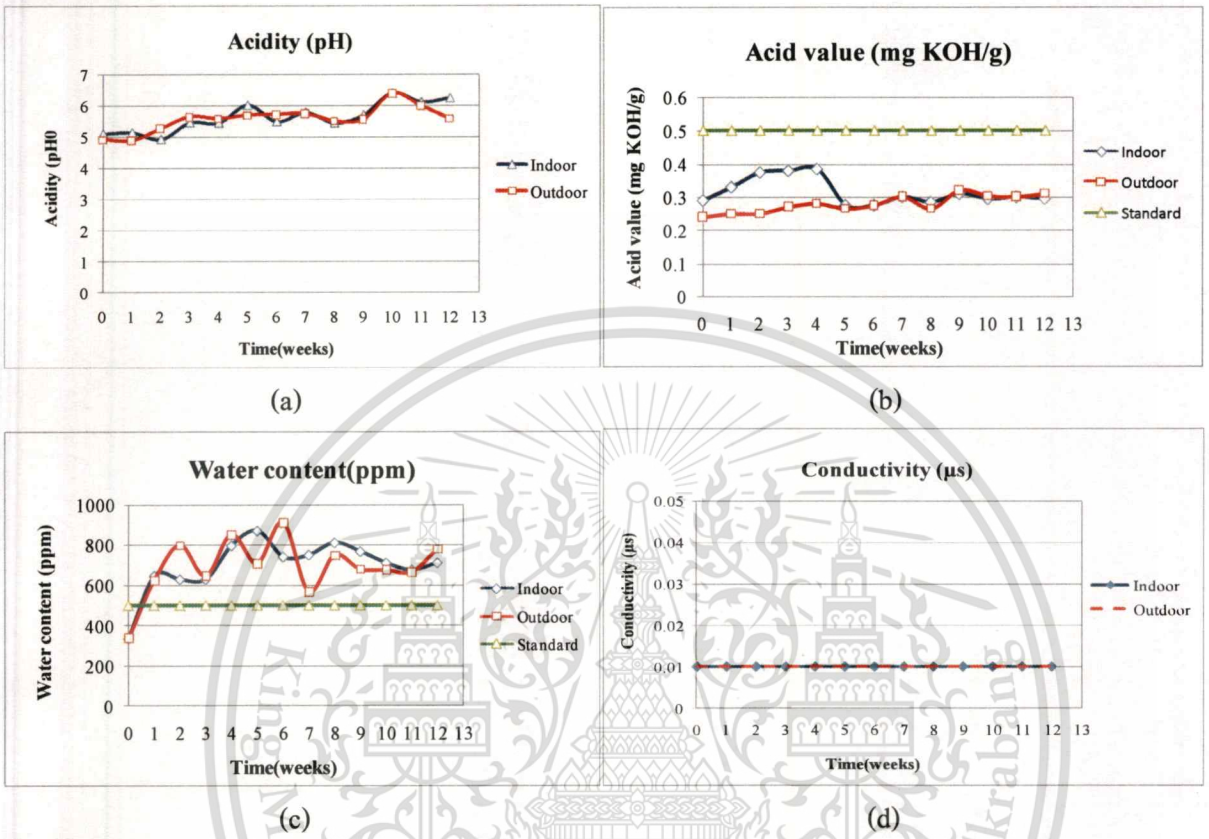

Fig. 5.2: Biodiesel property evaluations: (a) pH value, (b) acid value (mg KOH/g), (c) water content (ppm), and (d) conductivity value (µs).

Fig. 5.2(a) shows the results of pH values of biodiesel measured by pH meter. The pH values of the biodiesel stored in the fuel tanks placed both in the indoor and outdoor areas were gradually increasing with time. Since pH values of the biodiesel are lower than 7, these biodiesel samples were marked as acid substance. These results suggest that the fuel tank surface can be deteriorated from corrosion.

The acidity of biodiesel was also determined by automatic titrator, which could be compared to the standard value [1]. The results from Fig. 5.2(b) show that the acid values of the used biodiesels are slightly increased with time. These results agreed very well with the previous ones in Fig. 5.2(a). Nevertheless, the values were still within the specification of 0.5 mg KOH/g oil [1]. Please note that the acid values of the first 4 weeks are unusually high because of bad silicone sealing at a fuel tank cap during the experiment. The opening let more air flow in the tank, and accelerates the oil degradation, in other words, increases its oxidation rate. However, this had a very small effect on the water content.

This material is reserved for educational use only, not allowed for commercial use.
Forbidden to modify the content, and cite the document when use.

Large fluctuation of water content over the tested period in Fig. 5.2(c) could be explained by large fluctuation of %RH in the surrounding environment because each week sampling required re-opening and closing of fuel tank lid, which could allow moisture from the ambient surrounding to interfere humidity inside the fuel tank. Note also that water contents for both indoor and outdoor conditions exceed a standard limit of 500 ppm after 1st week, the first opening of fuel tank for sampling.

Poor dehydrating techniques during biodiesel processing or contacting with excessive water during transportation or storage can cause the results of water content in Fig.5.2(c) to be out of specification. The standard suggests a water content of less than 500 ppm in general B100 for blending with diesel and used in vehicles. The excess water can lead to corrosion and provides an environment for microorganisms. Fuel oxidation can also raise sediment levels. This test can be used in conjunction with acid number and viscosity to determine the oxidation level of the fuel during storage.

Corrosion level of the fuel tank may be observed by means of conductivity of biodiesel, which represents amount of metallic ions dissolved in the biodiesel. From Fig. 5.2(d), the conductivity of biodiesel is rather constant. However, later experiment shows some corrosion inside the fuel tank. This can be implied that this measuring tool is not suitable for this experiment.

5.3 Fuel tank corrosion.

5.3.1 Area of corrosion

The corrosion of fuel tanks that contained biodiesel fuel located both indoor and outdoor area as shown in Fig.1 was investigated and shown in Fig.5.3. It can be found that for both locations, signs of corrosion appear all over the inside surface walls, especially in the areas of welding joints and metal sheets. Within the first month, fuel tanks, which have been placed indoors, have more corrosive area than those placed outdoor. This is caused by the effect of oxygen in the air that leaks into the tank through the tank lid. By the end of the second month, the corrosion of the tank from both locations are not significantly different. The corrosion of fuel tank placed outdoor has been accelerated to compete the indoor's as can be seen by larger area of corrosion in Fig. 5(f) than in Fig. 5(c). The main corrosion takes place on the metal plate inside biodiesel tank. This indicates the corrosion from higher evaporated moisture concentration inside the tank that caused by a larger temperature difference between daytime and nighttime outside the building.

This material is reserved for educational use only, not allowed for commercial use.
Forbidden to modify the content, and cite the document when use.

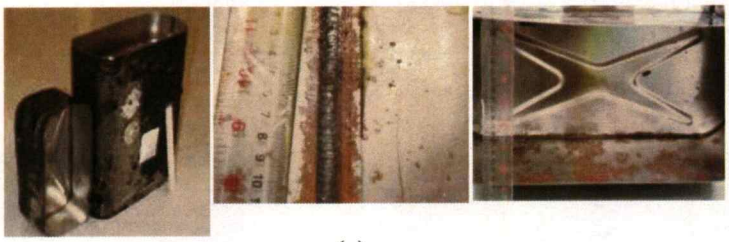

(a)

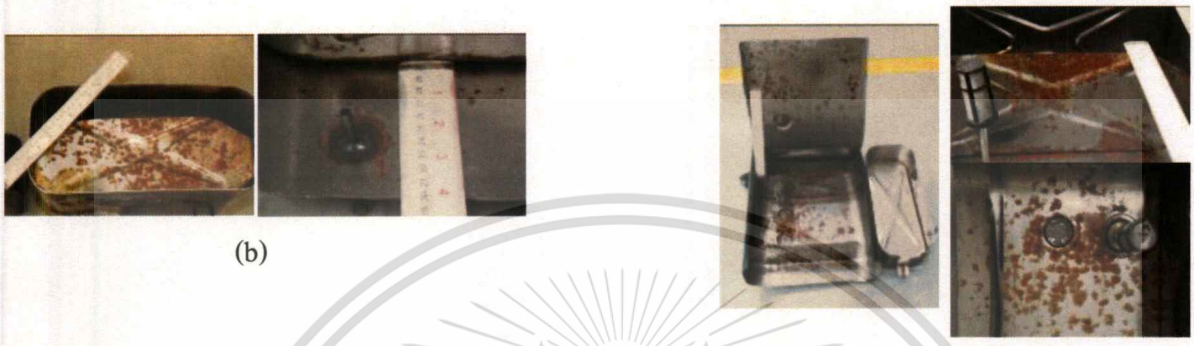

(b)

(c)

(d)

(e)

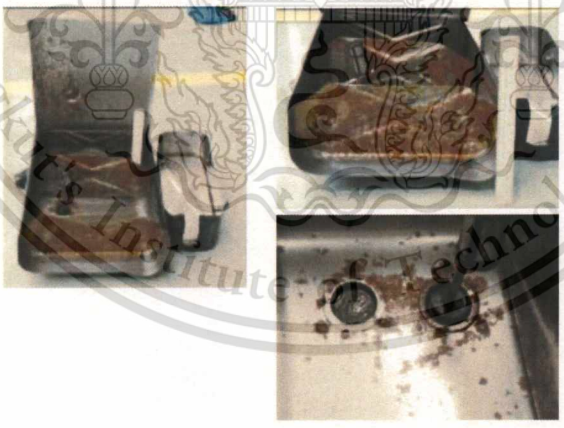

(f)

Fig. 5.3: The corrosion of fuel tank after containing biodiesel for : (a) 1 month at the indoor area, (b) 2 months at the indoor area, (c) 3 months at the indoor area (d) 1 month at the outdoor area, (e) 2 months at the outdoor area, and (f) 3 months at the outdoor area.

This material is reserved for educational use only, not allowed for commercial use.
Forbidden to modify the content, and cite the document when use.

5.3.2 Fuel tank observation by Scanning Electron Microscope (SEM).

Using SEM Technique, the biodiesel tank surfaces where corrosion occurred were evaluated in order to obtain more detailed information. Fig.5.4 and 5.5 show the surface of fuel tanks placed inside and outside the building, respectively at the resolution of 15x to 200,000x times to the original. It can be seen that the further the biodiesel has been left in the tanks, the larger and thicker corrosion products are detected. The results are even worse when the tanks are placed outdoor.

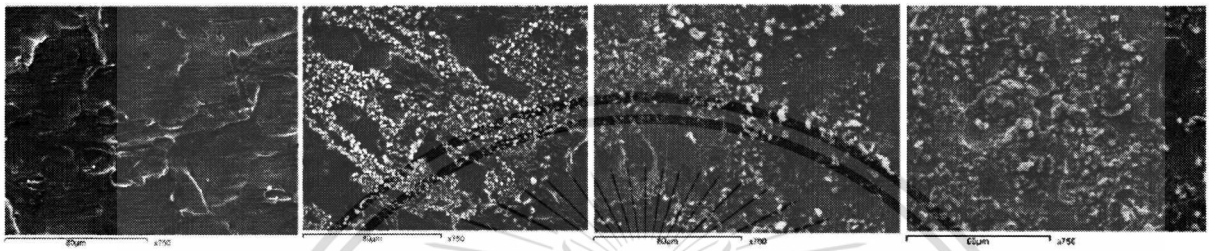

(a) (b) (c) (d)

Fig. 5.4: The corrosion of fuel tanks at indoor area taken by SEM during and after containing biodiesel for 3 months, (a) smooth surface without corrosion, (b) corrosion surface after 1 month, (c) corrosion surface after 2 months, (d) corrosion surface after 3 months.

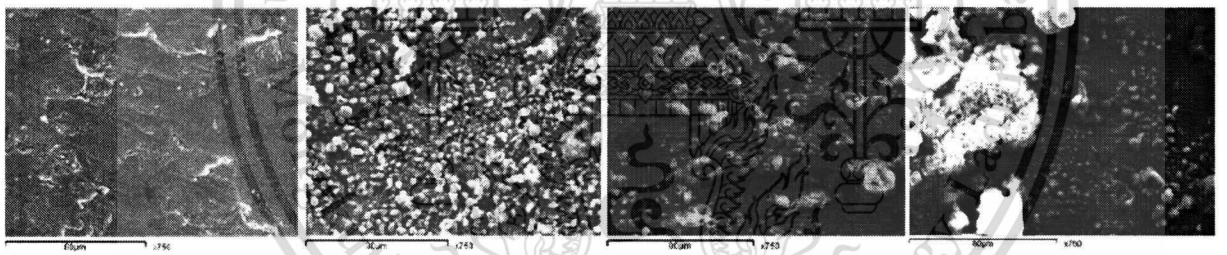

(a) (b) (c) (d)

Fig. 5.5: The corrosion of fuel tanks at the outdoor area taken by SEM during and after containing biodiesel for 3 months, (a) smooth surface without corrosion, (b) corrosion surface after 1 month, (c) corrosion surface after 2 months, (d) corrosion surface after 3 months.

5.3.3 Analysis of chemical components by EDS technique

The elemental composition of the corrosion products in Fig. 8 and Fig. 9 were determined by using EDS technique. Agree with the previous results in Fig.6 and 7, the results show that the high level of Iron (Fe) and Oxygen (O), which are the main components of metal rust (Fe_2O_3), can be detected in the corroded samples.

This material is reserved for educational use only, not allowed for commercial use.
Forbidden to modify the content, and cite the document when use.

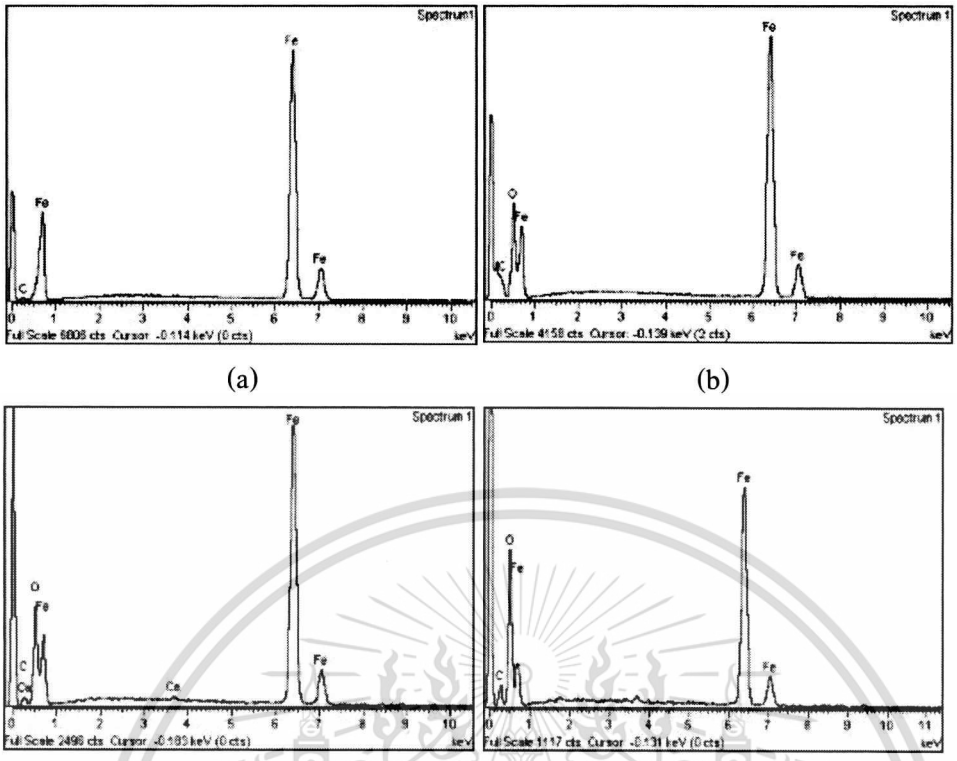

Fig.5.6: The chemical components of fuel tank by EDS technique at outdoor area , (a) the elemental compositions of the corrosion product for non-corroded surface, (b) the elemental compositions of the corrosion product after 1 month, (c) the elemental compositions of the corrosion product after 2 months, (d) the elemental compositions of the corrosion product after 3 months.

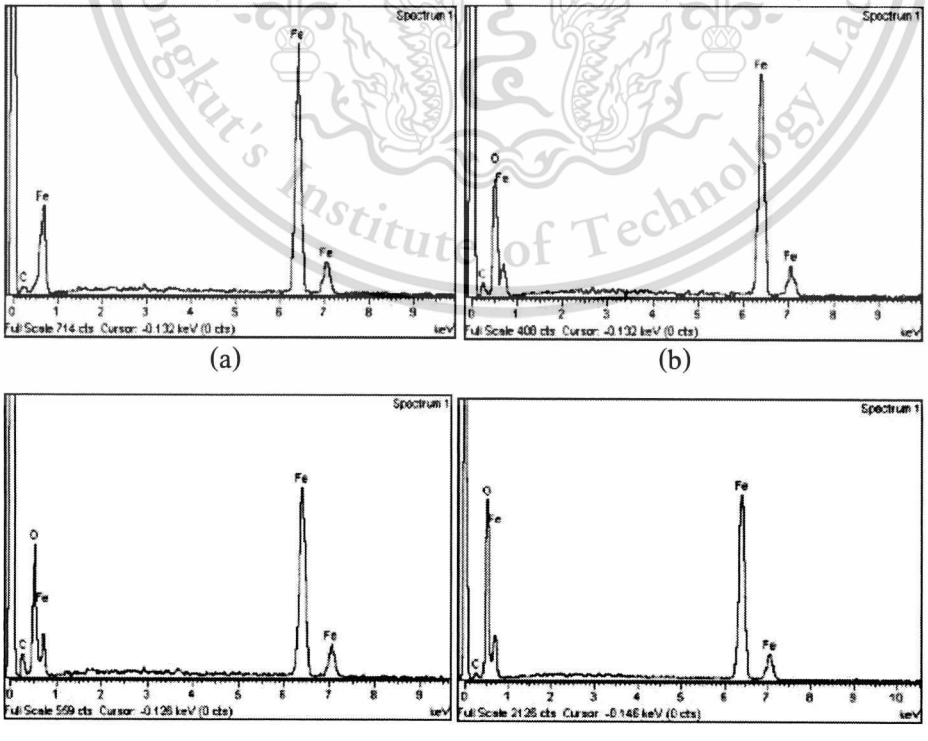

This material is reserved for educational use only, not allowed for commercial use.
Forbidden to modify the content, and cite the document when use.

Fig. 5.7: The chemical components of fuel tank by EDS technique at outdoor area , (a) the elemental compositions of the corrosion product for non-corroded surface, (b) the elemental compositions of the corrosion product after 1 month, (c) the elemental compositions of the corrosion product after 2 months, (d) the elemental compositions of the corrosion product after 3 months.

5.3.4 Corrosion of fuel tanks by using Reflected Light Microscope

To determine the thickness of corrosion area, the samples were cross sectioned and inspected by Reflected Light Microscope as can be seen in Fig.10 and 11. These show that a little loss of metal has been occurred from corrosion areas. These results are corresponding to the results in Fig. 4(d), in which the biodiesel conductivity was hardly detected. However, these results also suggest more metal loss in the case of outdoor location than the indoor one.

(a) (b) (c) (d)

Fig. 5.8: The cross section of fuel tank after containing biodiesel by using Reflected Light Microscope at the indoor area (a) the cross section of fuel tank for smooth surface, (b) the cross section of fuel tank after 1 month, (c) the cross section of fuel tank after 2 months, (d) the cross section of fuel tank after 3 month.

(a) (b) (c) (d)

Fig. 5.9: The cross section of fuel tank after containing biodiesel by using Reflected Light Microscope at the outdoor area :(a) the cross section of fuel tank for smooth surface, (b) the cross section of fuel tank after 1 month, (c) the cross section of fuel tank after 2 months, (d) the cross section of fuel tank after 3 months.

This material is reserved for educational use only, not allowed for commercial use.
Forbidden to modify the content, and cite the document when use.

CHAPTER 6

CONCLUSIONS AND SUGGESTIONS

6.1 Conclusions

6.1.1 The effect of B100 on fuel supply line

This research had been target for 510 hours test equivalent to 50,000 kilometers for evaluation the durability of fuel system when use B100. After 510-hour test, various parts of fuel system was disassembled, both of diesel and B100 system were investigated. The effects of B100 on fuel supply line can be concluded from this study as followings.

1) Weight of metal parts both of diesel and B100 system including of injector housing, needle, spring, delivery valve-holder, pump plunger are not significant different
2) Injector hole of B100 group and diesel group is not significant different. (0.6% different)
3) Injection pressure of B100 group and diesel group is not significant different which are within the operate range of 260 ±10 bar.
4) Stiffness of injector springs after using B100 and diesel for 510-hour is not significant different. (0.18% different)
5) Results of needle's diameters and needle tip's diameter show no significant different. (diameter of needle tip 1.5%different, diameter of needle 3.2%different)
6) Diameter of delivery-valve holder is not significant different. (Valve seat ID 0.015%different, OD 0.65%different)
7) Surface Roughness (Ra) of B100 group and diesel group is not significant different. (3.385%different)
8) Viscosities of B100 during test are within the standard range of 3.5-5 cSt/s according to ASTM D445.
9) Water content of B100 from initial test to 402 hours are within standard according to ASTM 6304(< 500 ppm), oxidation stability of B100 from initial test to 402 hours are within standard according to EN 14112 (> 10 hours), acid value of B100 from initial test to 402 hours are within standard according to ASTM D 664 (<0.5 mg KOH/g) but after 402 hours B100 properties water content, oxidation stability and acid vale are out of specification as a result of humidity fluctuation and temperature during test.

This material is reserved for educational use only, not allowed for commercial use.
Forbidden to modify the content, and cite the document when use.

6.1.2 The effect of B100 on fuel tank can be concluded from this study as followings.

1) Acid values of B100 were not significantly affected by the increased exposure time of fuel tanks to atmospheric environment, and still meet Thailand biodiesel standard following the Ministry of Energy.(below o.5 mg KOH/g)
2) Water content of B100 in the fuel tanks was higher than 500 ppm (standard), which might enhance corrosion of the fuel tanks.
3) Temperature fluctuation was a significant parameter of environments to influence corrosion behaviour of the fuel tanks.
4) Uniform corrosion was found on the inner surface of fuel tanks, in particular at susceptible areas of welds that the high level of Iron (Fe) and Oxygen (O), which are the main components of metal rust (Fe_2O_3), can be detected in the corroded samples.
5) More severe corrosion was obtained for the fuel tanks exposed to the outdoor environment.

6.2 Suggestions

6.2.1 Biodiesel (B100)

This section will describe considerations for B100 fuels. The considerations for storing, handling, and using B100 are very different than for B20 or lower biodiesel blend. This research can suggest only B100.

B100 has physical and chemical properties similar to petroleum based diesel and can in some cases be used in existing diesel applications with little or no modification to the engine or fuelling system. While B100 can be used as a pure fuel in diesel applications, there are important differences between B100 and conventional diesel fuels that must be taken into consideration when handling or using B100.

- B100 is a good solvent. It may loosen and/or dissolve sediments in fuel tanks and fuelling systems left by conventional diesel over time. If your system contains sediments, you should clean your existing tanks and fuel system before handling or using B100.
- B100 freezes at higher temperatures than most conventional diesel fuel and this must be taken into account if handling or using B100. Most B100 starts to cloud at between 35°F and 60°F, so heated fuel lines and tanks may be needed even in moderate climates. As B100 begins to gel, the viscosity also begins to rise, and it rises to levels much higher than most diesel fuel, which can cause increased stress on fuel pumps and fuel injection systems. Cold weather properties are the biggest reason many people use biodiesel blends.
- B100 is not compatible with some hoses and gaskets. B100 may soften and degrade certain types of rubber compounds found in hoses and gaskets and may cause them to leak and become

Forbidden to modify the content, and cite the document when use.

degraded to the point they crumble and become useless. This could cause a fuel spill on a hot engine, could ruin a fuel pump, or could result in filter clogging as the hose material gradually wears away. If using B100, extreme care should be taken to ensure that any part of the fuel system that touches the fuel is compatible with B100. Some systems already have biodiesel resistant materials but many do not because these materials are usually slightly more expensive.

- B100 is not compatible with some metals and plastics. Biodiesel will form high sediment levels if contacted for long periods of time with copper or copper containing metals (brass, bronze) or with lead, tin, or zinc (i.e. galvanized surfaces). These high sediment levels may cause filter clogging. Diesel systems are not supposed to contain these metals, but sometimes they can occur anyway. In addition, B100 may permeate some typical types of plastics (polyethylene, polypropylene) over time and they should not be used for storing B100.

There are other physical or chemical properties where biodiesel is substantially different from petroleum diesel and where these differences provide significant benefits. Biodiesel has significantly lower sulfur than today's diesel fuel, while providing a significant increase in lubricity. Most B100 already meets the EPA's new rule requiring all on-road diesel fuel to contain less than 15 ppm sulfur in 2006. The future 15 ppm diesel Ultra low sulfur diesel or ULSD can create lubricity problems as the new refining process tends to reduce the natural lubricity of diesel. Pure biodiesel, or biodiesel blended with ULSD restores fuel lubricity in levels as low as 1% or 2% biodiesel. Biodiesel also contains 11% oxygen by weight, as well as a slightly higher cetane number, which provides for more complete combustion and a reduction in most emissions.

6.2.2 Quality Specifications

B100 for this research are meet Thai standard (DOEB, 2007) but during the test of B100 on fuel system to at 402 hours, B100 is degraded because effect of humidity on fuel tank around pump test rig.

- Water and sediment refers to the presence of free water droplets and sediment particles. The allowable level for B100 is set at the same level allowed for conventional diesel fuel. Poor drying techniques during manufacturing or contact with excessive water during transport or storage can cause B100 to be out of specification for water content. Excess water can lead to corrosion and provides an environment for microorganisms. Fuel oxidation can also raise sediment levels, so this test can be used in conjunction with acid number and viscosity to determine if fuels have oxidized too much during storage.

This material is restricted for educational use only, not allowed for commercial use.
Forbidden to modify the content, and cite the document when use.

- A minimum viscosity is required for some engines because of the potential for power loss caused by injection pump and injector leakage. This is not an issue for B100 and the minimum is set at the same level as for petroleum diesel. The maximum viscosity is limited by the design of engine fuel injection systems. Higher viscosity fuels can cause poor fuel combustion that leads to deposit formation as well as higher in-cylinder penetration of the fuel spray which can result in elevated engine oil dilution with fuel. The maximum allowable viscosity in ASTM D975 for No. 2 diesel is 4.1 mm^2/s at 40°C although most engines are designed to operate on fuels of higher viscosity than 4.1 mm^2/s. ASTM D6751 allows for slightly higher viscosity than D975 primarily because that is where the normal viscosity of B100 lies. Consult your operational manual or your engine manufacturer if you intend to use a B100 in your engine that has a higher viscosity than what the engine or fuel system was designed for.
- Acid number for biodiesel is primarily an indicator of free fatty acids (natural degradation products of fats and oils) and can be elevated if a fuel is not properly manufactured or has undergone oxidative degradation. Acid numbers higher than 0.80 have been associated with fuel system deposits and reduced life of fuel pumps and filters.
- The D6751 specification also includes the following workmanship statement: "The biodiesel fuel shall be visually free of undissolved water, sediment, and suspended matter." B100 should be clear, although it may come in a variety of colors. Biodiesel color does not predict fuel quality.
- Currently there are ASTM specifications for B100 (D6751) and for petrodiesel (D975), but there is not a separate approved specification for biodiesel blends. Current practice to insure the quality of biodiesel blends is to use petrodiesel meeting D975 and biodiesel meeting D6751 prior to blending. Once blended, it is very difficult to determine the quality of the B100 used to make the blend. ASTM specifications for finished biodiesel blends up to B20 are under development, so please check with ASTM or the National Biodiesel Board (NBB) for updated information.

6.2.3 B100 Material Compatibility

B100 will degrade, soften, or seep through some hoses, gaskets, seals, elastomers, glues, and plastics with prolonged exposure. Some testing has been done with materials common to diesel systems but more data is needed on the wide variety of grades and variations of compounds that can be found in these systems, particularly with B100 in U.S. applications. Nitrile rubber compounds, polypropylene, polyvinyl, and Tygon materials are particularly vulnerable to B100. Before handling or using B100, contact the equipment vendor or OEM and ask if the equipment is suitable for B100 or Biodiesel. In some

This material is reserved for educational use only, commercial use is prohibited.
Forbidden to modify the content, and cite the document when use.

cases, the vendor may need the chemical family name for biodiesel (i.e. the methyl esters of fats and oils) to look up the information or even the exact chemical name of some of the biodiesel components such as methyl oleate, methyl linoleate, methyl palmitate, or methyl stearate. There have not been significant material compatibility issues with B20.

If your existing equipment or engine components are not compatible with B100, they should be replaced with those that are. Materials such as Teflon, Viton, fluorinated plastics, and Nylon are compatible with B100. B100 suppliers and equipment vendors should be consulted to determine material compatibility. Also consult other B100 vendors in other regions of the country to see what problems they may have experienced and what kind of replacement materials they are using. It is advisable to set up a monitoring program to visually inspect the equipment once a month for leaks, seeps, and seal decomposition. It would be wise to continue these inspections even after one year, as the experience is still relatively limited with B100.

Older vehicles, manufactured before approximately 1993, are more likely to contain seals, gaskets, etc., that will be affected by B100 over long periods of time. Modern rebuild kits or engines after 1993 may contain biodiesel compatible materials, but not always. Ask your dealership for recommendations.

Most tanks designed to store diesel fuel will store B100 with no problem. Acceptable storage tank materials include aluminum, steel, fluorinated polyethylene, fluorinated polypropylene, Teflon®, and most fiberglass. If in doubt, contact the tank vendor or check the National Biodiesel Board web site.

This research use 45-litre fuel tanks, normally used in 4-wheel truck, obtained from Sammitr Motor Co., Ltd were used in this experiment. This type of fuel tank is made of cold-rolled steel and may be corroded when contacting with moisture and degraded biodiesel. Others type of fuel tanks should to research

Brass, bronze, copper, lead, tin, and zinc may accelerate the oxidation of diesel and biodiesel fuels and potentially create fuel insolubles (sediments) or gels and salts when reacted with some fuel components. Lead solders and zinc linings should be avoided, as should copper pipes, brass regulators, and copper fittings. The fuel or the fittings will tend to change color and insolubles may plug fuel filters. Affected equipment should be replaced with stainless steel, carbon steel, or aluminium.

This research is simulation use B100 on fuel system of direct injection diesel engine, for common-rail engine should to research.

This material is reserved for educational use only, not allowed for commercial use.
Forbidden to modify the content, and cite the document when use.

REFERENCES

[1] Department of Energy Business (2007). Specification of commercial Fuels http://www.doeb.go.th/th/law/law_main_quality.html.

[2] Savita Kaul, R.C. Saxena, Ajay Kumar, M.S.Negi,A.K. Bhatnagar ,H.B. Goyal, A.K. Gupta, "Corrosion behavior of biodiesel from seed oils of Indian origin on diesel engine parts", Indian Institute of Petroleum, Dehradun, India.

[3] Wimonrat Trakarnpruk, Suriya Porntangjitlikit, "Palm oil biodiesel synthesized with potassiumloaded calcined hydrotalcite and effect of biodiesel blend on elastomer properties" Petrochemistry and Polymer Science, Department of Chemistry, Faculty of Science, Chulalongkorn University, Bangkok 10330, Thailand.

[4] K. Shaine Tyson, "Biodiesel Handling and Use Guidelines", National Renewable Energy Laboratory, U.S. Department of Energy.

[5] Nathan Hanson, Thomas Devens, Colin Rohde, Adam Larson, "The Effects of E20 on Automotive Fuel Pumps and Sending Units", Minnesota State Uniersity, Mankato.

[6] Bosch, R., **Diesel-engine management**, Stuttgart, Germany; Warrendale, PA : SAE Society of Automotive Engineers, 1999.

[7] Cengel, A., Y. and Boles A., M., **Thermo dynamics**, Second Edition (International Edition), McGraw-Hill, Inc., 1994.

[8] Challen, B. and Baranescu, r., **Diesel engine reference book**, 2nd ed., Oxford, Butterworth-Heinemann, 1999.

[9] Yamane, K., Kato, T., Okutani, H., and Shimamoto, Y., "Effect of Refining Process in Biodiesel Fuel Production on Fuel Properties, Diesel Engine Performance and Emissions," SAE Technical Paper, 2003.

This material is reserved for educational use only, not allowed for commercial use.
Forbidden to modify the content, and cite the document when use.

[10] Mongkol Jampamee, "Effects of biodiesel blended fuels on exhaust emissions of diesel engine ",Master. Science (Petrochemistry and Polymer Science), Chulalongkorn University. Bangkok (Thailand), 2004.

[11] B Terry, "Impact of biodiesel blend (B5,B20) on fuel system component durability", The Associated OctelCompany Limited , United Kingdom, 2005.

[12] Herbert H. Uhlig and R. Winston Revie, "Corrosion and Corrosion Control An Introduction to Corrosion Science and Engineering Third Edition." John Wiley & Sons, Inc. pp. 3-15, 1991.

King Mongkut's Institute of Technology Ladkrabang

This material is reserved for educational use only, not allowed for commercial use.
Forbidden to modify the content, and cite the document when use.

APPENDIX A

Proceeding

Appendix A-1: The 2nd Thammasat University International Conference on Chemical, Environmental and Energy Engineering (TU-ChEEE 2009), Bangkok, Thailand, March 3-4, 2009.

This material is reserved for educational use only, not allowed for commercial use.
Forbidden to modify the content, and cite the document when use.

APPENDIX B

ASTM STANDARD

B-1: Flash Point (ASTM D93)

This flash point test method is a dynamic test method, which depends on specified rates of heating to be able to meet the precision of the test method. The rate of heating may not in all cases give the precision quoted in the test method because of the low thermal conductivity of some materials. Flash point values are a function of the apparatus design, the condition of the apparatus used, and the operational procedure carried out. Flash point can therefore only be defined in terms of a standard test method, and no general valid correlation can be guaranteed between results obtained by different test methods, or with test apparatus different from that specified. The apparatus specifications are showed in Figure D1.

These test methods cover the determination of the flash point of petroleum products in the temperature range from 40 to 360°C by a manual Pensky-Martens closed-cup apparatus or an automated Pensky-Martens closed-cup apparatus. There are two procedures for this test method. First, procedure A is applicable to distillate fuels (diesel, kerosene, heating oil, turbine fuels), new lubricating oils, and other homogeneous petroleum liquids not included in the scope of Procedure B. Second, Procedure B is applicable to residual fuel oils, cutback residua, used lubricating oils, mixtures of petroleum liquids with solids, petroleum liquids that tend to form a surface film under test conditions, or is petroleum liquids of such kinematic viscosity that they are not uniformly heated

For calculating flash point value, the barometric pressure used in this calculation is the ambient pressure for the laboratory at the time of the test. Many aneroid barometers, such as those used at weather stations and airports, are precorrected to give sea level readings and would not give the correct reading for this test. Observe and record the ambient barometric pressure at the

This material is reserved for educational use only, not allowed for commercial use.
Forbidden to modify the content, and cite the document when use.

time of the test. When the pressure differs from 101.3 kPa (760 mm Hg), correct the flash point as follows:

$$\text{Corrected flash point} = C + 0.25\,(101.3 - K) \quad \text{(b1)}$$

$$\text{Corrected flash point} = F + 0.06\,(760 - P) \quad \text{(b2)}$$

$$\text{Corrected flash point} = C + 0.033\,(760 - P) \quad \text{(b3)}$$

Where: C = observed flash point, °C

F = observed flash point, °F

P = ambient barometric pressure, mm Hg, and

K = ambient barometric pressure, kPa.

After correction for barometric pressure, round the temperature to the nearest 0.5°C (1°F) and record

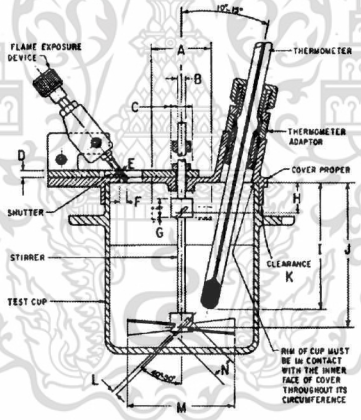

Figure D1 Test Cup and Cover Assembly.

B-2: Copper Strip Corrosion (ASTM D130)

This test method covers the determination of the corrosiveness by copper of aviation gasoline, aviation turbine fuel, automotive gasoline, cleaners solvent, kerosine, diesel fuel, distillate fuel oil, lubricating oil, and natural gasoline or other hydrocarbons having a vapor pressure no greater than 124 kPa (18 psi) at 37.8°C. Interpret the corrosiveness of the sample in accordance with one of the classifications of the ASTM Copper Strip Corrosion Standard as listed in Table D1.

This material is reserved for educational use only, not allowed for commercial use.
Forbidden to modify the content, and cite the document when use.

Table B2 Copper strip classifications (ASTM D130)

Classification	Designation	Description[A]
Freshly polished strip	...	[B]
1	slight tarnish	a. Light orange, almost the same as freshly polished strip b. Dark orange
2	moderate tarnish	a. Claret red b. Lavender c. Multicolored with lavender blue or silver, or both, overlaid on claret red d. Silvery e. Brassy or gold
3	dark tarnish	a. Magenta overcast on brassy strip b. Multicolored with red and green showing (peacock), but no gray
4	corrosion	a. Transparent black, dark gray or brown with peacock green barely showing b. Graphite or lusterless black c. Glossy or jet black

[A] The ASTM Copper Strip Corrosion Standard is a colored reproduction of strips characteristic of these descriptions.
[B] The freshly polished strip is included in the series only as an indication of the appearance of a properly polished strip before a test run; it is not possible to duplicate this appearance after a test even with a completely noncorrosive sample.

B-3: Carbon Residue (ASTM D524)

This test method covers the determination of the amount of carbon residue left after evaporation and pyrolysis of an oil, and it is intended to provide some indication of relative coke-forming propensity. This test method is generally applicable to relatively nonvolatile petroleum products, which partially decompose on distillation at atmospheric pressure. This test method also covers the determination of carbon residue on 10% (v/v) distillation residues. Petroleum products, containing ash-forming constituents as determined by Test Method D482, will have an erroneously high carbon residue, depending upon the amount of ash formed.

Calculate the carbon residue of the sample or of the 10 % distillation residue as follows:

$$\text{Carbon residue} = (A \times 100)/W \quad \text{(b4)}$$

where: A = mass of carbon residue, gram, and

W = mass of sample, gram.

B-4: Kinematic Viscosity (ASTM D445)

Dynamic viscosity (μ), viscosity describes a fluids resistance to flow. Dynamic viscosity (sometimes referred to as Absolute viscosity) is obtained by dividing the Shear stress by the rate of shear strain. The units of dynamic viscosity are: force/area x time. The Pascal unit (Pa) is used

This material is reserved for educational use only, not allowed for commercial use.
Forbidden to modify the content, and cite the document when use.

to describe pressure or stress = force per area. This unit can be combined with time (sec) to define dynamic viscosity, which is μ = Pa•s (1.0 Pa•s = 10 Poise = 1,000 Centipoise).

Kinematic Viscosity (ν), sometimes viscosity is measured by timing the flow of a known volume of fluid from a viscosity measuring cup. The timings can be used along with a formula to estimate the kinematic viscosity value of the fluid in Centistokes (cSt). The motive force driving the fluid out of the cup is the head of fluid. This fluid head is also part of the equation that makes up the volume of the fluid. Rationalizing the equations the fluid head term is eliminated leaving the units of Kinematic viscosity as area/time, which is ν = m^2/s (1.0 m^2/s = 10,000 Stokes = 1,000,000 Centistokes) and the kinematic viscosity can also be determined by dividing the dynamic viscosity by the fluid density.

For this test method specifies a procedure for the determination of the kinematic viscosity, ν , of liquid petroleum products, both transparent and opaque, by measuring the time for a volume of liquid to flow under gravity through a calibrated glass capillary viscometer. The dynamic viscosity, η, can be obtained by multiplying the kinematic viscosity, ν, by the density, ρ, of the liquid.

The result obtained from this test method is dependent upon the behavior of the sample, and is intended for application to liquids for which primarily the shear stress and shear rates are proportional (Newtonian flow behavior). If, however, the viscosity varies significantly with the rate of shear, different results may be obtained from viscometers of different capillary diameters. The procedure and precision values for residual fuel oils, which under some conditions exhibit non-Newtonian behavior, have been included.

Calculate each of the determined kinematic viscosity values, ν_1 and ν_2, from the measured flow times, t_1 and t_2, and the viscometer constant, C, by means of the following equation:

$$\nu_{1,2} = C \cdot t_{1,2} \qquad \text{(b5)}$$

where: $\nu_{1,2}$ = determined kinematic viscosity values for ν_1 and ν_2, mm^2/s,

C = calibration constant of the viscometer, mm^2/s^2, and

$t_{1,2}$ = measured flow times for t_1 and t_2, respectively, s.

Calculate the dynamic viscosity, η, from the calculated kinematic viscosity, ν, and the density, ρ, by means of the following equation:

$$\eta = \nu \times \rho \times 10^{-3} \qquad \text{(b6)}$$

where: η = dynamic viscosity, mPa·s,

This material is reserved for educational purposes only, not allowed for commercial use.
Forbidden to modify the content, and cite the document when use.

ρ = density, kg/m^3, at the same temperature used for the determination of the kinematic viscosity, and

ν = kinematic viscosity, mm^2/s.

B-5: Ash Content (ASTM D482)

This test method covers the determination of ash in the range 0.001–0.180 mass %, from distillate and residual fuels, gas turbine fuels, crude oils, lubricating oils, waxes, and other petroleum products, in which any ash-forming materials are normally considered to be undesirable impurities or contaminants. The test method is limited to petroleum products, which are free from added ash-forming additives, including certain phosphorus compounds.

Calculate the mass of the ash as a percentage of the original samples as follows:

$$\text{Ash, mass \%} = (w/W) \times 100 \quad \text{(b7)}$$

where: w = mass of ash, g, and

W = mass of sample, g.

B-6: Density (ASTM D4052)

This test method covers the determination of the density, relative density, and API Gravity of petroleum distillates and viscous oils that can be handled in a normal fashion as liquids at the temperature of test, utilizing either manual or automated sample injection equipment. Its application is restricted to liquids with total vapor pressures typically below 100 kPa and viscosities typically below about 15,000 mm^2/s at the temperature of test. The total vapor pressure limitation however can be extended 100 kPa provided that it is first ascertained that no bubbles form in the U-shaped, oscillating tube, which can affect the density determination. Some examples of products that may be tested by this procedure include: gasoline and gasoline-oxygenate blends, diesel, jet, basestocks, waxes, and lubricating oils.

Calculating Density Analyzers, using the observed T-value for the sample, and the T-value for water and appropriate instrument constants determined in Eq. d14 or d15, calculate the density or relative density using Eq. 2.2.12 and 2.2.13. Carry out all calculations to six significant figures and round the final results to four.

This material is reserved for educational use only, not allowed for commercial use.
Forbidden to modify the content, and cite the document when use.

For density: density, g/mL (kg/m^3) at t = $d_w + K_1(T_s^2 - T_w^2)$ (b8)

relative density, t/t = $1 + K_2(T_s^2 - T_w^2)$ (b9)

where: T_w = observed period of oscillation for cell containing water,

T_s = observed period of oscillation for cell containing sample,

d_w = density of water at test temperature,

K_1 = instrument constant for density,

K_2 = instrument constant for relative density, and

T = temperature of test, °C.

Using the observed T-values and the reference values for water and air (Eq. d16), calculate the instrument constant K using the following equations:

For density: $K_1 = [d_w - d_a][T_w^2 - T_a^2]$ (b10)

For relative density: $K_2 = [1.0 - d_a][T_w^2 - T_a^2]$ (b11)

where: T_w = observed period of oscillation for cell containing water,

T_a = observed period of oscillation for cell containing air,

d_w = density of water at test temperature, and

d_a = density of air at test temperature.

Calculate the density of air at the temperature of test using the following equation:

d_a, g/mL = 0.001293[273.15/T][P/760] (b12)

where: T = temperature, K, and

P = barometric pressure, torr.

B-7: Water Content (ASTM D6304)

This test method covers the direct determination of water in the range of 10 to 25,000 mg/kg entrained water in petroleum products and hydrocarbons using automated instrumentation. This test method also covers the indirect analysis of water thermally removed from samples and swept with dry inert gas into the Karl Fischer titration cell.

Calculate the water concentration in mg/kg or µL/mL of the sample as follows:

water, mg/kg or µg/g = W_1/W_2 or (b13)

This material is reserved for educational use only, not allowed for commercial use.

Forbidden to modify the content, and cite the document when use.

$$\text{water, } \mu L/mL = V_1/V_2 \quad \text{(b14)}$$

and calculate the water concentration, in mass or volume %, of the sample as follows:

$$\text{water, mass \%} = W_1/(10{,}000 \times W_2) \quad \text{or} \quad \text{(b15)}$$

$$\text{volume \%} = V_1/(10 \times V_2) \quad \text{(b16)}$$

where: W_1 = mass of water titrated, mg or μg (as appropriate),

W_2 = mass of sample used, kg or g (as appropriate),

V_1 = volume of water titrated, μL, and

V_2 = volume of sample used, mL.

Use the following equations for calculating the water content of the sample in units of volume % from mass %, or mass % from volume %.

water, (volume%) = mass% x [density of sample at t / density of water at t] (b17)

water, (mass%) = volume % x [density of sample at t / density of water at t] (b18)

where: t = test temperature.

This material is reserved for educational use only, not allowed for commercial use.
Forbidden to modify the content, and cite the document when use.

APPENDIX C

Diesel Standard of Department of Energy Business

Table C1 Characteristic and quality of Diesel fuel (Department of Energy Business, 1997)

Item	Description	Rates (low-high)	Diesel		
			High Speed		Low speed
			Normal	B5	
1	Specific Gravity at 15.6 °C	Not lower than	0.81	0.81	-
		And not higher than	0.87	0.87	0.92
2	Cetane Number				
	or Calculated Cetane Index				
	Before January 1, 2012	Not lower than	47	47	45
	Form January 1, 2012	Not lower than	50	50	45
3	Viscosity, cSt				
	3.1 at 40 °C or	Not lower than	1.8	1.8	-
		And not higher than	4.1	4.1	8
	3.2 at 50 °C	Not higher than	-	-	6
4	Pour Point, °C	Not higher than	10	10	16
5	Sulphur, %wt.				
	Before January 1, 2012	Not higher than	0.035	0.035	1.5
	Form January 1, 2012	Not higher than	0.005	0.005	1.5
6	Copper Strip Corrosion	Not higher than	N. 1	N. 1	-
7	Oxidation Stability, g/m^3	Not higher than	-	25	-
8	Carbon Residue, %wt	Not higher than	0.05	0.05	-
9	Water and Sediment, %vol	Not higher than	0.05	0.05	0.3
10	Ash, %wt	Not higher than	0.01	0.01	0.02
11	Flash Point, °C	Not higher than	52	52	52
12	Distillation (90% recovered), °C	Not higher than	357	357	-
13	Polycyclic Aromatic Hydrocarbon, % wt				
	Before January 1, 2012	-	-	-	-
	Form January 1, 2012	Not higher than	11	11	-
14	Colour				
	14.1 Hue		-	Blue	-
	14.2 Dye , mg/L	Not lower than	-	7.0	-
	14.3 Intensity	Not lower than	-	-	4.5
		And not higher than	4.0	-	7.5
15	Methyl Ester of Fatty Acid, %vol	Not lower than	1.5	4	-
		And not higher than	2	5	-
16	Lubricity, µm	Not higher than	460	460	-
17	Additive	According to the regulation of Department of Energy Business			

This material is reserved for educational use only, not allowed for commercial use.
Forbidden to modify the content, and cite the document when use.

BIOGRAPHY

Name: Mr. Khemmachat Rungsawat

Date of Birth: January 13, 1984

Place of Birth: Yala, Thailand

Education:

2002-2005 B. Eng. in Mechanical Engineering, Kasetsart University

2007-2011 M. Eng. in Automotive Engineering (International program), International College, King Mongkut's Institute of Technology Ladkrabang (KMITL)

Scholarships:

2007-2009 Full scholarship for study in the master degree from National Science and Technology Development Agency (NSTDA)

Publications:

1. Rungsawat, K., Chollacoop, N., Topaiboul, S., Charoenphonphanich,c., and Takahashi, K., Effect of biodiesel on fuel tank in automotive fuel system, The 2nd Thammasat University International Conference on Chemical, Environmental and Energy Engineering (TU-ChEEE 2009), Bangkok, Thailand, March 356-362, 2009.

This material is reserved for educational use only, not allowed for commercial use.
Forbidden to modify the content, and cite the document when use.